TP 14366E

Tank-Car Thermal Protection Defect Assessment: Fire Tests of 500-Gallon Tanks with Thermal Protection Defects

Prepared for

Transportation Development Centre
of
Transport Canada

by

Department of Mechanical and Materials Engineering
Queen's University
Kingston, Ontario

March 2005

105-04881/

TP 14366E

Tank-Car Thermal Protection Defect Assessment: Fire Tests of 500-Gallon Tanks with Thermal Protection Defects

by

A.M. Birk, D. Poirier, C. Davison, and C. Wakelam
Department of Mechanical and Materials Engineering
Queen's University
Kingston, Ontario

March 2005

This report reflects the views of the authors and not necessarily those of the Transportation Development Centre of Transport Canada or co-sponsoring organization.

The Transportation Development Centre and the co-sponsoring agencies do not endorse products or manufactures. Trade or manufacturers' names appear in this report only because they are essential to its objectives.

Since some of the accepted measures in the industry are imperial metric measures are not always used in this report.

Project team

A.M. Birk
D. Poirier
C. Davison
C. Wakelam

Un sommaire français se trouve avant la table des matières.

Transport Canada Transports Canada

PUBLICATION DATA FORM

1. Transport Canada Publication No.
TP 14366E

2. Project No.
5422

3. Recipient's Catalogue No.

4. Title and Subtitle
Tank-Car Thermal Protection Defect Assessment:
Fire Tests of 500-Gallon Tanks with Thermal Protection Defects

5. Publication Date
March 2005

6. Performing Organization Document No.

7. Author(s)
A.M. Birk, D. Poirier, C. Davison and C. Wakelam

8. Transport Canada File No.
2450-FP654-5

9. Performing Organization Name and Address
Department of Mechanical and Materials Engineering
McLaughlin Hall
Queen's University
Kingston, Ontario
Canada K7L 3N6

10. PWGSC File No.
MTB-3-00363

11. PWGSC or Transport Canada Contract No.
T8200-033505/001/MTB

12. Sponsoring Agency Name and Address
Transportation Development Centre (TDC)
800 René Lévesque Blvd. West
Suite 600
Montreal, Quebec
H3B 1X9

13. Type of Publication and Period Covered
Final

14. Project Officer
A. Vincent

15. Supplementary Notes (Funding programs, titles of related publications, etc.)
Co-sponsored by Transport Canada's Transport Dangerous Goods Directorate

16. Abstract

A series of fire tests was carried out to measure the effect of defects in thermal protection systems on fire-engulfed propane tanks.

Dangerous goods tank-cars are protected from accidental fire impingement by thermal protection systems. One common system includes a 13 mm thick blanket of high-temperature ceramic-fibre thermal insulation covered with a 3 mm steel jacket. Recent inspections revealed tanks with significant defects in these thermal protection systems. The tests conducted in this study were designed to establish acceptable levels of defect from a safety standpoint.

Tests were conducted using 1890 L (500 US gal.) ASME code propane tanks as approximate one-third scale models of 112J type tank-cars. These tanks were tested in the baseline state (i.e., no thermal protection) and in a thermally protected state with defects. The defect sizes tested covered approximately 8% and 16% of the tank surface area. The tanks were 25% engulfed in a fire that simulated a hydrocarbon pool fire with an effective blackbody temperature of approximately 870°C. At this scale, it was expected that the 500-gal. tanks would fail in about one third the time of a full-scale tank-car. This was confirmed by results from baseline tests.

The fire testing showed that even relatively small defects could result in tank rupture when the defect area is engulfed in a severe fire and not wetted by liquid lading.

17. Key Words
Fire test, thermal protection defects, failure prediction, dangerous goods tank-car, 500-gallon propane tank

18. Distribution Statement
Limited number of copies available from the Transportation Development Centre

19. Security Classification (of this publication)
Unclassified

20. Security Classification (of this page)
Unclassified

21. Declassification (date)
—

22. No. of Pages
xviii, 70, apps

23. Price
Shipping/ Handling

CDT/TDC 79-005
Rev. 96

Canada

Transports Canada Transport Canada

FORMULE DE DONNÉES POUR PUBLICATION

1. N° de la publication de Transports Canada TP 14366E	2. N° de l'étude 5422	3. N° de catalogue du destinataire

4. Titre et sous-titre

Tank-Car Thermal Protection Defect Assessment:
Fire Tests of 500-Gallon Tanks with Thermal Protection Defects

5. Date de la publication

Mars 2005

6. N° de document de l'organisme exécutant

7. Auteur(s)

A.M. Birk, D. Poirier, C. Davison et C. Wakelam

8. N° de dossier - Transports Canada

2450-FP654-5

9. Nom et adresse de l'organisme exécutant

Department of Mechanical and Materials Engineering
McLaughlin Hall
Queen's University
Kingston, Ontario
Canada K7L 3N6

10. N° de dossier - TPSGC

MTB-3-00363

11. N° de contrat - TPSGC ou Transports Canada

T8200-033505/001/MTB

12. Nom et adresse de l'organisme parrain

Centre de développement des transports (CDT)
800, boul. René-Lévesque Ouest
Bureau 600
Montréal (Québec)
H3B 1X9

13. Genre de publication et période visée

Final

14. Agent de projet

A. Vincent

15. Remarques additionnelles (programmes de financement, titres de publications connexes, etc.)

Coparrainé par la Direction générale du transport des marchandises dangereuses de Transports Canada

16. Résumé

Une série d'essais au feu ont été réalisés afin de mesurer l'effet de défauts du système de protection thermique de citernes de propane lorsque celles-ci sont enveloppées par des flammes.

Les wagons-citernes pour marchandises dangereuses sont dotés d'un système de protection thermique qui les protège contre l'effet des flammes en cas d'accident. Un système de protection typique est formé d'un matelas isolant de fibre céramique haute température de 13 mm d'épaisseur recouvert d'une jaquette en acier de 3 mm d'épaisseur. Des inspections récentes ont révélé la présence de défauts importants dans ces systèmes de protection thermique. Le but des essais menés au cours de la présente étude était de déterminer le degré de détérioration acceptable du point de vue de la sécurité.

Les essais ont été réalisés sur des citernes à propane de 1 890 L (500 gallons US) conformes au code de l'ASME, et représentant plus ou moins des modèles à l'échelle un tiers de wagons-citernes de type 112J. Ces citernes ont été testées dans deux configurations : sans protection thermique (configuration de référence) et avec une protection thermique défectueuse. Les défauts de protection étudiés couvraient environ 8 p. 100 et 16 p. 100 de la surface de la citerne. Les citernes étaient plongées au quart dans un feu qui simulait l'incendie d'une nappe d'hydrocarbures produisant une température de corps noir effective d'environ 870 °C. À cette échelle, on s'attendait à la rupture des citernes de 500 gallons en trois fois moins de temps qu'un wagon-citerne en vraie grandeur. Cela a été confirmé par les essais en configuration de référence.

Les essais au feu ont révélé que même des défauts de dimensions relativement faibles peuvent entraîner la rupture de la citerne lorsque la zone où se trouve le défaut est exposée à un feu intense et qu'elle n'est pas mouillée par le liquide transporté.

17. Mots clés Essai au feu, défauts de protection thermique, prévision de défaillance, wagon-citerne pour marchandises dangereuses, citerne à propane de 500 gallons	18. Diffusion Le Centre de développement des transports dispose d'un nombre limité d'exemplaires.

19. Classification de sécurité (de cette publication) Non classifiée	20. Classification de sécurité (de cette page) Non classifiée	21. Déclassification (date) —	22. Nombre de pages xviii, 70, ann.	23. Prix Port et manutention

Executive Summary

A series of fire tests was carried out to measure the effect of defects in thermal protection systems on fire-engulfed propane tanks. The tests were conducted at Defence R&D Canada – Valcartier's Munitions Experimental Test Centre during the summer of 2004.

Dangerous goods tank-cars are protected from accidental fire impingement by thermal protection systems designed so that a tank will not rupture for 100 minutes in a defined engulfing fire, or 30 minutes in a defined torching fire. One common system includes a 13 m thick blanket of high-temperature ceramic-fibre thermal insulation covered with a 3 m steel jacket. Recent inspections revealed tanks with significant defects in these thermal protection systems. The tests conducted in this study were designed to establish what levels of defect are acceptable from a safety standpoint.

The tests were conducted using 1890 L (500 US gal.) ASME code propane tanks as approximate one-third scale models of 112J type tank-cars. The model tanks have a diameter of 0.96 m, a wall thickness of 7.1 mm and an overall length-to-diameter ratio (L/D) of about 3. The 112J type tank-cars have a diameter of about 3 m, a wall thickness of 16 mm and an L/D of about 6. At this scale, it is expected that the 500-gal. tanks will fail in about one third the time of a full-scale tank-car.

Tanks were tested in the baseline state (i.e., no thermal protection) and in a thermally protected state with defects. The defects tested covered approximately 8 and 16 percent of the tank surface area.

The tanks were 25 percent engulfed in a fire that simulated a hydrocarbon pool fire with an effective blackbody temperature of approximately 870°C. The fire consisted of an array of 25 liquid-fuelled propane burners that provided a sheet of gentle luminous flame. This system was used rather than a pool fire because it allowed better control and gave better test-to-test consistency than an open pool fire. However, even with the burners, the strength and direction of the wind could strongly influence the effectiveness of the fire. For this reason, testing was conducted when wind conditions looked to be most favourable.

A total of six tests were conducted with the 500-gal. tanks. Two tests were baseline, unprotected tanks, one of which failed in 8 minutes, as expected. The other failed in 46 minutes due to poor fire conditions for the first 38 minutes of the test. If scaling the failure time by the tank diameter is correct, then we would expect an unprotected 112 type tank-car to fail after 24 minutes in an engulfing fire. This agrees very well with the RAX 201 test of a full-scale tank-car.

Tests were then conducted with 16 and 8 percent insulation defects from bottom to top on one side of the tank. Failure times (corrected for poor fire conditions) were 24 and 36 minutes, respectively. This would scale to about 72 and 109 minutes, respectively,

for a full-scale tank-car. These tanks failed with fill levels near 70 percent, which means the vapour spaces in the tanks were relatively small at the time of failure.

The fire testing demonstrated that even relatively small insulation defects can result in tank rupture if the defect area is engulfed in a severe fire, and the defect area is not wetted by liquid lading.

The main conclusions from this work are:

i) The baseline test resulted in tank failure in 8 minutes. If this is scaled by the tank diameter, then an unprotected tank-car failure would be expected at 24 minutes. This agrees well with the RAX 201 test and suggests that the scaling approach is valid.

ii) The fire temperature ranged between about 700 and 927°C. When the fire was below 816°C it was not considered credible and adjustments to some tests were necessary. In most cases, the fire was between about 820 and 890°C, which is in line with fire-test standards. Credible liquid hydrocarbon pool fires range from 800 to 950°C.

iii) The entire vapour space got very hot, including areas not exposed to fire and under thermal protection. This is partly due to high vapour temperatures before the pressure relief valve (PRV) is activated. With small defects, the PRV can take a long time to pop and this gives very high vapour temperatures (> 300°C).

iv) The jacket temperatures were in line with expectations based on thermal modelling. With good fire contact, the jacket temperatures ranged from 780 to 860°C. This would be quite close to the effective fire temperature.

v) The vapour space wall temperatures were higher than expected based on thermal modelling. This is most likely due to assumptions in the vapour space heat transfer model. When convection coefficients were reduced and liquid surface radiation properties adjusted (emissivity of surface reduced), much better agreement between model and experiments were achieved.

vi) The cooling effect of the liquid surface did not appear to be as strong as previously believed. The tanks failed with high fill levels (higher than 70 percent). The high liquid levels did not save the tanks by cooling the vapour space wall.

vii) Tank pressurization was in line with expectations. The tank pressurizes much faster than predicted by single-node thermal models such as AFFTAC. The time to PRV action is inversely proportional to the defect fraction. It is also known from previous testing that pressurization depends on the fill level and the location of the heating.

viii) The SA 455 steel used in the tanks was significantly stronger than required by the material specification minimum requirements (minimum UTS = 480 Mpa; actual test steel was approximately 610 MPa). Modelling based on minimum properties of SA 455 suggest that the wall should fail when the wall temperature achieves about

650°C. The wall temperatures reached 720°C at failure. The SA 455 as tested had tensile and stress rupture properties very similar to the TC 128B used in tank-cars.

ix) For the tanks tested, with the fire conditions used, an 8 percent insulation defect resulted in tank failure in about 36 minutes (corrected for poor fire). This scales to about 109 minutes for a rail tank-car if scaled by the tank diameter. This suggests that the 8 percent insulation defect on the tanks tested is near the upper limit of allowable defect. However, if this defect size is scaled up to a rail tank-car based on wall thickness, then the allowable defect area on the tank-car is only about 4 percent of the tank-car surface area.

Sommaire

Une série d’essais au feu ont été réalisés afin de mesurer l’effet de défauts du système de protection thermique de citernes de propane lorsque celles-ci sont enveloppées par des flammes. Ces essais ont eu lieu au Centre d’essais et d’expérimentation des munitions (CEEM) de Recherche et développement pour la défense Canada – Valcartier, au cours de l’été 2004.

Les wagons-citernes pour marchandises dangereuses sont protégés contre l’effet des flammes en cas d’accident par un système de protection thermique conçu pour protéger la citerne de la rupture pendant 100 minutes lorsque soumise à des flammes enveloppantes, ou 30 minutes, lorsque soumise à une flamme de chalumeau. Un système de protection typique est formé d’un matelas isolant de fibre céramique haute température de 13 mm d’épaisseur recouvert d’une jaquette en acier de 3 mm d’épaisseur. Des inspections récentes ont révélé la présence de défauts importants dans ces systèmes de protection thermique. Le but des essais menés au cours de la présente étude était de déterminer le degré de détérioration acceptable du point de vue de la sécurité.

Les essais ont été réalisés sur des citernes à propane de 1 890 L (500 gallons US) conformes au code de l’ASME et représentant plus ou moins des modèles à l’échelle un tiers de wagons-citernes de type 112J. Les citernes modèles ont un diamètre de 0,96 m, une paroi de 7,1 mm d’épaisseur et un rapport longueur/diamètre (L/D) d’environ 3. Quant aux wagons-citernes de type 112J, leur citerne a un diamètre d’environ 3 m, une paroi de 16 mm d’épaisseur et un rapport L/D d’environ 6. À cette échelle, on s’attendait à la rupture des citernes de 500 gallons en trois fois moins de temps qu’un wagon-citerne en vraie grandeur.

Les citernes ont été testées dans deux configurations : sans protection thermique (configuration de référence) et avec une protection thermique défectueuse. Les défauts de protection étudiés couvraient environ 8 p. 100 et 16 p. 100 de la surface de la citerne.

Les citernes étaient plongées au quart dans un feu qui simulait l’incendie d’une nappe d’hydrocarbures produisant une température de corps noir effective d’environ 870 °C. Le feu émanait d’un ensemble de 25 brûleurs au propane liquide, qui produisaient de douces flammes blanches. Ce système a été préféré à un feu en nappe parce qu’il était plus facile à commander et qu’il donnait des résultats plus constants, d’un essai à l’autre, qu’un feu en nappe ouvert. Il reste que même avec des brûleurs, la force et la direction du vent pouvaient avoir une grande influence sur l’efficacité du feu. C’est pourquoi les essais ont eu lieu lorsque les conditions du vent semblaient le plus favorables.

Six essais au total ont été menés sur les citernes de 500 gallons. Deux essais portaient sur la configuration de référence (sans protection thermique). Dans un cas, la rupture s’est produite après 8 minutes, comme prévu. Dans l’autre cas, la rupture est survenue après 46 minutes, à cause de mauvaises conditions de feu pendant les 38 premières minutes de l’essai. En supposant que le temps avant défaillance est proportionnel au diamètre de la citerne, on peut s’attendre qu’un wagon-citerne de type 112J sans protection thermique se

rompe au bout de 24 minutes d'enveloppement par des flammes. Cela concorde tout à fait avec les résultats de l'essai RAX 201 d'un wagon-citerne en vraie grandeur.

Des essais ont ensuite été menés sur des citernes comportant des défauts d'isolation sur 16 p. 100 et sur 8 p. 100 de leur surface, de bas en haut, sur un côté de la citerne. Les temps avant défaillance (corrigés pour de mauvaises conditions de feu) ont été de 24 et de 36 minutes, respectivement. Cela correspondrait à 72 et 109 minutes, respectivement, pour un wagon-citerne en vraie grandeur. La rupture des citernes est survenue à des niveaux de remplissage avoisinant les 70 p. 100. Le volume de la phase gazeuse à l'intérieur de la citerne était donc relativement faible au moment de la rupture.

Les essais au feu ont révélé que même des défauts de dimensions relativement faibles peuvent entraîner la rupture de la citerne lorsque la zone où se trouve le défaut est exposée à un feu intense et qu'elle n'est pas mouillée par le liquide transporté.

Voici les principales conclusions tirées des travaux :

i) L'essai en configuration de référence a entraîné la rupture de la citerne en 8 minutes. En supposant que le temps avant défaillance est proportionnel au diamètre de la citerne, on peut s'attendre que la rupture d'un wagon-citerne sans protection thermique surviendrait après 24 minutes d'exposition aux flammes. Cela concorde avec les résultats de l'essai RAX 201 et tend à valider la méthode de changement d'échelle.

ii) La température du feu variait de 700 °C à 927 °C environ. En deçà de 816 °C, les conditions de feu étaient considérées non crédibles et les résultats de certains essais ont dû être rajustés. Dans la plupart des cas, la température du feu était à peu près comprise entre 820 °C et 890 °C, ce qui respecte les normes des essais au feu. Dans la réalité, des feux en nappe d'hydrocarbures liquides atteignent des températures qui oscillent de 800 °C à 950 °C.

iii) Toute la zone au-dessus de la marge de remplissage est devenue très chaude, même les endroits non exposés au feu et protégés par l'isolant. Cela est partiellement attribuable aux températures élevées atteintes par les gaz avant l'ouverture de la soupape de sûreté. En présence de petits défauts, la soupape peut prendre beaucoup de temps à s'ouvrir, ce qui donne le temps aux gaz d'atteindre des températures très élevées (> 300 °C).

iv) Les températures de la jaquette étaient conformes aux attentes, selon le modèle thermique. Un contact étroit avec le feu a entraîné des températures de 780 °C à 860 °C dans la jaquette en acier, soit des températures assez proches de celle du feu.

v) La température des parois dans la zone au-dessus de la marge de remplissage était supérieure aux attentes, d'après le modèle thermique. Cela est tout probablement dû aux hypothèses posées par le modèle concernant le transfert de chaleur dans la zone au-dessus de la marge de remplissage. Après réduction des coefficients de convection et rajustement des propriétés de rayonnement de la surface du liquide (réduction de l'émissivité de la surface), les expériences étaient beaucoup plus conformes au modèle.

vi) L'effet de refroidissement produit par la surface du liquide ne s'est pas révélé aussi puissant qu'on l'avait envisagé. De fait, la rupture des citernes est survenue à de forts niveaux de remplissage (plus de 70 p. 100). Ainsi, les niveaux élevés de liquide n'ont pas réussi à refroidir suffisamment la paroi au-dessus de la marge de remplissage.

vii) La mise en pression des réservoirs était conforme aux attentes. La citerne monte en pression beaucoup plus vite que prévu par les modèles thermiques à nœud unique, comme le modèle AFFTAC. Le temps avant l'ouverture de la soupape de sûreté est inversement proportionnel à la surface du défaut. On sait aussi, par des essais antérieurs, que la montée en pression est fonction du niveau de remplissage et de l'emplacement de la source de chaleur.

viii) Les citernes étudiées étaient faites d'acier SA 455, un acier beaucoup plus résistant que ne l'exige la spécification relative aux matériaux (résistance à la traction minimale de 480 Mpa; la résistance de l'acier testé était d'environ 610 MPa). La modélisation fondée sur les propriétés minimales de l'acier SA 455 indique une rupture de la paroi lorsque celle-ci atteint une température d'environ 650 °C. Or, les températures des parois atteignaient 720 °C à la rupture. Notons que l'acier SA 455 testé présentait des propriétés d'élasticité et de rupture par fluage très semblables à celles de l'acier TC 128B utilisé dans les wagons-citernes.

ix) Pour les citernes mises à l'essai, dans les conditions de feu mises en oeuvre, un défaut d'isolation de 8 p. 100 a mené à la rupture de la citerne en 36 minutes environ (temps corrigé pour les mauvaises conditions de feu). Cela revient à environ 109 minutes pour un wagon-citerne, en supposant que le temps avant défaillance est proportionnel au diamètre de la citerne. Cela donne à penser que le défaut d'isolation de 8 p. 100 des citernes étudiées est près de la limite supérieure du défaut acceptable. Toutefois, si l'étendue du défaut est augmentée à l'échelle de l'épaisseur de paroi d'un wagon-citerne, la superficie du défaut acceptable dans le wagon-citerne n'est plus que de 4 p. 100 environ de la surface.

Table of Contents

1.0 Introduction **1**

1.1 Background 1
1.2 Objectives 2
1.3 Scope 2

2.0 Theory **3**

2.1 Tank Failure 3
2.2 Tank Failure – Scale Effects 3
2.3 Scaling of Critical Defect Size 7
2.4 Non-Ideal Scaling 8

3.0 Approach **10**

3.1 Experimental Design 10
3.2 Test Layout 13
3.2.1 Test Site 13
3.2.2 Test Tanks 14
3.2.3 Burners 17
3.2.4 Pressure Relief System 19
3.3 Instrumentation and Control 24
3.3.1 Instrumentation 24
3.3.2 Data Acquisition System and Control 27
3.4 Test Procedure 28

4.0 Results and Analysis **29**

4.1 Overview 29
4.2 Fire Condition 29
4.3 Baseline Tests 33
4.3.1 Baseline Test 04-1 33
4.3.2 Baseline Test 04-6 37
4.4 Large Thermal Defect Tests 42
4.4.1 Large Thermal Defect Test 04-2 43
4.4.2 Large Thermal Defect Water Tank Test 04-W5 47
4.4.3 Large Thermal Defect Test 04-3 49
4.5 Large Thermal Defect, Low Hoop Stress, Test 04-4 55
4.6 Small Thermal Defect, Test 04-5 60
4.7 Results Summary 63

5.0 Conclusions **67**

6.0 Recommendations **68**

References **69**

Appendix A: Fire Condition Verification

Appendix B: Lading Temperatures

Appendix C: Tank Fill Level

Appendix D: Water Fill Tank Tests Data Plots

Appendix E: Test Data Plots

Appendix F: Error Analysis

Appendix G: Field Test Check Lists

Appendix H: Data Acquisition Software User's Guide

Appendix I: Wall Thermocouple Fabrication

Appendix J: Burner Development

List of Figures

Figure 3.1: PRV field trials site map ... 15
Figure 3.2: Standard ASME 1890 L test tank (from manufacture's drawing) ... 15
Figure 3.3: Burner array and evaporator set-up ... 18
Figure 3.4: Burner array configuration ... 19
Figure 3.5: Nominal flame width and location relative to tank insulation defects and steel jacket ... 19
Figure 3.6: Original tank PRV (250 psig, 1 in. diameter, 2565 scfm) ... 20
Figure 3.7: Tank 04-01 with burners in place ... 21
Figure 3.8: PRV, PRV piping, and nozzle sketch ... 22
Figure 3.9: Computer-controlled PRV (air reservoir, control valve, backup PRV stack valve, nozzle plate) ... 22
Figure 3.10: PRV nozzle operating with steam flow ... 24
Figure 3.11: Lading thermocouple locations ... 25
Figure 3.12: Wall thermocouple layout for Test 04-6 ... 26
Figure 4.1: Burner system in operation (note luminous pool-fire-like flame, and flame wrapping around tank with wind from right to left (northwest wind)) ... 30
Figure 4.2: Wall thermocouple layout for water tank Test 04-W4 ... 31
Figure 4.3: Wall temperature, Test 04-W4 (water tank test, no shell/insulation, 80% fill) ... 31
Figure 4.4: Picture showing poor fire contact on tank top (wind from east (right to left)) ... 32
Figure 4.5: Wall thermocouple layout for Test 04-1 ... 33
Figure 4.6: Wall temperature, Test 04-1 (baseline test, no insulation, no steel jacket, 78% fill) ... 34
Figure 4.7: BLEVEd tank, Test 04-1 ... 35
Figure 4.8: Tank pressure, Test 04-1 ... 36
Figure 4.9: Lading temperature (TC bundle 1), Test 04-1 ... 37
Figure 4.10: Wall thermocouple layout for Test 04-6 ... 38
Figure 4.11: Wall temperature, Test 04-6 (baseline test, no insulation, no steel jacket, 78% fill) ... 39
Figure 4.12: Tank after failure, Test 04-6 ... 40
Figure 4.13: Tank failure, Test 04-6 ... 40
Figure 4.14: Tank pressure, Test 04-6 ... 41
Figure 4.15: Lading temperature (TC bundle 1), Test 04-6 ... 42
Figure 4.16: Location and size of tank insulation defects and protective steel jacket ... 43
Figure 4.17: Fire condition at beginning of Test 04-02 ... 44
Figure 4.18: Lading temperature (TC bundle 1), Test 04-2 ... 44
Figure 4.19: Wall thermocouple layout for Test 04-2 ... 45
Figure 4.20: Wall temperature, Test 04-2 (16% area insulation defect, 71% fill). Run aborted due to insufficient burner fuel flow ... 45
Figure 4.21: Tank pressure, Test 04-2 ... 46
Figure 4.22: Fire condition for Test 04-W5 ... 47
Figure 4.23: Wall thermocouple layout for Test 04-W5 ... 48
Figure 4.24: Wall temperature, Test 04-W5 (16 % area insulation defect, 50% fill) ... 48

Figure 4.25: Lading temperature (TC bundle 1), Test 04-W5 49
Figure 4.26: Wall thermocouple layout for Test 04-3 50
Figure 4.27: Wall temperature, Test 04-3 (16% area insulation defect) 50
Figure 4.28: Tank pressure, Test 04-3 51
Figure 4.29: Test 04-03 burned vapour space wall under insulated area (not under fire) 52
Figure 4.30: Test 04-03 tank after rupture. The steel jacket split open at the top tack weld 53
Figure 4.31: Lading temperature (TC bundle 1), Test 04-3 53
Figure 4.32: Tank failure, Test 04-3 54
Figure 4.33: Wall thermocouple layout for Test 04-4 56
Figure 4.34: Wall temperature, Test 04-4a (16% insulation defect, low hoop stress). Run aborted to increase fuel pressure 56
Figure 4.35: Wall temperature, Test 04-4b (16% insulation defect, low hoop stress) .. 57
Figure 4.36: Test 04-04 rupture with split jacket. Note burned vapour space 58
Figure 4.37: Tank rupture, Test 04-04. Note jagged tear, suggesting wall made contact with jacket and jacket provided some support 58
Figure 4.38: Lading temperature (TC bundle 1), Test 04-4 59
Figure 4.39: Wall thermocouple layout for Test 04-5 60
Figure 4.40: Wall temperature, Test 04-5 (8% insulation defect). Flame lifted or shifted for approximately 1200 seconds of the test duration 61
Figure 4.41: Tank pressure, Test 04-5 62
Figure 4.42: Test 04-5, small rupture with small insulation defect. Again, tank wall contact with the outer steel jacket is suspected 62
Figure 4.43: Tank wall temperature for tests 04-3, 04-4, 04-5, and 04-6. Thermocouple located at top and centre of the tank 65

List of Tables

Table 3.1: Comparison between the 500-gallon tank and 112J tank-car 11
Table 3.2: Comparison of full-scale fire tests 12
Table 3.3: Test matrix 13
Table 3.4: Test tank specifications 16
Table 3.5: Comparison of 112J tank and 500-gallon ASME code propane tank 16
Table 3.6: Insulation and jacket specifications 17
Table 3.7: Summary of ceramic fibre insulation properties (Unifrax, tank-car insulation, 72 kg/m3 density, new condition) 17
Table 3.8: DAQ instrumentation list 24
Table 3.9: Thermocouple locations (bundle 1) 26
Table 4.1: Fill level effect on wall temperature during burner calibration tests 32
Table 4.2: Comparison of results for high and low hoop-stress test pair 59
Table 4.3: Test summary 64

Glossary

AFFTAC	Analysis of Fire Effects on Tank Cars
ASME	**A**merican **S**ociety of **M**echanical **E**ngineers
BLEVE	**B**oiling **L**iquid **E**xpanding **V**apour **E**xplosion
CFD	**C**omputational **F**luid **D**ynamics
CGSB	**C**anadian **G**eneral **S**tandards **B**oard
DAQ	**D**ata **A**c**q**uisition
METC	**M**unitions **E**xperimental **T**est **C**entre
PRV	**P**ressure **R**elieve **V**alve
UTS	**U**ltimate **T**ensile **S**trength

1.0 Introduction

This report describes the results of a series of fire tests carried out by A.M. Birk and his team from the Department of Mechanical and Materials Engineering of Queen's University at Kingston, Ontario. The purpose of the study was to measure the effect of defects in thermal protection systems on fire-engulfed propane tanks.

The tests were conducted at Defence R&D Canada – Valcartier's Munitions Experimental Test Centre during the summer of 2004.

1.1 Background

Certain dangerous goods tank-cars must be thermally protected so they can survive accidental fire impingement. The requirement for thermal protection systems for pressure tank-cars is specified in CAN/CGSB-43.147-2002, section 15.8, which states:

If a thermal protection system is specified by this standard, the system must be capable of preventing the release of any dangerous goods from the tank car, except release through the pressure relief device, when subjected to the following conditions:

> *(1) A pool fire for 100 min, and*
> *(2) A torch fire for 30 min.*

It is known from field surveys that some operating dangerous goods tank-cars have defective thermal protection systems. With the size of the North American fleet of tank-cars, it is not feasible to fix all of these defects immediately, due to both cost and logistical reasons. This research program was intended to help identify which tanks need immediate attention.

Several published reports have been prepared by A.M. Birk and his team in connection with this issue [1, 2, 3, 4].

The work has led us to the point where a computer model has been developed to predict critical thermal protection defect sizes on tank-cars. This thermal model requires some additional data and final validation before it can be used to assess defects in the field. The following data is needed to further support the theoretical work:

i) Obtain high temperature stress-rupture data (by test) of tank-car steels, including both old steels and new (to cover the true condition of the tank-car fleet) [5].
ii) Conduct a CFD (computational fluid dynamics) study to obtain predictions for the pressurization of tanks with fire heating of localized thermal protection defects.
iii) Obtain medium-scale fire test data of tanks with defective thermal protection for validation of failure times.

This report presents the results of the fire testing of medium-scale propane tanks with thermal protection defects. The stress-rupture testing and CFD study of pressurization rates will be published separately.

1.2 Objectives

The overall objective of this work was to provide detailed data on how tanks with thermal protection defects respond to fire impingement.

The objectives were to determine:

i) how defect size affects the wall heating rates;
ii) how defect size affects the time to PRV opening;
iii) the smallest defect size that can lead to rupture in the allotted time frame.

1.3 Scope

The scope of the test was limited to one test series in the summer of 2004. The testing involved six tests of 500-gal. tanks. Two tests, done without thermal protection, served as baseline tests, and the remainder were done with two levels of thermal protection defect (8 and 16% of tank surface area).

2.0 Theory

This study examined the role that thermal insulation defects play in the survivability of a tank when exposed to fire. This chapter presents relevant background theory.

2.1 Tank Failure

Tank failure by fire impingement is due to high wall temperatures in the vapour space of the tank. With a properly working and sized pressure relief valve (PRV), the tank can fail due to wall material degradation at high temperature, even though the tank pressure is within design limits. Numerous fire tests have shown this [6, 7, 8, 9].

Thermal protection is used to provide a barrier to the fire heat flux [10]. This slows the rate of wall heating and delays failure. If there are gaps or defects in the thermal protection, local hot spots can develop in the tank wall. If these hot spots are large and hot enough, they can result in a local rupture of the wall.

2.2 Tank Failure – Scale Effects

Consider two tanks, a full sized 112J tank-car and a reduced-scale tank, where the following is true for both tanks:

i) Same shape (meaning same length-to-diameter (L/D) ratio) and same end types
ii) Wall thickness scaled to give same hoop stress at same pressure
iii) Same wall material (i.e. same ultimate tensile strength UTS, density, thermal conductivity, specific heat, etc.)
iv) PRV size based on tank surface area and fire heat flux so that pressure does not exceed 120% of PRV set pressure during fire exposure
v) Same PRV pressure setting

These two tanks are then exposed to fires that have the same heat flux (kW/m^2). The pool fire standard for tank-car thermal protection requires a fire in the range of 816 to 927°C effective blackbody temperature. This has been determined to be the fire environment seen by the RAX 201 test of a full-scale tank-car [6].

Let us also consider that the tanks start with the same fill level and initial temperature.

The question is – will the small-scale tank behave the same as the full-scale tank? What will be different? Can we account for these differences in some way?

From the above, the tanks only differ in tank diameter, tank length and wall thickness. All of these would be related to the full-scale tank by a single scale factor, λ. For example, we could choose to test with a tank one third the diameter of the full-scale tank. This means the tank length, diameter and wall thickness are all one third that of the full-scale tank. In this case the volume would be 1/27 that of the full-scale tank.

Tank failure in a fire is dictated by the following:

i) wall temperature in the vapour space
ii) tank stress in the heated area
iii) wall material properties at the elevated temperature

Since the tank will be scaled to have the same material and stress, issues influencing wall temperature remain to be considered. The wall temperature rise rate depends on:

i) fire heat flux
ii) wall thickness, density, thermal conductivity and specific heat
iii) convection in the vapour space
iv) radiation in the vapour space

The fire must be large and luminous for the heat transfer to be dominated by thermal radiation [11]. Previous fire testing [12] has demonstrated that large, massive, cool objects actually cool the fire and reduce the heat flux. However, if a tank is thermally protected, this effect does not apply since the cool object is insulated from the fire. We also know from testing that the small-scale tank will see higher fire heating due to convection [13]. For an engulfing hydrocarbon pool fire, the heat flux is dominated by thermal radiation and the difference caused by convection is small. Therefore, we expect the heat flux to be similar for the two different scales but probably a little higher (worse) for the small scale (i.e. small scale is conservative).

Here again we note that both tanks are made of steel with similar density, thermal conductivity and specific heat. Surface emissivities should also be similar [14] for similarly aged tanks.

The convection and radiation in the vapour space depends on the liquid level and on the action of the PRV. The shape of the vapour space is important. For horizontal, round cylinders, the shape of the vapour space is similar for different scales for similar fill levels. Smaller tanks will have higher convective heat transfer coefficients in the vapour space, which will slightly reduce the wall temperature. Small tanks will have higher fire convection effects, which will tend to increase the wall temperature [13]. Consequently, we expect a small difference in wall temperature from small to large scale, but it should not be significant.

For radiative heat transfer, the vapour space shape is important and, as previously noted, would be the same for the different scales, provided the fill is the same. The surface emissivities must be the same between scales. Emissivity does not vary with scale but depends on materials and surface properties, which are the same between the scales considered here.

Boiling heat transfer effects will change slightly with scale since the vapour bubbles will be the same size for both large and small tank (both have propane)[15] . This will affect liquid swell. This is most important at very high fill levels. Since tanks usually don't fail at very high fill levels, this should not be a significant factor in failure prediction.

The rate of increase of the wall temperature in the vapour space is determined by heat received from the fire, the heat loss by convection and radiation on the inside (backside), and the tank wall heat capacity. In mathematical terms this can be written as (see, for example, Holman [16]):

$$\frac{dT_w}{dt} = \frac{(q_{fire} - q_{back})A}{\rho c A w} \propto \frac{1}{w} \tag{1}$$

where

T_w = wall temperature
t = time
w = wall thickness.
ρ = density of wall material
c = wall specific heat
A = wall area exposed to heating
q = heat flux

Equation 1 shows that the temperature rise rate depends on wall thickness, if the heat flux is similar. The thicker the wall, the slower it heats up. Therefore, the smaller tank will heat up faster and fail faster. This will scale with the wall thickness, which also happens to scale with the tank diameter. This has been seen in numerous tests of small-scale tanks.

The tank stress depends on:

i) tank pressure P
ii) wall thickness t
iii) tank diameter D
iv) tank L/D
v) end types
vi) heating pattern

The nominal hoop stress = PD/2t. For tanks of similar shape with the same t/D and L/D ratio the stress field will be the same for the same heating pattern.

Stress rupture data [17] provides time to failure as a function of nominal tensile stress and sample temperature under constant load conditions. The size of the sample is not a strong factor. This is the basis of tensile testing. Therefore, a 7.1 mm wall should behave the same as a 16 mm wall as far as stress rupture is concerned, provided the stress is the same and there are no large defects in the steel. Therefore, the time to failure for a given stress and temperature should be the same for the different scales.

The size of the failure or rupture will depend on the wall thickness. Therefore, failure length is expected to scale with the wall thickness. For the assumed tanks, this means the failure length scales linearly with tank diameter.

Tank pressurization depends on:

i) fire heat flux
ii) PRV setting and capacity
iii) tank fill

Tanks with higher fill levels pressurize faster because of the small vapour space and large surface area of liquid wetted wall [7].

For the same fill level, the tank initial pressurization rate depends on the temperature rise rate in the liquid boundary layer. This is determined by the ratio of heated surface area covered by liquid to the heated liquid boundary layer volume. It is the heating of the liquid boundary layer that determines pressure inside the tank. The boundary layer volume is determined by the wetted surface area and the boundary layer thickness, δ:

$$\frac{dT_{bl}}{dt} = \frac{qA_w}{\rho c V_{bl}} = \frac{q\pi DL}{\rho c \pi DL\delta} \propto \frac{1}{\delta} \tag{2}$$

The boundary layer thickness δ is a weak function of the tank diameter – it is probably related to $D^{1/4}$ (based on the laminar thin conduction layer model for free convection in an enclosure, see [18]). In other words, if you test with a one-third scale tank, you expect the smaller tank boundary layer to heat up about 31% faster than a full-scale tank. For a near full unprotected tank-car, this means the difference between the PRV popping in 2 minutes for the full scale tank-car [6] versus 1.5 minutes for a tank with one third the diameter. There is a difference, but it is not very significant. Test experience suggests that the difference is even smaller than stated above and is lost in the fire variability.

The heating rate of the bulk liquid depends on the heated surface area and the liquid volume. In mathematical terms this is:

$$\frac{dT_{bulk}}{dt} = \frac{qA_w}{\rho c V_{liq}} = \frac{4q\pi DL}{\rho c \pi D^2 L} \propto \frac{1}{D} \tag{3}$$

As the tank diameter gets bigger, more time is required to heat up the bulk liquid. This has been observed in numerous previous tests.

The final tank pressure is determined by the PRV setting and the PRV capacity. If the PRV is properly sized, the pressure will be limited to about 120% of the PRV setting. In most cases the tank fails some time after the pressure has reached the PRV set pressure. In large unprotected tanks, the pressure will be at the PRV set pressure before the wall heats up to failure conditions. For example, with RAX 201 the PRV opened in 2 minutes and the tank failed in 24 minutes. It is possible that in small tanks the wall will reach dangerous temperatures before the PRV is activated. In thermally protected tanks, both the tank pressure and wall temperature are delayed. However, if there are thermal protection defects, the wall temperature may reach dangerous levels in the defect area before the PRV is activated. We need a computer model to consider all the possibilities.

Considering tanks of similar shape (same L/D ratio) in similar fires with similar material UTS and similar stress (i.e. wall thickness scaled by *D*), the following assumptions should be valid:

i) The rate of wall temperature rise depends on *D* – the bigger the *D*, the longer it takes to heat the wall.
ii) The rate of initial pressurization depends on fill, and only weakly on *D*.
iii) The rate of bulk heating of the liquid depends on *D*.
iv) The failure time depends only on wall *T* (since stress and material are the same), and this depends on initial fill and *D*.

In other words, failure time scales with tank *D* if all other factors are fixed. For severe heating, the failure time is almost linear with *D*. This means that if the diameter is doubled, the failure time should double. We expect failure of an unprotected 112-type tank-car to take about 24 minutes (based on RAX 201). If we test with a one-third scale tank under similar conditions, we expect it to fail in approximately 8 minutes. For less intense heating, the failure time is dictated by stress-rupture considerations.

2.3 Scaling of Critical Defect Size

Consider a square defect with side dimensions *S* x *S* on a plate with thickness *w* under the defect. From a conduction heat-transfer standpoint, the defect heat transfer depends on the thermal properties of the steel and the plate dimensions *S* and *w*.

Consider the case of the same fire heat flux (i.e. same fire blackbody *T*). The rate of temperature rise of the plate is a function of the (heat input)/(plate mass), which relates to $S^2/(S^2w)$ or just $1/w$. Since the tank wall, *w*, depends on the tank diameter, *D*, we can say that the defect temperature rise rate depends on the tank *D*. The larger the tank, the slower the defect heats up.

The temperature gradients in the defect area also depend on *S* and *w*. If one has the same S/w ratio, then you get the same temperature distribution over the defect area. This assumes the backside heat transfer is the same. This is not exactly true for small and large scale, but it is close.

The local stress field in the bulging steel plate is a function of the heated length *S* and wall thickness *w* [19]. The bulge geometry will be similar as long as the temperature and stress fields are similar, and this will be true if the ratio S/w is the same. Therefore, we must scale the critical defect length for failure based on the wall thickness, *w*. In other words, the critical defect length for the 112J tank-car = (*w* for tank-car)/(*w* for small-scale tank) x critical defect length for the small-scale tank.

2.4 Non-Ideal Scaling

Perfect scaling is usually not achieved in real-world testing. This section shows that our scale model tests had some scaling differences with the 112J tank-car. These include:

i) material UTS
ii) tank L/D ratio
iii) tank t/D ratio
iv) hemi heads vs. elliptical heads
v) nominal PRV pressure setting and flow capacity
vi) tank initial fill

The fire conditions were also probably not exact.

Material UTS can be accounted for in the stress-rupture analysis. The different PRV set pressure is also accounted for in any hoop stress calculation. The tank w/D ratio is also accounted for in the stress analysis. The PRV flow capacity does not matter much as long as the PRV can maintain the pressure near the set pressure. As long as the PRV is oversized, it will either sit partially open or it will cycle open and closed between its pop and re-close pressure.

The different tank ends mean the stress will be different in the end regions. However, end region failure is not of significant interest here and therefore end type is not important.

The different L/D ratio means the cylinder stress field will be more affected by end effects. However, in the middle of the tank these end effects will be small.

For heat transfer, the L/D ratio is important because for the same defect length to wall thickness ratio S/w, the defect will take up a smaller fraction of the total tank surface area on a tank with a larger L/D ratio. This means the defect will see more cool wall, resulting in slightly reduced wall *T* in the defect. Again, this can be accounted for in a good thermal model.

Tank fill level is important. Tank-cars can be filled to 95% or more. Normal propane storage tanks are usually filled to about 80%. A fire-engulfed tank-car is more likely to go liquid full and this can delay failure. The full-scale propane railway tank test by BAM in Germany [20] showed a 22% full tank would fail in about 17 minutes when engulfed in fire. The full-scale test RAX 201 [6] with a 94% fill failed in 24 minutes in an engulfing fire. Both failed at about the same peak vapour space wall temperature and tank pressure. The RAX 201 tank failed when it was about 40-50% full. The extra initial fill (95% vs 22%) in the RAX 201 test delayed failure by 7 minutes.

This means some adjustments need to be done to compensate for these differences. These adjustments can be made with our thermal model of the tank. If the model is properly validated and if it accounts properly for the physics of the problem, the predictions will be reasonable. The model predictions are not expected to be perfect or exact. There will always be some uncertainty in the analysis and therefore one should try to be conservative when generating estimates.

3.0 Approach

The effect of thermal protection defects on a tank's response to a fire was studied experimentally during the summer of 2004. Testing involved exposing six instrumented ASME code 500-gal. propane tanks to controlled fire conditions. Two of the tanks were baseline-unprotected tanks so the tank behaviour could be compared to the full-scale unprotected tank test of RAX 201. The remaining four tests considered defects covering 8 and 16% of the tank surface area. A number of burner development and water tank tests were conducted in preparation for the propane tank tests. A general description of the propane tank field trials is presented in this chapter. More detail, including information on the preliminary testing is presented in the various appendices to this report.

3.1 Experimental Design

In this test series, 500-gal. tanks were used as approximate one-third scale models for 33,000-gal. tank cars. The testing required some adjustments to the 500-gal. tank and the fire conditions to ensure proper scaling or controllable test conditions. These adjustments included the following:

i) Engulfing fire replaced with 25% partially engulfing.
ii) Pool fire replaced with array of liquid propane burners.
iii) Mechanical PRV replaced with computer controlled valve.
iv) PRV set pressure increased to give same stress/strength condition.
v) Initial fill reduced.

The fire was designed to represent a full-scale pool fire with an effective blackbody temperature in the range of 871 ±56°C.

The plan was to have similar stress and wall strength conditions in the tanks so that scaled failure times would be similar. It is known from the RAX 201 test that the unprotected 112J type tank will fail when the tank wall reaches about 650°C. The 500-gal. tank steel is slightly weaker than tank-car steel (480 vs. 550 MPa minimum ultimate tensile strength) and the 500-gal. tank has a larger tank wall thickness-to-diameter ratio than the tank-car, $w/D = 0.0071/0.96$ vs. $0.016/3.0$. For this reason, the PRV setting on the 500-gal. tank had to be adjusted upward so that the tank would fail with a wall temperature around 650°C like in the tank-car. The same stress condition was achieved by increasing PRV set pressure on the 500-gal. tank to 381 (pop) psig. Table 3.1 summarizes how the PRV was set.

The tests were conducted with about 25% fire engulfment. This condition gives vapour space peak wall temperatures similar (but slightly lower) to 100% engulfment. However, the tank will pressurize and empty through the PRV about four times slower (i.e., one quarter the total heat input). This means the tanks with 25% fire should fail a little later (order of 1 minute later) than if they were 100% engulfed.

Table 3.1: Comparison between the 500-gallon tank and 112J tank-car

	Nominal 500 gal.	**500 gal. as per test**	**112J Tank-Car 33,000 US gal.**
D (m)	0.95	0.95	3.0
t (mm)	7.1	7.1	16
Nominal fill by volume	80%	70-80%	95%
P set (MPa) range	1.72 (250 psi) 1.72 – 1.89	2.44 (354 psi) 2.44 – 2.68	1.93 (280 psi) 1.93-2.12
Hoop stress at Pset (MPa)	116	165	181
σ_{ult}			
at 20°C	505	505	550
at 650°C	155	155	170
FOS at 650°C and PRV set based on hoop stress	1.23-1.35	0.85-0.94	0.85-0.94

The fill level in these tests was lower than in the 112J type tank. This was done because the computer-controlled PRV could not tolerate the tank going liquid full. With a fill level of 95% it is expected that the thermally protected tank will go liquid full before the PRV is popped by vapour pressure. The higher fill level in the tank-car is known to delay failure (compare RAX 201 [6] to BAM fire test [20]). Table 3.2 compares results from two full-scale tank tests where the main difference in failure was due to initial fill level.

As can be seen from the table, the reduced-fill tank failed 7 minutes earlier than the 95% full tank. This suggests that the higher fill case delayed failure due to wall cooling by the high fill level. Therefore, the same effect is expected to be true for our testing. This can be adjusted later using the tank thermal model.

Table 3.2: Comparison of full-scale fire tests

Condition	**RAX 201 Full-Scale Tank-Car Test [6]**	**BAM Full-Scale Test [20]**
Fire	Engulfing hydrocarbon pool fire	Engulfing hydrocarbon pool fire
Tank D	3 m	2.9 m
Wall Thickness	16 mm	14.5 mm
Material UTS	550-620 MPa	550-660 MPa
Volume	125 m^3	45 m^3
Initial Fill	94%	22%
Fail Time	24 min	17 min
P at failure	2.4 MPa	2.45 MPa
Wall T at Failure	645°C	650°C
Fill at Failure	40-50%	25-30%

Scale considerations predict the following:

i) The 500-gal. tank will fail in about one third the time of the RAX 201 test if the tank scaling and fire conditions are correct (500-gal. tank should fail in 8 minutes vs. 24 minutes for RAX 201).

ii) The reduced fill condition in the baseline 500-gal. tank could cause early failure by about 1-2 minutes.

iii) The tank will pressurize in about the same time the full-scale tank pressurizes; however, because there is only 25% fire engulfment, the PRV will pop about 4 times later than for the case of 100% engulfment. This means the tank is expected to pop its PRV in about 8 minutes.

Insulation defects of 8 and 16% of the tank surface area were tested. Baseline tests were conducted where no insulation and no jacket were used. Table 3.3 shows a summary of the test matrix.

The effect of reduced hoop stress on tank survivability was examined in a single test, where the PRV was set to open at a gauge pressure of 2.12 MPa (308 psi) and close at 1.93 MPa (280 psi) (blowdown of 9%). Since failure is dominated by the high wall temperature, a small reduction in stress should only add a few minutes to the time of failure.

Table 3.3: Test matrix

Test No.	Settings	Purpose
04-01 04-06	No insulation or steel jacket	Baseline test for tank model and fire condition validation
04-02 04-03	Large defect (16% of tank surface)	Defect size effect on survivability
04-04	Large defect, reduced hoop stress	Hoop stress effect on survivability
04-05	Small defect (8% of tank surface)	Defect size effect on survivability

3.2 Test Layout

The physical test layout followed the same basic design used during 500-gal. tank tests conducted in the summers of 2000, 2001 and 2002 [21]. The main difference was the type and number of burners used to simulate the engulfing fire, and the modelled thermal protection system.

3.2.1 Test Site

The Munitions Experimental Test Centre (METC) at the Defence R&D Canada site at Valcartier, Quebec, was chosen as the location of the field trials. This location was ideal for the testing because of its 800 m x 600 m test plateau.

The tanks and burner stands were placed on a concrete pad in the centre of the plateau. Approximately 35 m from the concrete pad was an instrument bunker located behind a 0.61 m thick concrete block wall. The instrument bunker contained the main data acquisition equipment, high-speed and regular video cameras, computers, and other related equipment.

As in previous tests, the mechanical PRV was removed and replaced with a computer-controlled fast opening ball valve. This was done to eliminate the variability of real PRVs [22] from the test. The computer-controlled PRV and nozzle were located at the end of the tank behind a protected concrete block wall.

Again, as in previous tests, a pool fire was not used because these types of fires are very difficult to control. We needed to have test-to-test repeatability of fire conditions. To do this, we used an array of liquid propane burners. These burners are not perfect but they are more consistent than a pool fire. The propane burner supply tank was located approximately 50 m from the test tank and was protected by a concrete wall.

A remote bunker was used for controlling and observing the tests and was located approximately 370 m from the tank. This ensured that personnel were a safe distance from thermal radiation and blast hazards, and greatly reduced the risk of projectile hazards. The general layout of the test site can be seen in Figure 3.1.

3.2.2 Test Tanks

Standard ASME code 1890 L (500 US gal.) steel LPG storage tanks were used for the field-testing. The tanks were designed and manufactured according to ASME Pressure Vessel Code (for LPG service). The test tanks were horizontal steel cylinders with one longitudinal weld at the bottom of the tank and hemispherical end caps. A sketch of a test tank can be seen in Figure 3.2. The design gauge pressure for the test tanks at 46°C was 1.72 MPa (250 psig). A minimum wall thickness was specified for all of the test tanks, as indicated in the figure. Table 3.4 shows more test tank specifications. The burst pressure $\left[P_{burst} = \frac{2 \cdot \sigma_{ult} \cdot t}{D}\right]$ in Table 3.4 is calculated using an ultimate strength of 480 MPa at 46°C for SA-455 ASME Steel.

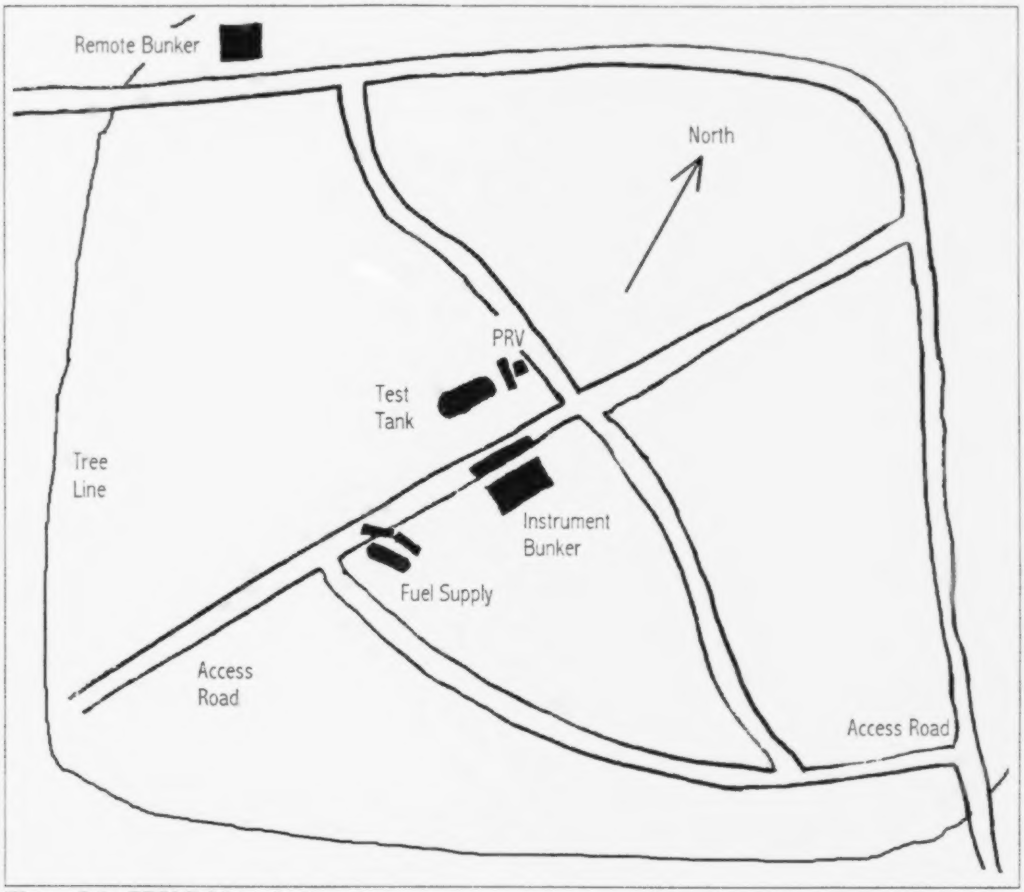
Remote Bunker
North
PRV
Test Tank
Tree Line
Instrument Bunker
Fuel Supply
Access Road
Access Road

Figure 3.1: PRV field trials site map

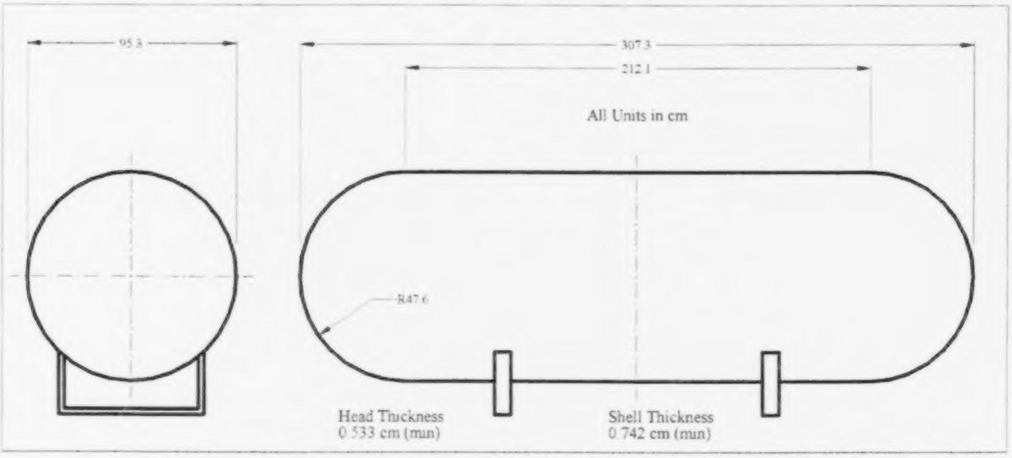
95.3
307.3
212.1
All Units in cm
R47.6
Head Thickness 0.533 cm (min)
Shell Thickness 0.742 cm (min)

Figure 3.2: Standard ASME 1890 L test tank (from manufacturer's drawing)

Table 3.4: Test Tank Specifications

Specification	Property
Capacity	1890 L
Length	3.07 m (end to end)
Diameter	0.953 m
Minimum Wall Thickness-Shell	7.1 mm
Minimum Wall Thickness-Head	5.3 mm
Material-Shell	SA-455 ASME Steel
Material-Head	SA-414 gr.C ASME Steel
Design Pressure	1.72 MPa at 46°C
Calculated Burst Pressure	7.1 MPa at 46°C

In this test program, we are using the 500-gal. tank as a model of a 33,000-gal. 112J type tank-car. Table 3.5 gives a comparison of these two tanks. The 500-gal. tank has hemi heads versus the elliptical head of the 112J tank. This end effect should have little impact on the time to tank failure since the failure occurs in the cylinder section where the defects are located. End failures have not been studied here. There are differences in the PRV set pressure, material UTS, etc. These differences are described in more detail in Chapter 4.

Table 3.5: Comparison of 112J tank and 500-gallon ASME code propane tank

	500-gallon tank	**112J tank**
Description	horizontal cylinder	horizontal cylinder
Heads	hemi	2:1 elliptical
Diameter D	0.96 m	3.05 m
L/D	3	6
Wall thickness (cylinder)	7.1 mm	16 mm
PRV setting	1.72 MPa	1.93 MPa
PRV capacity	2600 scfm	33000 scfm
Material	SA 455	TC 128
Minimum UTS at 20°C	480 MPa	550 MPa

Modifications were necessary to accommodate five bundles of thermocouples and two pressure transducers to be attached to the tank from below. Seven ¾ in. NPT couplings were welded onto the bottom of the tank for this instrumentation. In addition to the instrumentation couplings, a 2 in. pipe coupling at the top of the tank was required for the pressure relief piping.

The tank cylinders were made from SA 455 carbon steel with minimum UTS of 480 MPa. The mill test report showed actual UTS near 610 MPa, almost 30% greater than required. This is nearly identical to typical TC 128 steel (TC 128 minimum UTS = 550 MPa.).

Additionally, the tanks were covered to different degrees with thermal blanket insulation in most of the tests (no insulation was used on baseline tests). This insulation was itself covered with a 3 mm steel jacket in the flame impingement zone. Specifications of the insulation and steel jacket are given in Tables 3.6 and 3.7. Note that the thermal conductivity of the insulation is a function of temperature. At high temperature the thermal conductivity increases rapidly. Also, note that the thermal conductivities shown depend on the blanket density, which will increase if the blanket is crushed. These tests were conducted with a blanket in like-new condition.

Table 3.6: Insulation and jacket specifications

Property	**Insulation**	**Steel Jacket**
Material	"Tank Car Scroll" Ceramic Fibre Blanket	Carbon Steel
Width	1.2 m	
Thickness	13 mm	3 mm

Table 3.7: Summary of ceramic fibre insulation properties (Unifrax, tank-car insulation, 72 kg/m^3 density, new condition)

Temperature (°C)	**thermal conductivity k (W/mK)**	**Comment**
-20	0.03	
100	0.05	liquid wetted wall temperature
300	0.09	
500	0.15	protected vapour space wall temperature
650	0.20	
800	0.30	jacket temperature in engulfing fire

3.2.3 Burners

Fire testing of this type is often carried out using liquid hydrocarbon-fuelled pool fires. This type of fire is very difficult to control, since even slight winds can greatly affect the fire's behaviour. A pool fire also poses additional complications to the data acquisition process. For these reasons, an array of burners was developed to simulate a partially engulfing pool fire.

The objective of the burner system design was to:

- simulate an engulfing pool fire with an estimated blackbody temperature in the range of 871 ± 56°C (Canadian General Standards Board standard CAN/CGSB 43.147-2002)
- deliver the heat in a uniform, repeatable way from test to test

A 5 x 5 array of propane torches and a liquid propane evaporator, shown in Figure 3.3, was designed from simple modified pipe fittings. It was developed and tested to simulate conditions from a credible pool fire. Note the luminous flame, as is characteristic of pool fires.

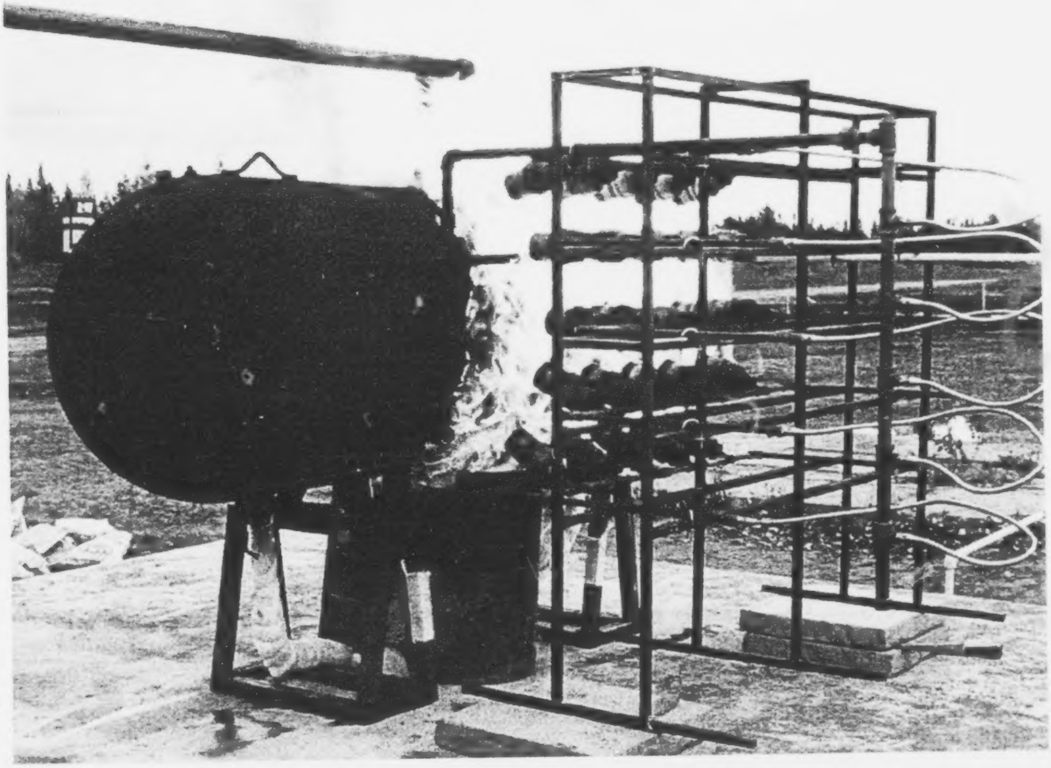

Figure 3.3: Burner array and evaporator set-up

Figures 3.4 and 3.5 show the relative position and size of the tank, insulation, steel jacket, and burner system. Liquid propane was supplied to the evaporator at approximately 205 kPa (30 psi). The burner array was positioned to engulf both the liquid space and the vapour space.

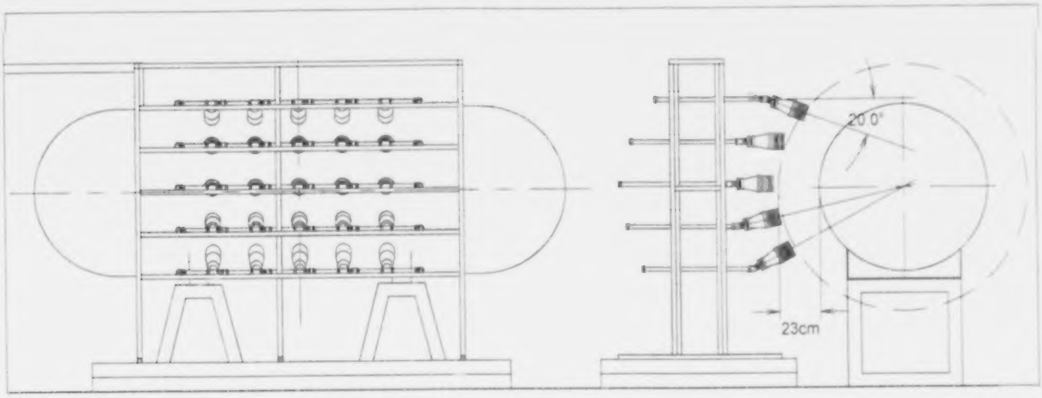

Figure 3.4: Burner array configuration

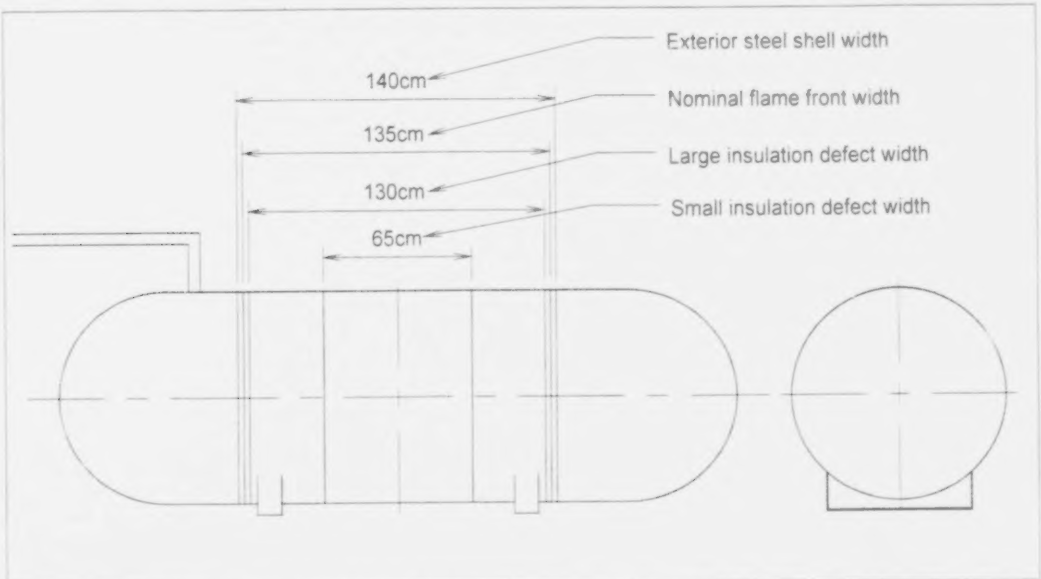
Exterior steel shell width
Nominal flame front width
Large insulation defect width
Small insulation defect width
140cm
135cm
130cm
65cm

Figure 3.5: Nominal flame width and location relative to tank insulation defects and steel jacket

The burner system was developed and tested in the laboratory before fieldwork was started. Some test results from the burner development work appear in Appendix J.

3.2.4 Pressure Relief System

To ensure repeatable test results, it was vital to have good control over the tank pressure regulation. Previously conducted fire tests [23] showed that small to medium sized PRVs can have highly variable performance. Since repeatable pressure control was not possible with commercial PRVs, the original PRV was removed and replaced with a computer-controlled high-speed ball valve. This required bringing a pipeline off the top (vapour space) of the tank and using a fast-acting valve to control flow out of the tank. An instrumented flow nozzle was used on the outlet side of the valve. Because of the potential for large explosions and the expense of the valves and nozzle, the pipeline was routed behind a concrete wall. A sketch of the layout can be seen in Figure 3.8.

3.2.4.1 Original Pressure Relief Valve

It was important for the pressure relief system to mimic the original PRV while maintaining complete control over the valve operation. Figure 3.6 shows a photo of one of the original PRVs that would have been installed on the test tanks.

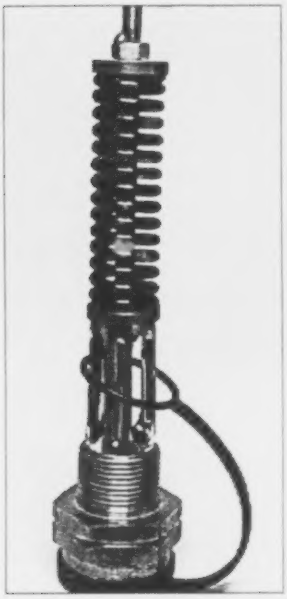

Figure 3.6: Original tank PRV (250 psig, 1 in. diameter, 2565 scfm)

Some of the specifications of this valve are below:

- Set Pressure = 250 psig (1.72 MPag)
- Size = 1 in. (25.4 mm) NPT
- Flow Capacity = 2565 standard cubic feet per minute (1.21 m^3/s) of air at 20% overpressure (300 psig or 2.07 MPag).
- Liquefied Petroleum Gas Safety Relief Valve
- Stamped by the Underwriters' Laboratories Inc. (ULC/ORD-C132-1992)
  - -Set pressure tolerance is 0 to 10% on first opening (first opening is defined as start-to-discharge pressure)
  - -Valve must pop fully open by 120% pressure in order to give full capacity flow
  - -Resealing must occur by at least 90% of start-to-discharge pressure
  - -Subsequent openings must be greater than 85% of initial start-to-discharge pressure
  - -Subsequent resealing must occur by at least 80% of start-to-discharge pressure

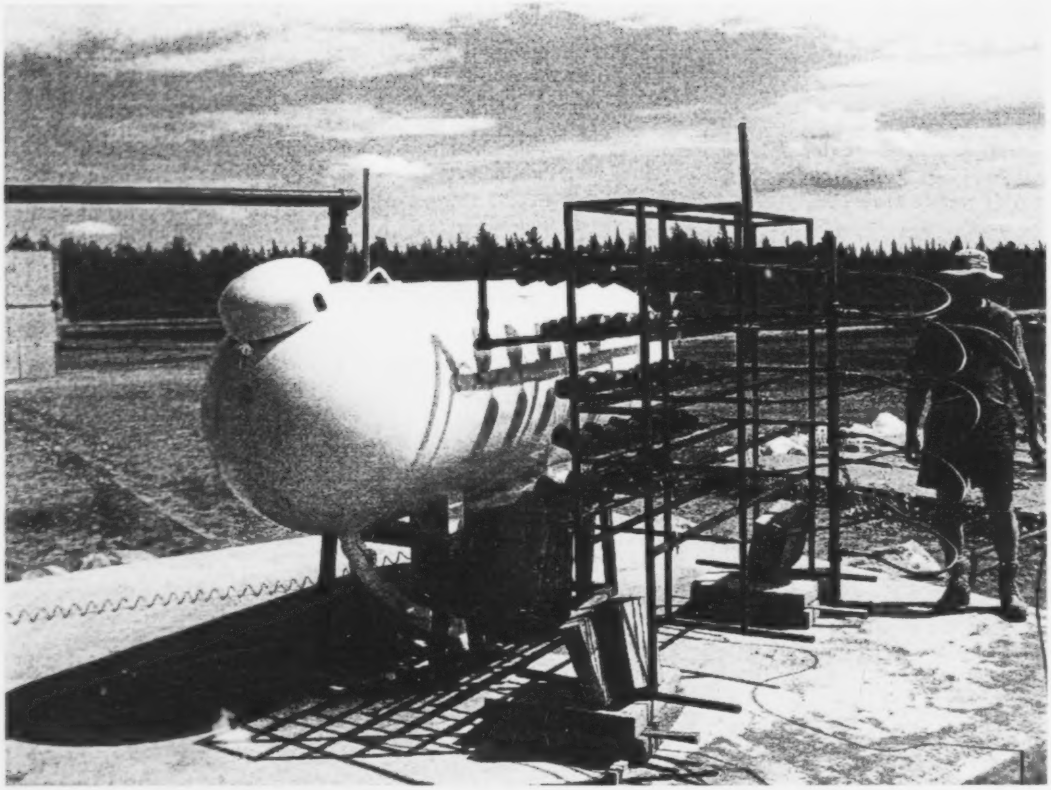

Figure 3.7: Tank 04-01 with burners in place

3.2.4.2 Computer-Controlled Pressure Relief Valve

A rapid acting valve was required to keep up with the changing pressure. The valve used was a normally closed, full port ball valve with a pneumatic, double acting actuator and a 110 VAC solenoid.

The control system used a pressure signal from a pressure transducer located on the bottom of the tank, as indicated by P1 in Figure 3.8. A second pressure transducer, P2, was placed in the piping between the tank and the valve. The reading from this transducer was used as a redundant measurement of tank pressure when there was no flow through the PRV piping. When the computer-controlled valve was open or cycling, the second pressure reading provided information on the response of the system and pressure losses through the piping. Figure 3.9 shows the computer-controlled PRV. A third pressure transducer, P3, was placed at the exit nozzle, Figure 3.8. This was used primarily for determining the mass flow through the nozzle, but also provided information on losses through piping.

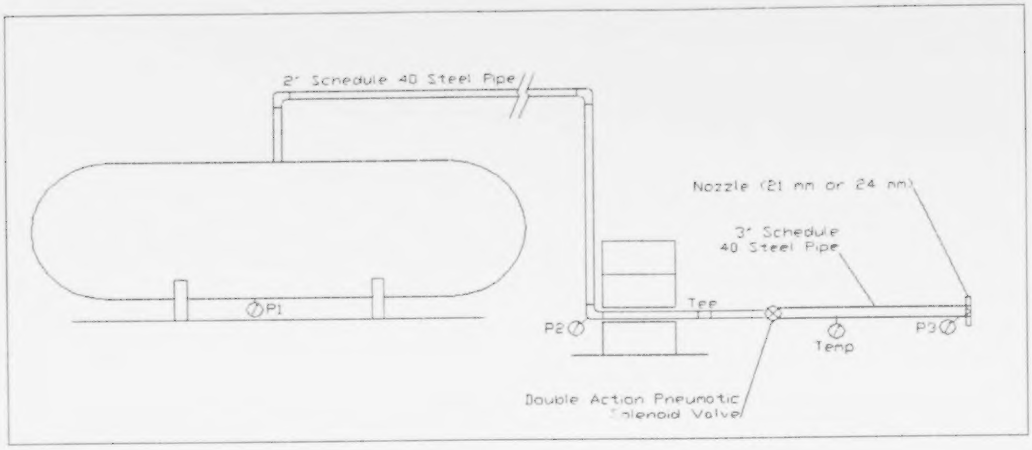
2" Schedule 40 Steel Pipe
Nozzle (21 mm or 24 mm)
3" Schedule 40 Steel Pipe
P1
P2
Tee
Temp
P3
Double Action Pneumotic Solenoid Valve

Figure 3.8: PRV, PRV piping, and nozzle sketch

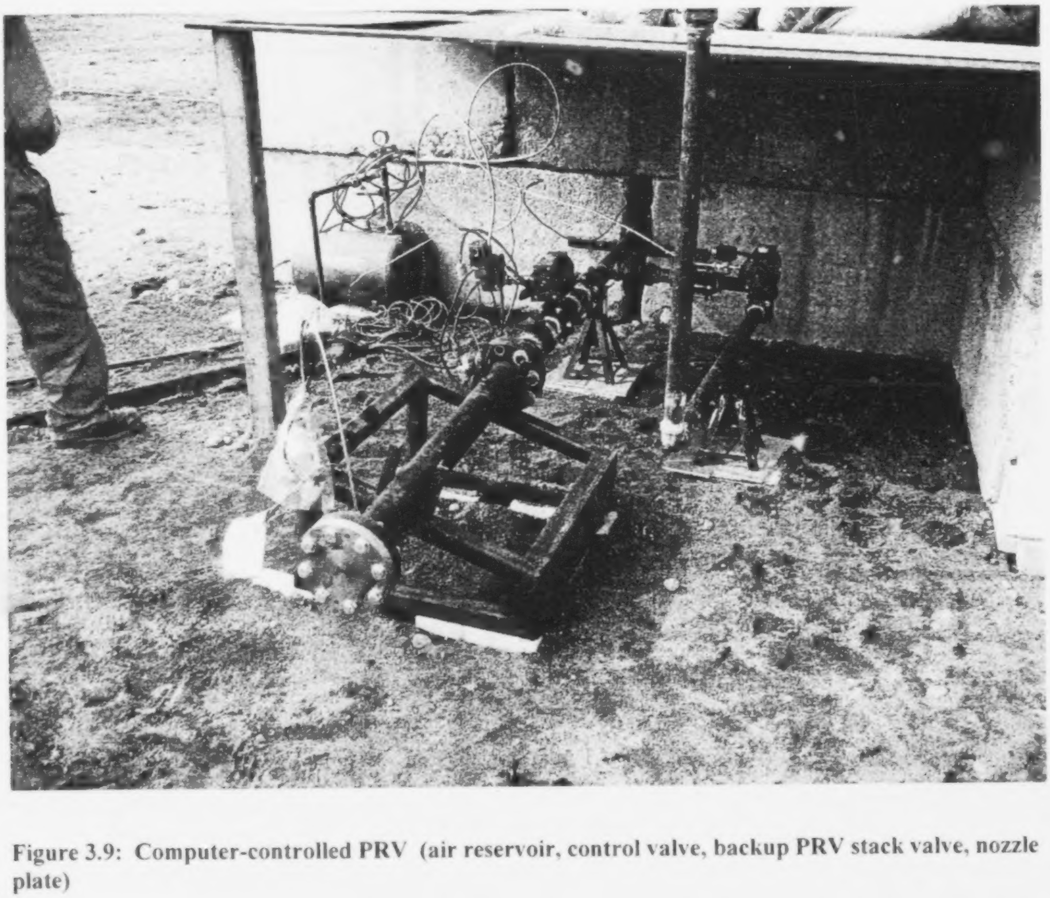

Figure 3.9: Computer-controlled PRV (air reservoir, control valve, backup PRV stack valve, nozzle plate)

The field tests required the PRV to open when the tank pressure reached a set pressure and to close again when the pressure dropped to a second, lower, set pressure. In five of the six tests, the simulated PRV was set to open at a gauge pressure of 2.63 MPa (381 psi) and close at 2.39 MPa (346 psi), a blowdown of 9%. The 500-gal. tank steel was supposed to be slightly weaker than the tank car steel (480 MPa ultimate vs. 550 MPa) and the 500-gal. tank had a larger tank wall thickness-to-diameter ratio than the tank-car – i.e., 0.0071/0.96 vs. 0.016/3.0. The same stress condition was achieved by increasing the PRV set pressure on the 500-gal. tank to 381 (pop) psig.

The effect of reduced hoop stress on tank survivability was examined in a single test. The PRV was set to open at a gauge pressure of 2.12 MPa (308 psi) and close at 1.93 MPa (280 psi) (a blowdown of 9%).

3.2.4.3 PRV Flow Capacity

The PRV piping and metered nozzle were designed to control the pressure in the tank and also to be easily controlled by the computer. An oversized valve could cause the pressure to drop very rapidly and would require very rapid pressure sampling by the computer. If the computer was not fast enough, the oversized valve could result in the pressure dropping too far before the PRV is closed.

The nozzle used at the end of the pressure relief piping was designed for choked flow, just like an actual PRV. A smooth converging nozzle with a diameter of 15 mm was used in all the tests. This size nozzle gives a flow capacity of about 1500 scfm air at 2.07 MPa. This is more than adequate to control the tank pressure with the fire conditions (25% engulfing) and thermal protection used in this testing. Figure 3.10 shows the flow nozzle operating with steam flow.

Refer to Appendix C for more details of the pressure relief system.

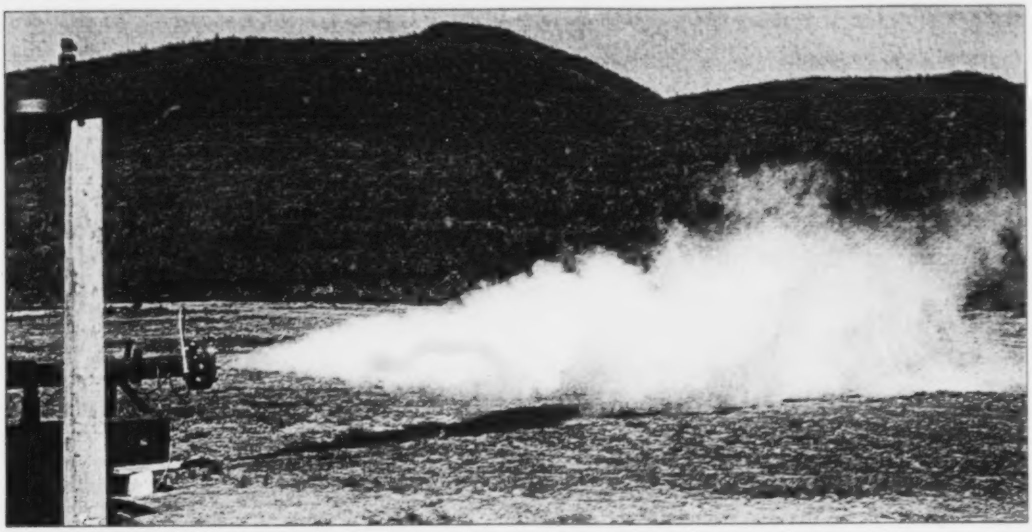

Figure 3.10: PRV nozzle operating with steam flow

3.3 Instrumentation and Control

3.3.1 Instrumentation

Each test tank was instrumented with 48 sheathed lading thermocouples, one static pressure transducer, and from 11 to 17 wall thermocouples (Table 3.8). The lading thermocouples were contained in five vertical bundles, with each bundle containing a full range of thermocouple lengths.

Table 3.8: DAQ instrumentation list

Measurement	Device	Quantity
Lading Temperature	Type K Thermocouple (3.175 mm, stainless steel, sheathed)	48
Tank Wall Temperature	Type K Thermocouple (24 gauge, unsheathed)	11 -- 17
Tank Pressure	3.45 MPa (500 psi) Pressure Transducer	1
PRV Pipe Pressure	3.45 MPa (500 psi) Pressure Transducer	1
PRV Nozzle Pressure	3.45 MPa (500 psi) Pressure Transducer	1
PRV Nozzle Temperature	Type K Thermocouple (3.175 mm, stainless steel, sheathed)	1

Figure 3.11 shows a sketch of the location of the lading thermocouples. The centre bundle (Bundle 1) was located at the tank mid plane in the centre. Bundles 2 and 3 were

located at the two ends of the tank. Bundles 4 and 5 were located in the mid plane of the tank on either side of Bundle 1.

The large number of thermocouples was used in the lading in order to better understand the temperature gradients and thermal stratification. Each thermocouple represents a specific fill level, as shown in Table 3.9 for Bundle 1. See Appendix B for more information on thermocouple locations.

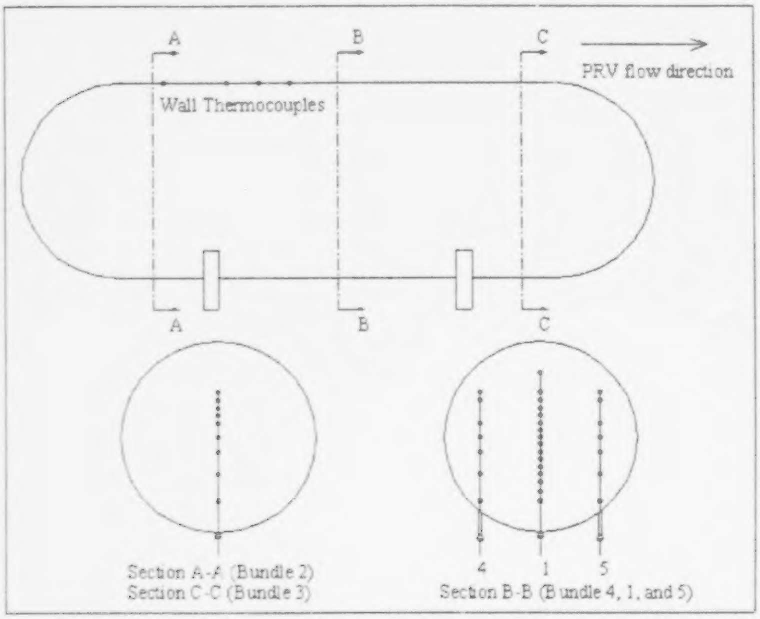
A
B
C
PRV flow direction
Wall Thermocouples
A
B
C
Section A-A (Bundle 2)
Section C-C (Bundle 3)
4
1
5
Section B-B (Bundle 4, 1, and 5)

Figure 3.11: Lading thermocouple locations

Table 3.9: Thermocouple locations (bundle 1)

Thermocouple	% Fill	Location
T0	90	Highest
T1	80	
T2	75	
T3	70	
T4	65	
T5	60	
T6	55	
T7	50	
T8	45	
T9	40	
T10	35	
T11	30	
T12	25	
T13	20	
T14	15	
T15	10	Lowest

The tank wall in the vapour space was instrumented with 11 to 17 unsheathed thermocouples, typically located as shown in Figure 3.12. The wall thermocouples were spot welded directly to the wall of the tank using the fabrication procedure presented in Appendix I.

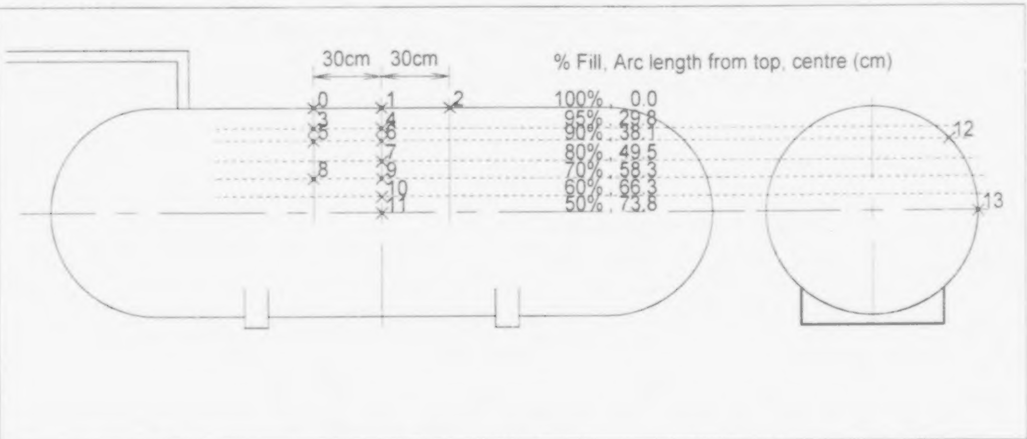
30cm
30cm
% Fill, Arc length from top, centre (cm)
0
1
2
3
4
5
6
7
8
9
10
11
12
13
100% , 0.0
95% , 29.8
90% , 38.1
80% , 49.5
70% , 58.3
60% , 66.3
50% , 73.8

Figure 3.12: Wall thermocouple layout for Test 04-6

Still photography, video, and high-speed video (500 frames/second) were also used to collect data during the fire tests. Three camera shacks were located at various points around the tank, each with an SLR still camera and a video camera. A video camera and the high-speed camera were in the instrument bunker, viewing the event through a 13 mm thick piece of plexiglass. Still cameras and a video camera were also located at the remote bunker, 370 m from the test tank, along with a high powered, 30x telescope for the test personnel to use during the tests.

3.3.2 Data Acquisition System and Control

A PC-based data acquisition system was used for the low frequency measurement recording and for all process control. The data acquisition card was a Sciemetric System 200 with 96 input channels, a solid-state relay module, and a digital input/output board. All static pressure and temperature measurements were digitally recorded using the Sciemetric System. The pressure transducers and the thermocouple in the nozzle were sampled at a rate of 10 Hz, while all other thermocouples were sampled once per second.

The Sciemetric System was controlled using LABVIEW programmed logic and was used to accomplish the following control tasks, in addition to recording the temperature and pressure measurements:

- Control a shut-off valve for the propane burner's fuel supply.
- Control pneumatically operated valves used for the tank pressure relief. During the tests, the control system used the pressure signal from the pressure transducer on the tank to determine when to open and close the main PRV.
- Digitally record when the PRV was open and when it was closed. Using this information and the recorded nozzle temperature and pressure, the PRV mass flow rate could be calculated.

Necessary hardware for data acquisition and control was located in the instrument bunker (see Figure 3.1). The entire system was controlled remotely from the safety bunker over a fibre-optic network link using PC-Anywhere software (Symantec).

In case of a loss of power and control, a normally open, pneumatic valve was placed off the tee shown in Figures 3.8 and 3.9. On the other side of the valve, a standard 1.72 MPa (250 psig) PRV was located. During testing, the normally open valve was energized so no fluid would flow through the conventional PRV, but if power was lost, the pneumatic valve would open and the conventional PRV would be available to control the tank pressure.

In addition to the computer control, the system has a manual backup control, which can do the following:

i) open the computer-controlled PRV
ii) shut off propane fuel
iii) trigger the still cameras

Appendix H gives more information on the data acquisition software.

3.4 Test Procedure

The following procedure was used for each of the six propane tests:

- The tank, burner stands, and required number of burners were positioned.
- Instrumentation was installed and cables were protected with ceramic insulation wherever possible.
- In all but the baseline tests, the tank was covered in ceramic insulation and then covered with a steel jacket in the area where the fire made direct contact.
- The tank was pressure tested for leaks using air from an air compressor at 689 kPag (100 psig).
- The air was vented through the converging nozzle by opening the pneumatic powered PRV.
- The tank was purged of air and then filled to 70-80% capacity with commercial propane.
- The air compressor, receiver, and lines were charged to 689 kPag (100 psig) for the main solenoid valve.
- The burner fuel lines were pressurized to 276 kPag (30 psig).
- The data acquisition system and recorders and cameras were powered up.
- Test conditions (i.e., blowdown) were programmed into control logic. A PRV opening pressure of 2.63 MPag (381 psig) was used in all but one test.
- Video cameras and high-speed video were started.
- Personnel were moved to the remote bunker.
- Data recording on the Sciemetric System was initiated.
- Flares were ignited near the exit of the PRV nozzle so that releases would be ignited.
- Burner fuel flow was started.
- The propane burners were manually ignited.
- Still cameras were triggered when tank failure began (once tank started to open).
- After tank failure, the burner fuel was shut down, and video cameras and data recording were stopped.
- Data was recorded until the tank failed.

Appendix G gives some checklists that were used in the field. These checklists give more information about the test sequence.

4.0 Results and Analysis

This chapter presents the results of the testing. Appendix E contains a more comprehensive compilation of test data plots and figures.

4.1 Overview

The test program started with final calibration of the fire burner system. This was followed by the propane tests. The basic test progress was as follows:

i) Water tests for fire calibration
ii) Test 04-01 baseline (late failure due to wind change)
iii) Test 04-02 16% defect (test aborted due to burner system problem)
iv) Test 04-W5 water test (to reset burners using tank from 04-02)
v) Test 04-03 16% defect repeat
vi) Test 04-04 16% defect, reduced pressure
vii) Test 04-05 8% defect
viii) Test 04-06 baseline repeat

The baseline unprotected tank with a consistent fire failed in about 8 minutes. If scaled by the tank diameter, this would predict a failure time of 24 minutes for the full-scale tank. This is in good agreement with the RAX 201 test. This suggests the fire condition and the tank scaling were appropriate.

The tanks with thermal protection defects of 8 and 16% failed in about 36 and 24 minutes, respectively. This is with adjustment for periods of poor fire engulfment. If these are scaled for the full-size tank, the failure times would be 109 and 72 minutes, respectively. These then need to be adjusted for the different tank fills (70% for 500 gal., 95% for the 112J tank) and the different tank shapes and sizes. This will be done using the validated thermal model [24].

4.2 Fire Condition

Fire tests on 500-gal. tanks containing water were conducted as a final calibration check of the burner system. Burners were to deliver a flame that was equivalent to an engulfing fire with an effective blackbody temperature of 871 ±56°C.

The burner fuel pressure necessary to achieve the desired fire intensity was 30 psig. This was determined from Water Tests 1 and 2, where the pressure was 20 and 40 psig, respectively. Twenty-five burners were set about 9-10 in. from the tank surface, angled as depicted in Figure 4.1.

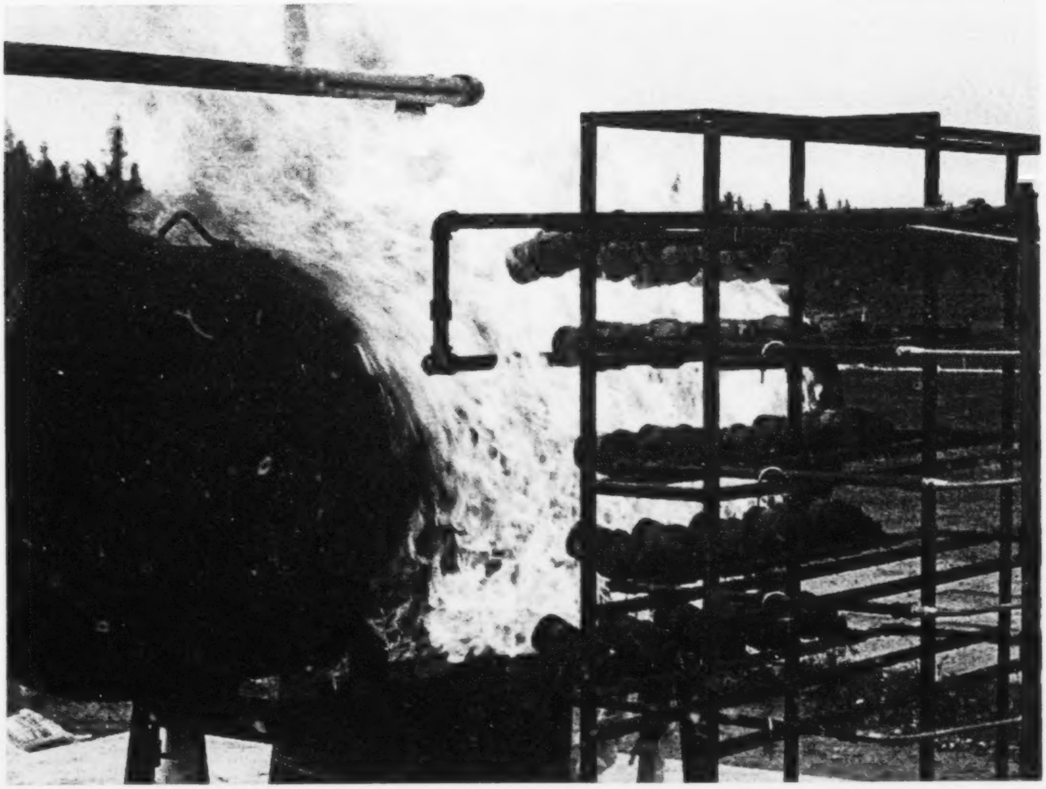

Figure 4.1: Burner system in operation (note luminous pool fire-like flame, and flame wrapping around tank with wind from right to left (northwest wind))

Burner flames were sooty and luminous, and produced a flame that looked very much like a hydrocarbon pool fire. The effective blackbody temperature was estimated to be in the range of 800-900°C. See Appendix A for details.

Flame contact was excellent when the wind was W or WNW (Figure 4.1). Contact was poor when wind was from the east. Prevailing winds at the test site are from the west; therefore, it was decided to attempt to conduct tests with west winds only.

It should be noted that the fire system used here had a fire buildup time of about 2 minutes. Once it reached steady conditions, the fire remained constant except for wind effects. It has been noted in various pool fire tests (see for example [7]) that pool fire intensity tends to drop with time. This was not modelled here since it is not clear what causes this effect (in some tests it is probably a fuel delivery problem).

Figure 4.2 shows the wall thermocouple layout used in Water Tank Test 04-W4, while Figure 4.3 shows the wall temperature results. During time spans (0 to 200 and 1200 to 1800 seconds) where the wind was < 10 km/h and from an optimal direction (W to WNW), vapour space wall thermocouples show nearly the same temperature reading.

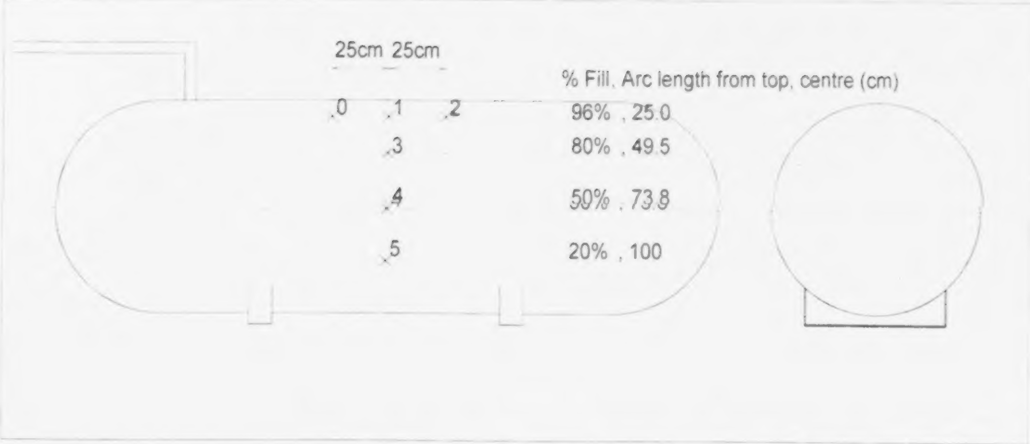
25cm 25cm
% Fill, Arc length from top, centre (cm)
0
1
2
3
4
5
96% , 25.0
80% , 49.5
50% , 73.8
20% , 100

Figure 4.2: Wall thermocouple layout for Water Tank Test 04-W4

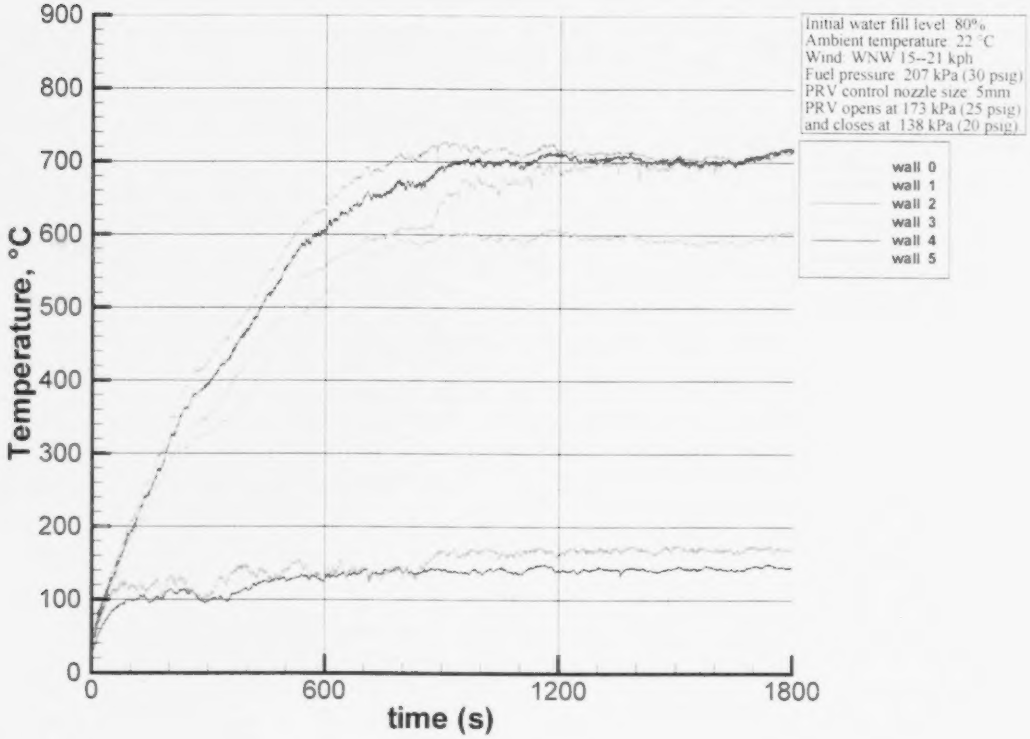

Figure 4.3: Wall temperature, Test 04-W4 (water tank test, no shell/insulation, 80% fill)

When the wind was strong or from an undesirable direction, wall temperatures diverged from each other. This effect can be used as an indicator of the test quality.

Figure 4.4 shows how the wind affected the fire contact on the tank top.

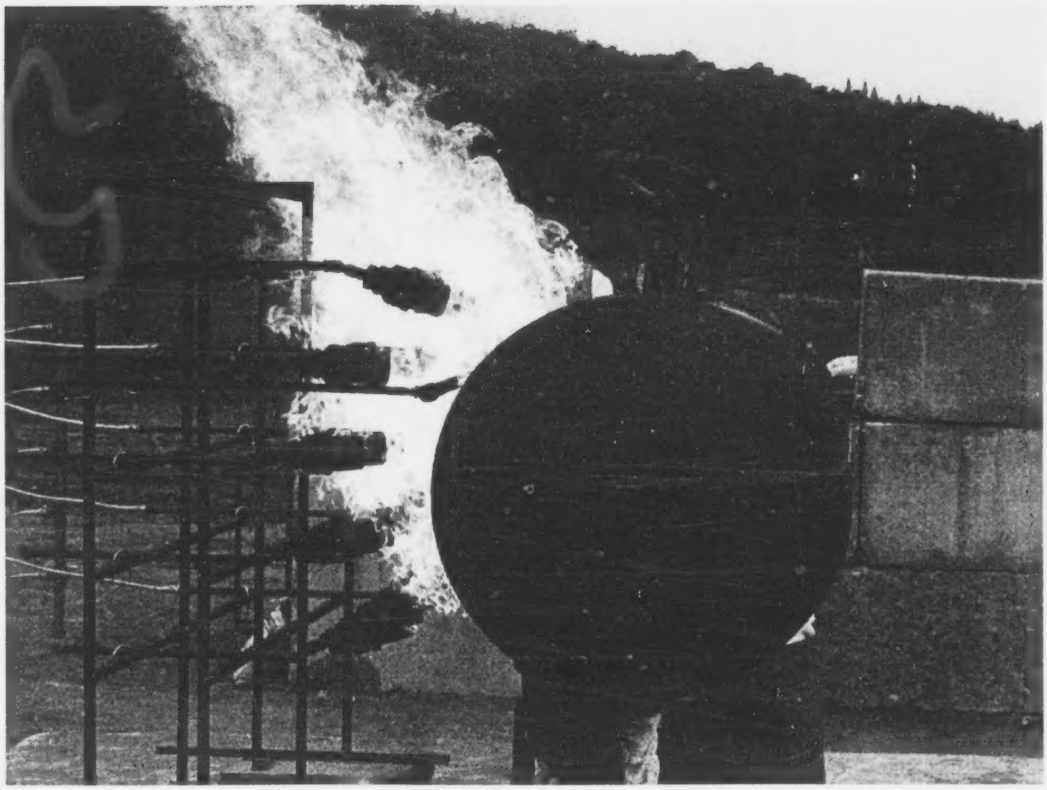

Figure 4.4: Picture showing poor fire contact on tank top (wind from east (right to left))

With the wind from the west, fire exposure was about 25% of the total tank surface area when a 5 x 5 array of burners was used. Final calibration tests were done with the tank filled 50% (Water Test 04-W3) and 80% (Water Test 04-W4). Fill level clearly affected the equilibrium wall temperature, as shown in Table 4.1. One would expect the higher fill level to pull the peak wall temperature down due to wall conduction and increased free convection.

Table 4.1: Fill level effect on wall temperature during burner calibration tests

	Water Fill Level	**Equilibrium Wall T, °C**	**Time to 650°C Wall**	**Notes**
Water Test 3	50%	750	350 sec	Wind < 10 km/h
Water Test 4	80%	700	650 sec Wall T's cover range from 550-650°C	Wind 15-21 km/h

Based on these two tests, it was decided that the tests with propane-filled tanks be conducted when the wind was below 10 km/h, when possible.

It was expected that the baseline unprotected tank with propane would fail with wall temperatures in the range of 650 – 700°C. Based on the wall temperatures achieved in the water tests, failure was expected after about 8-10 minutes of fire exposure.

More results from burner development and water tank tests are presented in Appendices J and D, respectively.

4.3 Baseline Tests

The baseline tests involved tanks with no thermal protection. The first test failed due to a change in the wind direction. This caused late failure, but it is clear from the data that it was a wind effect on the fire. A second baseline test was necessary. The results from both tests are presented here for the sake of completeness.

4.3.1 Baseline Test 04-1

The tank was filled and purged with 1460 L of propane, 78% fill by volume. The computer-controlled PRV was set to pop at 2.63 MPa (381 psig) and close at 2.39 MPa (346 psig). The simulated PRV had a 15 mm orifice. If the scaling and the fire were correct, the tank should fail when the peak wall temperature reached about 650°C. It was predicted that the tank would fail in the 8-10 minute time frame.

Light drizzle with no wind or slight wind (2-4 km/h from the east) was encountered during the test. This slight wind pushed the flame off the tank, which had a dramatic effect on the heating of the tank. This resulted in a late PRV activation and wall temperatures that did not exceed 500°C for the first 38 minutes of the test. Figures 4.5 and 4.6 show wall thermocouple layout and temperature results, respectively.

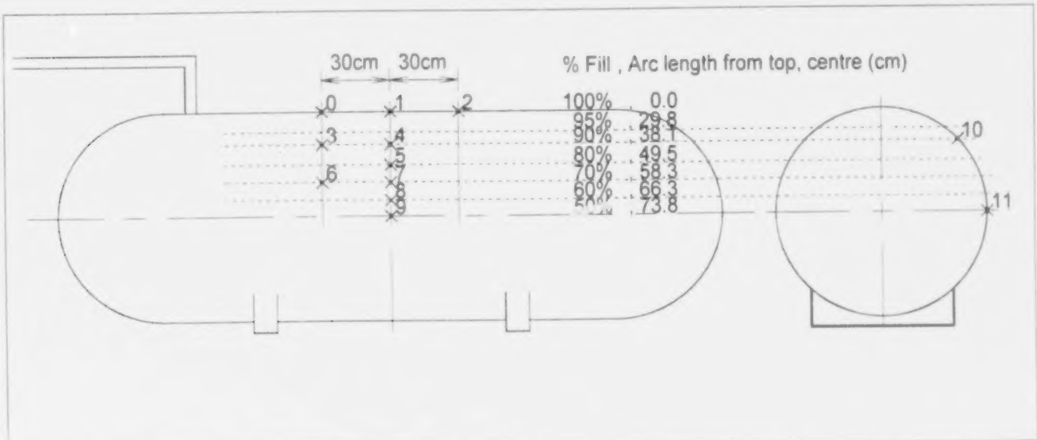

Figure 4.5: Wall thermocouple layout for Test 04-1

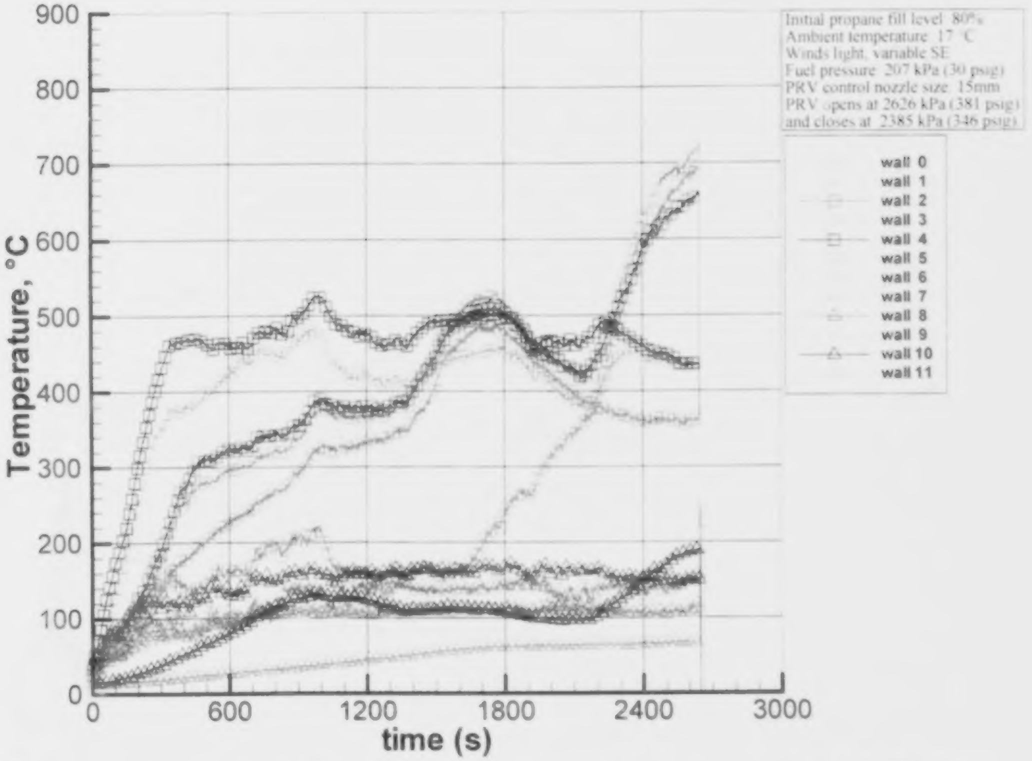

Figure 4.6: Wall temperature, Test 04-1 (baseline test, no insulation, no steel jacket, 78% fill)

Late in the test, the wind direction changed to WNW, pushing the flame over the tank, causing a rapid increase in wall temperatures to over 650°C. The tank failed with a powerful BLEVE at about 46 minutes. Review of video footage showed there was a brief initial rupture and jet release before the tank opened completely. The jet lasted about 3-4 frames (about 100 ms). Figure 4.7 shows the tank remnants.

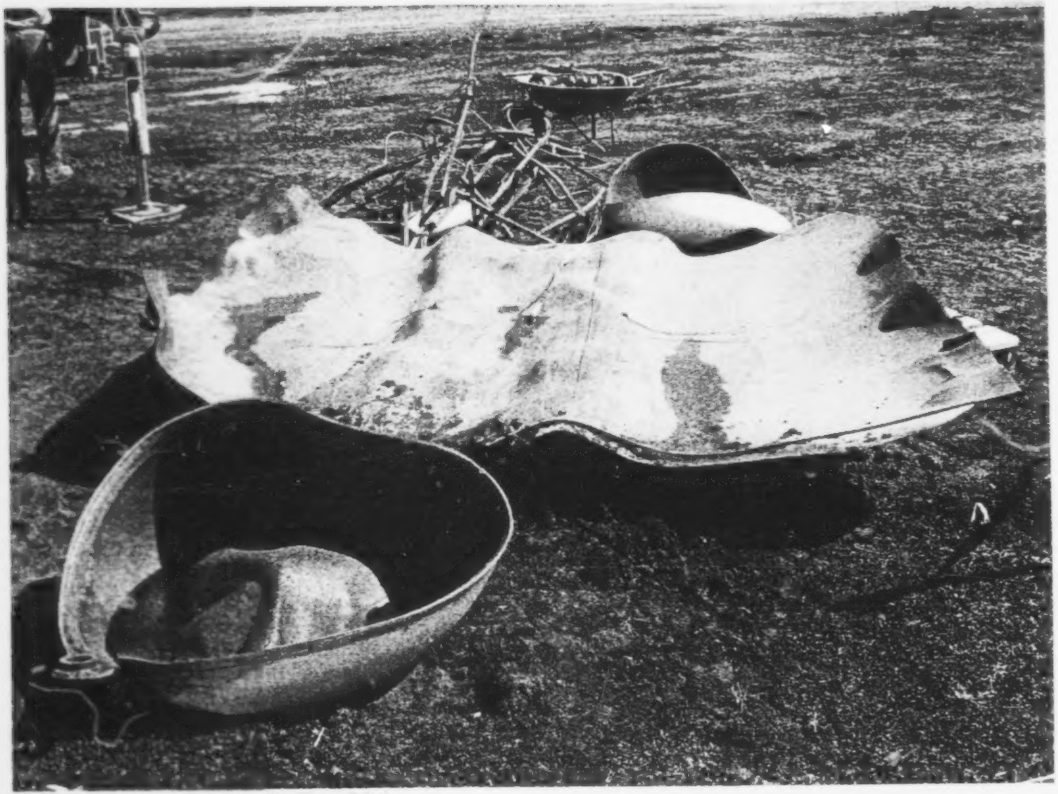

Figure 4.7: BLEVEd tank, Test 04-1

The blast was very strong and the fireball large and long lasting. The blast broke windows in a trailer about 170 m from the tank. Predicted [25] window breakage range for this size tank is about 140 m.

The PRV opened for the first time at 800 seconds (13.3 minutes), as shown in Figure 4.8. This is much later than expected and was due to the poor wall heating. The PRV had been predicted to open in a 100% engulfment case in about 2 minutes. For a 25% engulfment case, it would be expected to open in about four times longer, or 8 minutes. The PRV was activated 44 times for about one to two seconds each time. This represents about 150-200 L of propane being vented. Therefore, the tank was still about 60-70% full at failure.

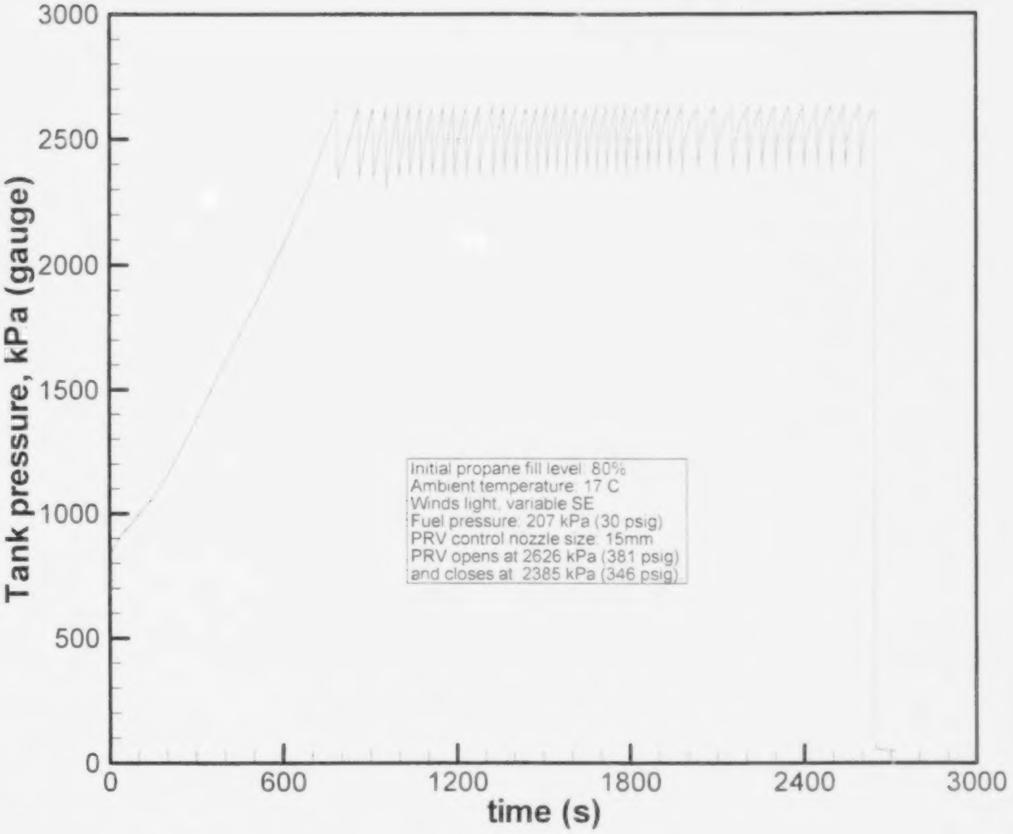

Figure 4.8: Tank pressure, Test 04-1

The liquid temperature was not de-stratified at the time of failure, as shown in Figure 4.9. Liquid temperature ranged from about 69°C at the liquid top to nearly 49°C near the bottom of the liquid. The peak vapour space temperature was 93°C.

The original cylindrical portion of the tank was opened flat on the ground, with the end caps separated from the cylinder.

Extrapolation of the wall temperature data, Figure 4.6, suggests the tank would have failed in 9-10 minutes if the flame had been effective from the start of the test. From 38 minutes to 46 minutes, the wall temperatures increased from about 430°C to over 700°C. The tank was expected to fail when the wall exceeded about 650°C.

Since the tank failure was at a wall temperature well above 700°C, it is believed the SA 455 steel in the tank was much stronger than the minimum ratings.

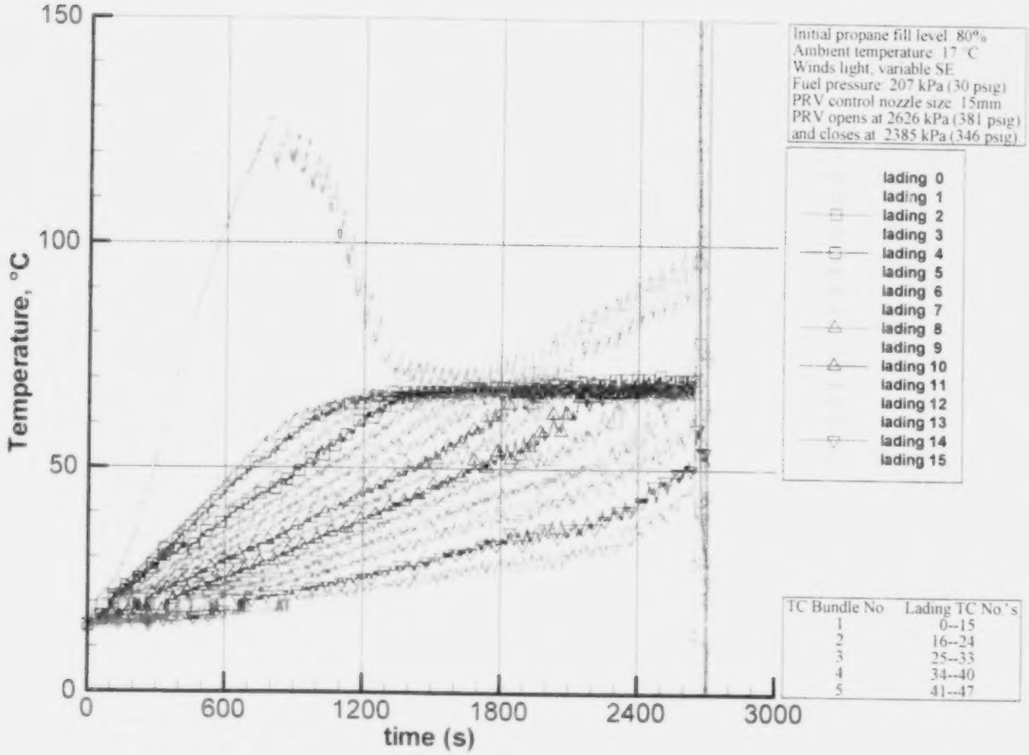

Figure 4.9: Lading temperature (TC bundle 1), Test 04-1

This test was a good example of how the fire drives the test outcome. The tank failure is determined by the fire details. We must use our judgement to decide whether the fire was a credible engulfing fire. In this test, the fire was blown off the tank top for the first 36 minutes and this delayed failure. At around 36 minutes the wind turned and the tank failed within a few minutes. It is obvious from the measured wall temperatures that this took place. Therefore we can correct the failure time and say that the tank would have failed in about 10-11 minutes.

4.3.2 Baseline Test 04-6

It was evident that Baseline Test 04-1 was strongly affected by poor wind conditions that developed during the course of the test. It was clear that the fire was a problem and that failure could be estimated at 10-11 minutes from the results. It was decided to repeat the baseline test with the last available tank in the series.

As in Test 04-1, the tank was filled and purged with 1460 L of propane, about 78% fill by volume. The PRV was set to pop at 2.63 MPa (381 psig) and close at 2.39 MPa (346 psig). The simulated PRV had a 15 mm orifice.

Figures 4.10 and 4.11 show wall thermocouple layout and temperature results, respectively.

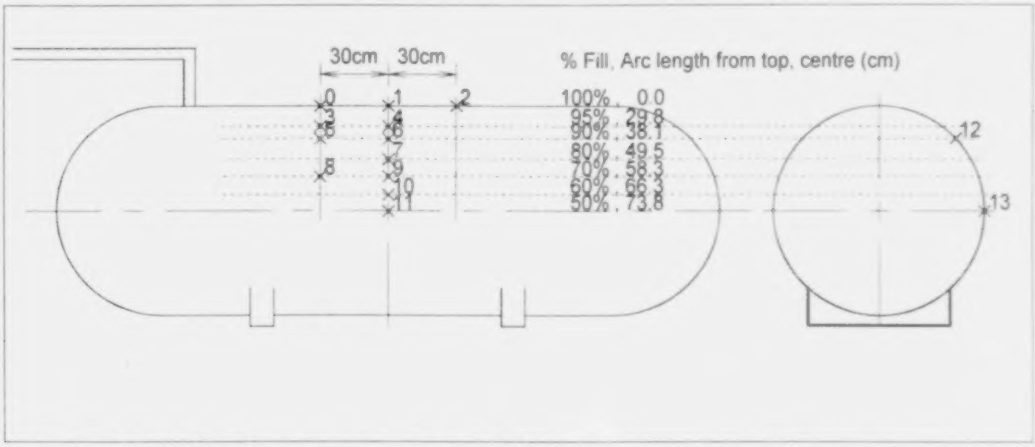
30cm
30cm
% Fill, Arc length from top, centre (cm)
100% , 0.0
95% , 29.8
90% , 38.1
80% , 49.5
70% , 58.3
60% , 66.3
50% , 73.8
0
1
2
3
4
5
6
7
8
9
10
11
12
13

Figure 4.10: Wall thermocouple layout for Test 04-6

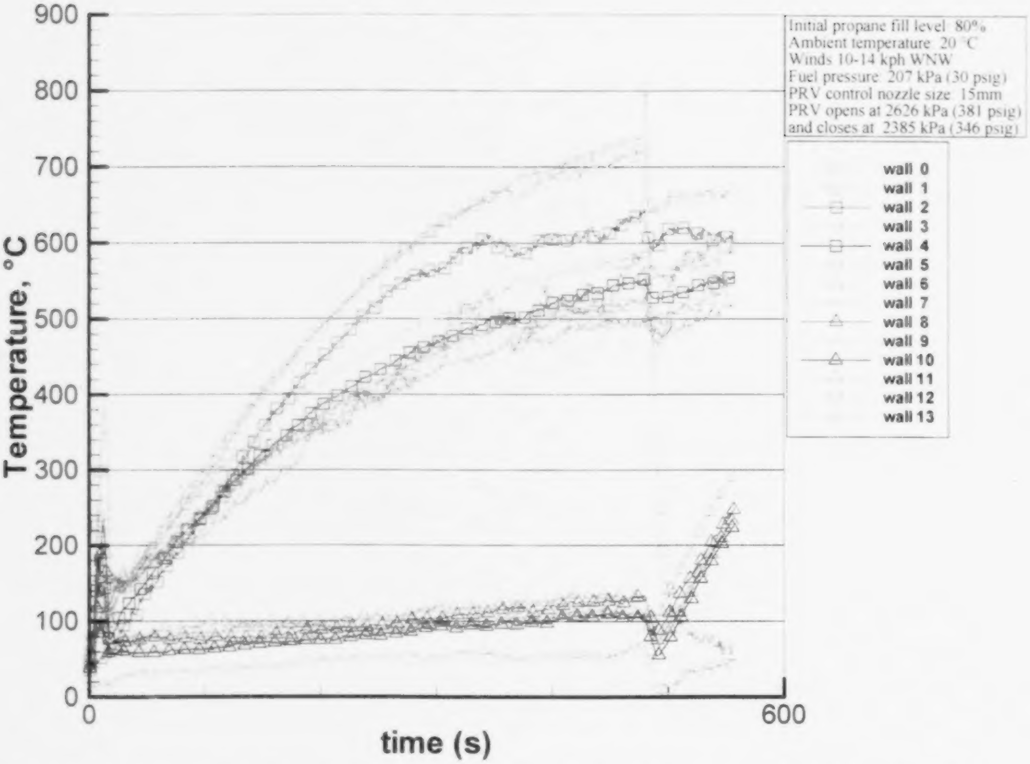

Figure 4.11: Wall temperature, Test 04-6 (baseline test, no insulation, no steel jacket, 78% fill)

Wind conditions were near ideal for this test, the best in the series. The fire was started and, as predicted, the tank failed with a large jet release in 8 minutes. Figures 4.12 and 4.13 show the tank and the failure opening. The failure tear length was 368 mm, with a maximum opening width of 45 mm and a vertical deformation from the top of the tank of 89 mm. Wall thinning was evident along the edge of the opening.

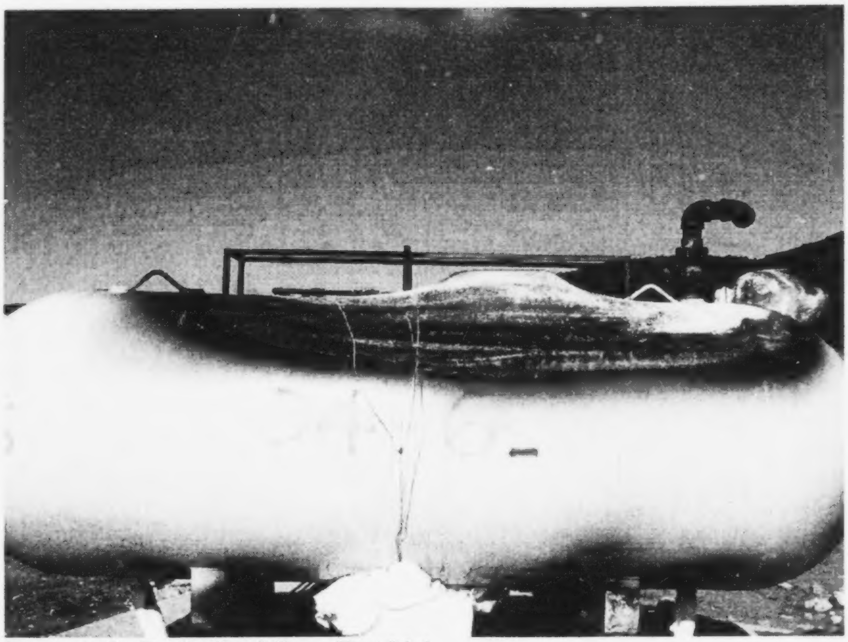

Figure 4.12: Tank after failure, Test 04-6

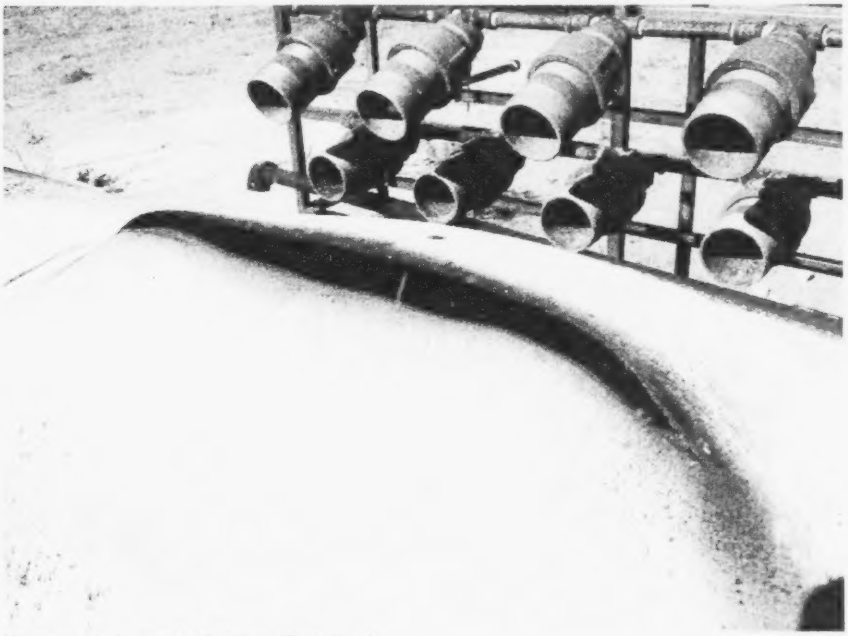

Figure 4.13: Tank failure, Test 04-6

The PRV did not open over the course of the test. Tank pressure at failure was about 2.4 MPa (375 psig), very near the point of activating the PRV, Figure 4.14. Peak wall temperature was about 740°C. There was no BLEVE because the liquid lading was not fully heated to saturation and the wall was only locally heated. The crack stopped in cool strong steel.

Because the failure was so rapid, the liquid temperature was not de-stratified at the time of failure, Figure 4.15. The liquid temperature ranged from 50°C at the liquid top to around 32°C near the liquid bottom. This reduced the energy available in the liquid to do work on the tank wall during the rupture process. The peak vapour space temperature was close to 160°C.

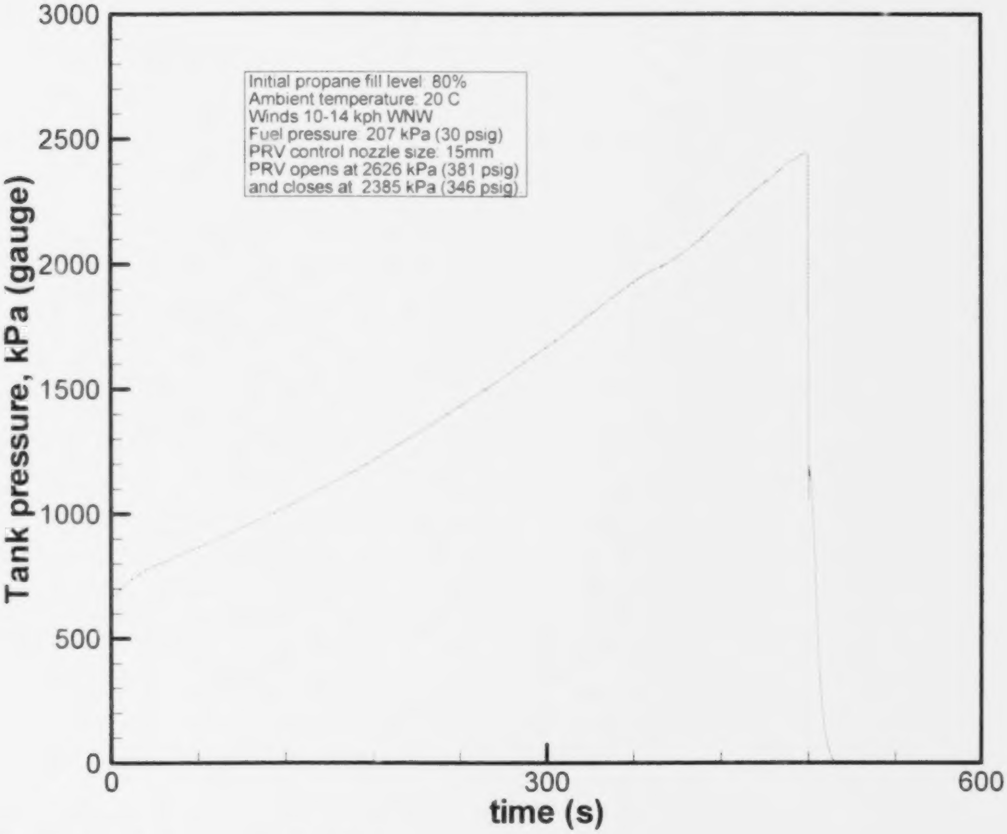

Figure 4.14: Tank pressure, Test 04-6

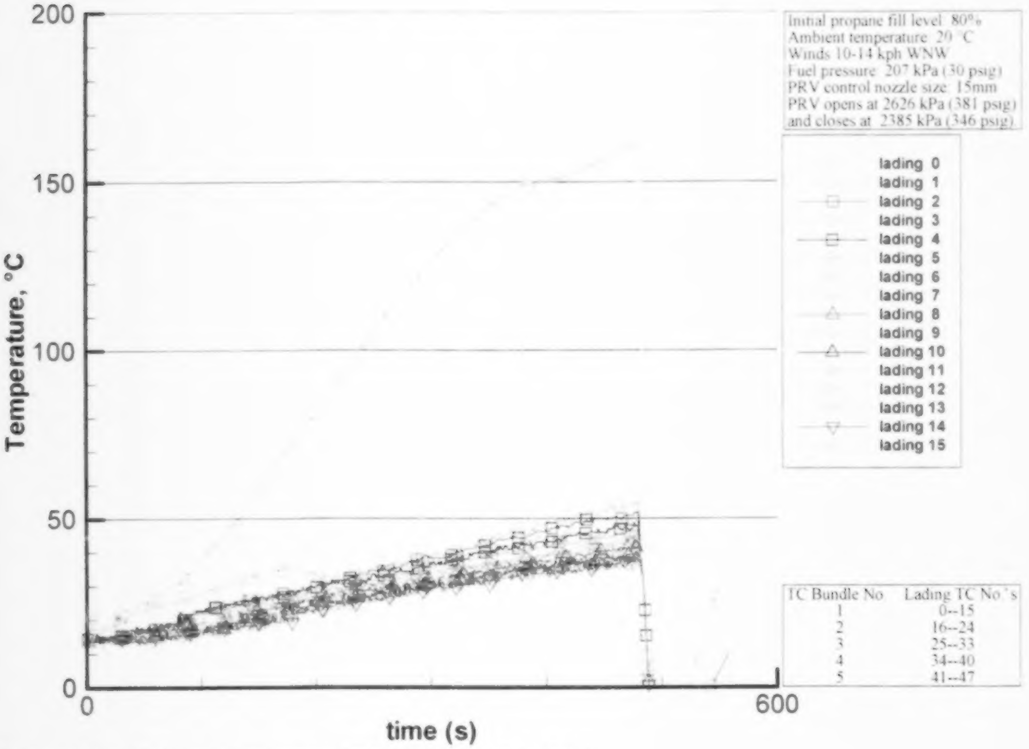

Figure 4.15: Lading temperature (TC bundle 1), Test 04-6

It should be noted that the first baseline test (Test 04-1) resulted in a very powerful BLEVE. This happened for the following reasons:

i) Liquid energy was higher (liquid was hotter and near uniform in temperature).
ii) Failure was later at lower fill level (larger area of wall was at high temperature).
iii) Stress-rupture damage in the wall was more widespread (more time for widespread damage to take place).

The tank in Test 04-6 was tested with a slightly different burner system than the first baseline test and this probably explains the earlier failure time (8 minutes versus an estimated 10-11 minutes). This change is described in section 4.4.3.

4.4 Large Thermal Defect Tests

These tests considered cases of 8 and 16% thermal protection defects. The defects were on one side of the tank and spanned an area from near the bottom of the tank to the top.

Figure 4.16 shows location and size of both large and small insulation defects and the protective steel jacket used. The large defect was 1.30 m wide and spanned almost the entire tank circumference except for the bottom 20-30 degrees. The remainder of the tank was insulated with 133 mm tank car ceramic fibre insulation. The white tank was painted black in the region of the defect to ensure a high emissivity.

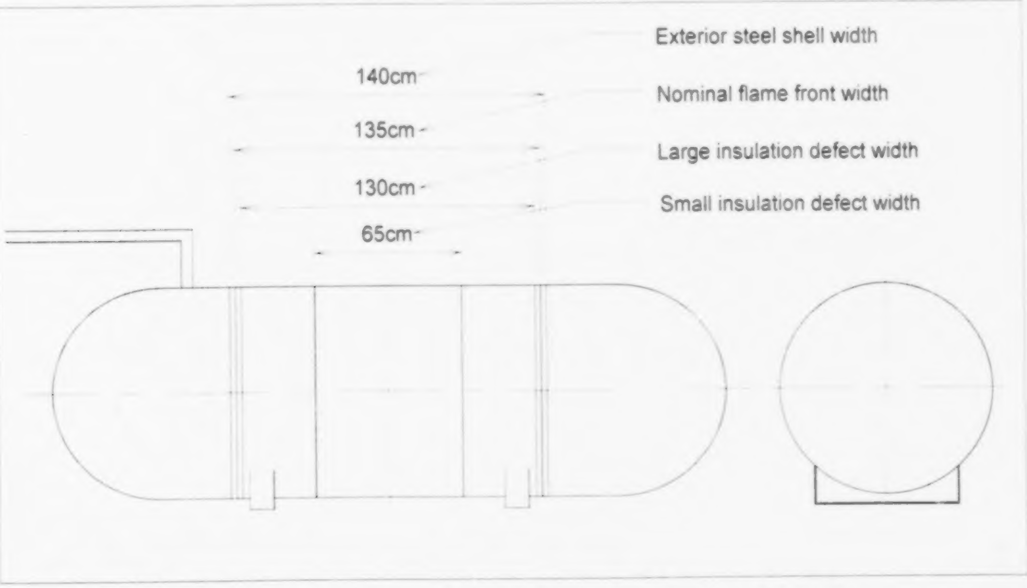

Exterior steel shell width
140cm
Nominal flame front width
135cm
Large insulation defect width
130cm
Small insulation defect width
65cm

Figure 4.16: Location and size of tank insulation defects and protective steel jacket

Test 04-2, the first large defect test, was aborted early in the test due to poor fire conditions caused by a restriction in the burner fuel supply line just before the burner system evaporator. Corrections were made to the fuel delivery system and a final check of the fire conditions was made on the tank used in Test 04-2, but with water fill. After the fire condition proved satisfactory, a repeat of Test 04-2 was conducted, Test 04-3.

Results from all three tests are presented here for the sake of completeness.

4.4.1 Large Thermal Defect Test 04-2

The tank was filled and purged with 1300 L of propane, about 71% fill by volume. The PRV was set to pop at 2.63 MPa (381 psig) and close at 2.39 MPa (346 psig). The simulated PRV had a 15 mm orifice.

Figure 4.17 shows fire conditions at the beginning of the test. The wind started at 7-16 km/h from the west but then turned southwest. This wind direction blew the flame along the tank side instead of over the tank. The fire did not look good, and this was confirmed by very slow heating rate of the tank lading and low wall temperatures (Figures 4.18, 4.19 and 4.20).

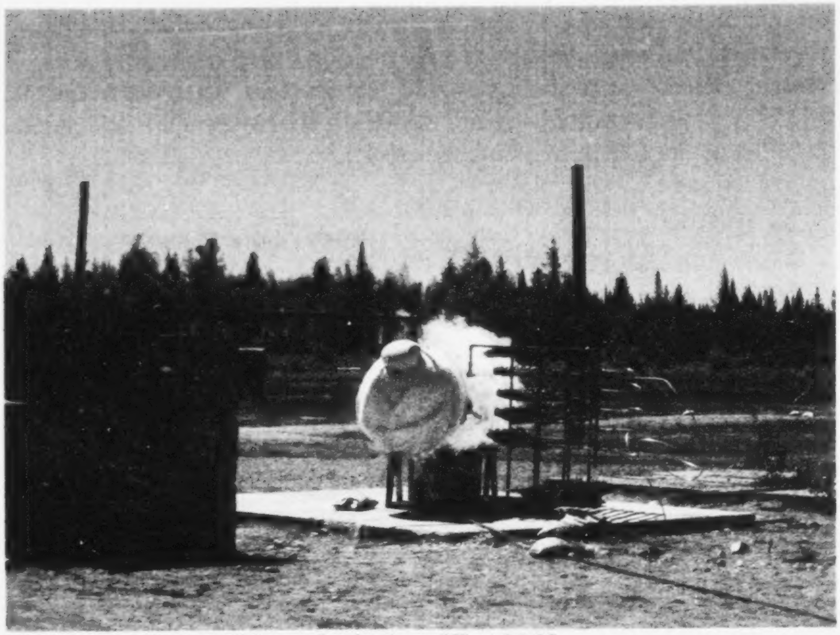

Figure 4.17: Fire condition at beginning of Test 04-02

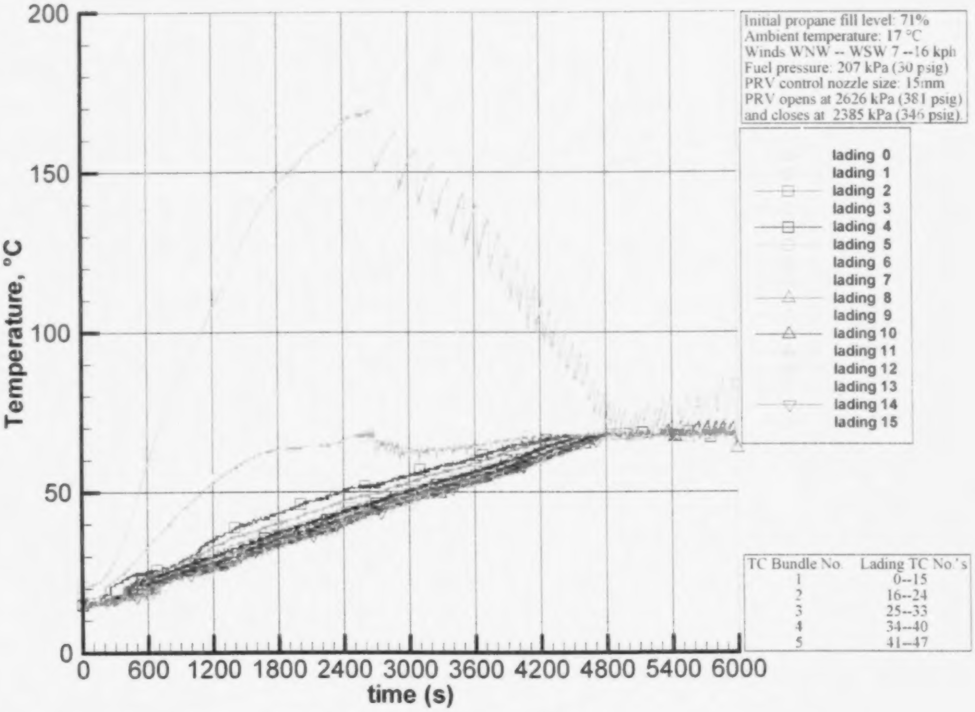

Initial propane fill level: 71%
Ambient temperature: 17 °C
Winds WNW -- WSW 7 --16 kph
Fuel pressure: 207 kPa (30 psig)
PRV control nozzle size: 15mm
PRV opens at 2626 kPa (381 psig)
and closes at 2385 kPa (346 psig).

TC Bundle No.	Lading TC No.'s
1	0--15
2	16--24
3	25--33
4	34--40
5	41--47

Figure 4.18: Lading temperature (TC bundle 1), Test 04-2

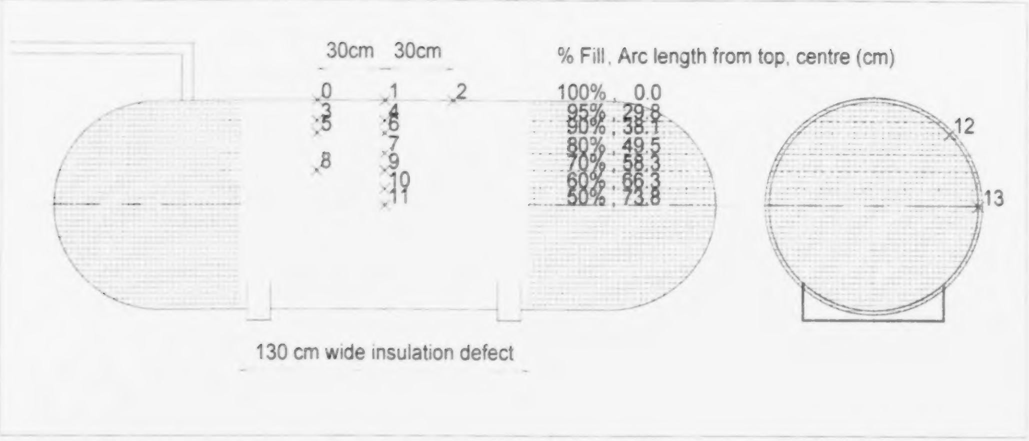
30cm
30cm
% Fill, Arc length from top, centre (cm)
0
1
2
3
4
5
6
7
8
9
10
11
100% , 0.0
95% , 29.8
90% , 38.1
80% , 49.5
70% , 58.3
60% , 66.3
50% , 73.8
12
13
130 cm wide insulation defect

Figure 4.19: Wall thermocouple layout for Test 04-2

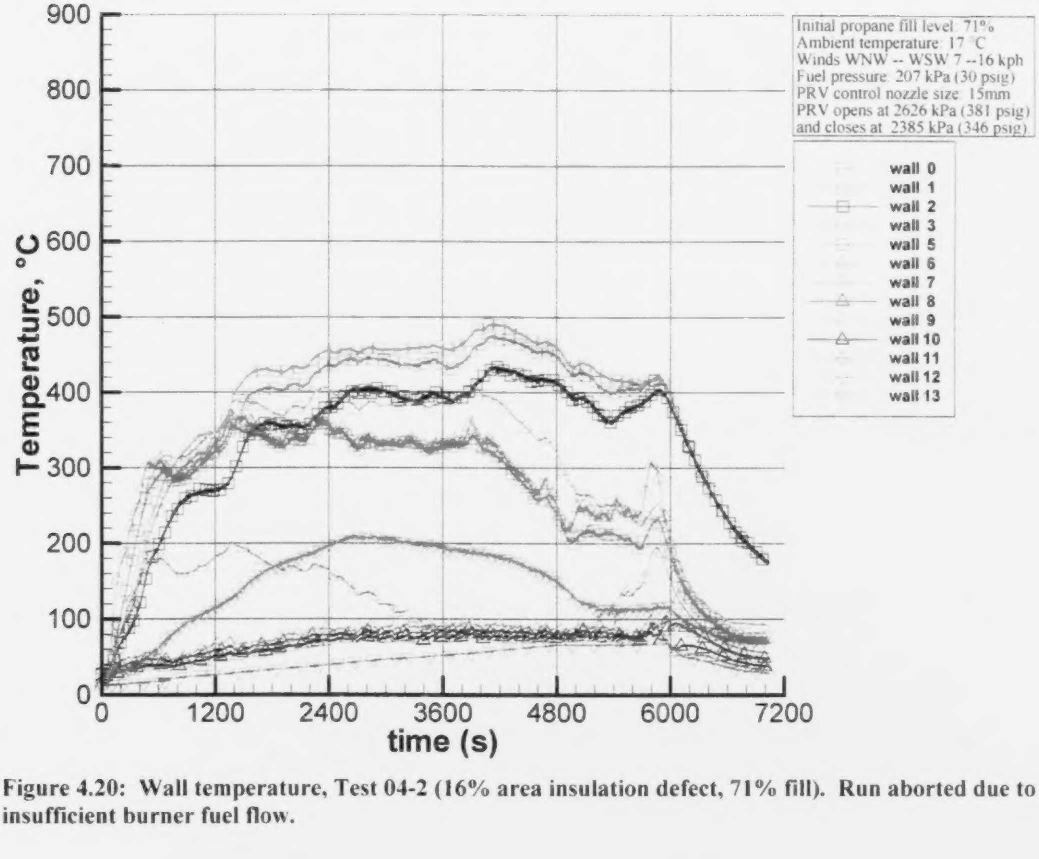

Figure 4.20: Wall temperature, Test 04-2 (16% area insulation defect, 71% fill). Run aborted due to insufficient burner fuel flow.

The test was continued for 100 minutes in hope that the wind would turn back, but it did not. Wall temperature readings did not reach 500°C, well below what was expected. The test was a failure due to low fire heat flux. The test was aborted and the tank lading was dumped and flared off using an emergency dump line.

The PRV opened at 2700 sec and cycled 41 times before the test was stopped. The tank pressure was well controlled using the 15 mm PRV nozzle, Figure 4.21.

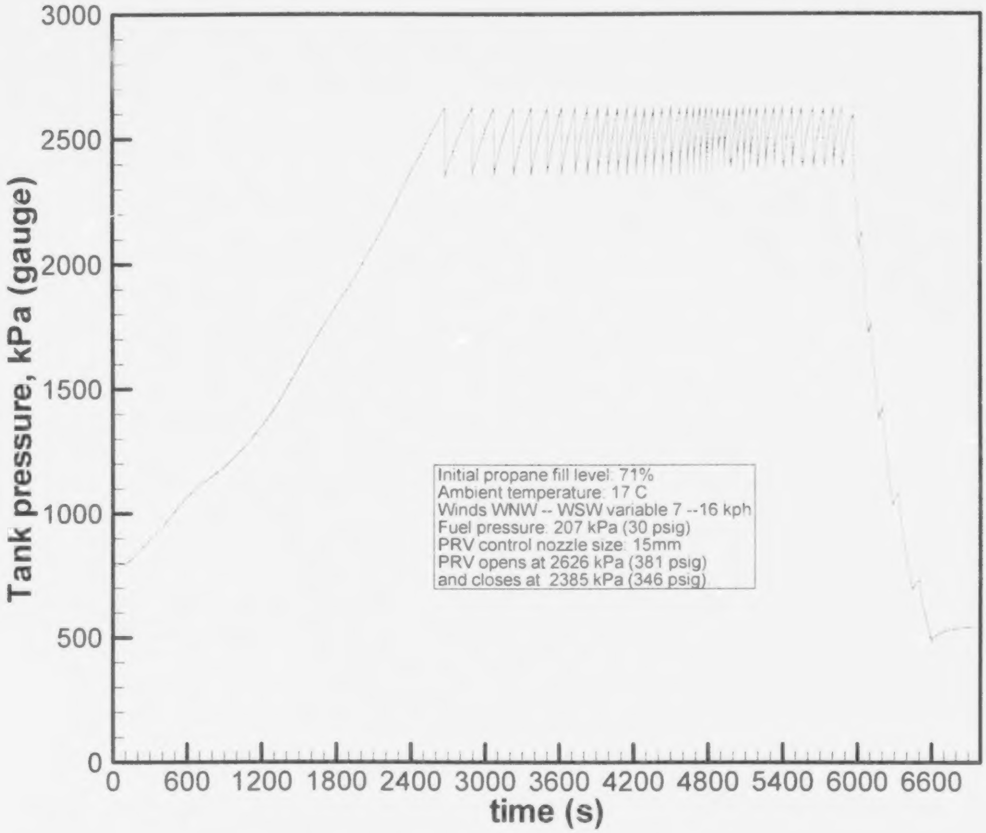

Figure 4.21: Tank pressure, Test 04-2

The problem with the fire was not entirely due to wind conditions. It was later determined that the fuel flow to the burners was low due to an over-length piece of 0.5 in. copper tube that jointed the liquid propane fuel supply pipe to the burner system evaporator. This line was longer than in the earlier water tests and caused a fuel flow restriction that reduced the fuel flow by about 40-50%.

Earlier water tests used about 50% of the propane fuel tank in 100 minutes of testing; this test only used about 30% of the fuel in 100 minutes. From this point on, the copper line was replaced by 1 in. diameter pipe.

4.4.2 Large Thermal Defect Water Tank Test 04-W5

The tank from aborted Test 04-2, with the jacket and large defect, was filled to 50% with water. The portion of the burner fuel line consisting of 0.5 in. copper tube was replaced with 1 in. pipe to alleviate fuel flow restriction. The fire was started and it was immediately apparent that the fire condition had significantly improved, Figure 4.22.

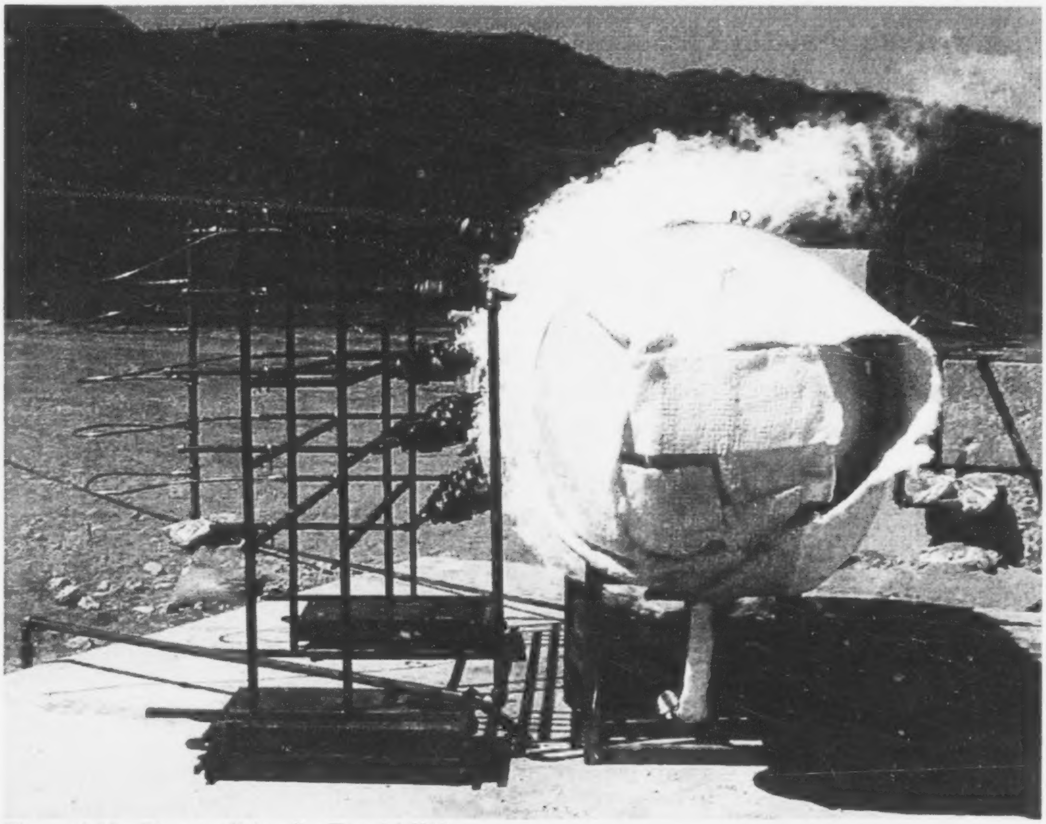

Figure 4.22: Fire condition for Test 04-W5

Figures 4.23 and 4.24 show wall thermocouple layout and temperature results, respectively. Wall temperatures under the jacket increased rapidly and by 730 seconds the wall was at 500°C. By 25 minutes the wall temperature under the jacket peaked at about 640°C. This was 20-40°C hotter than expected from simulations.

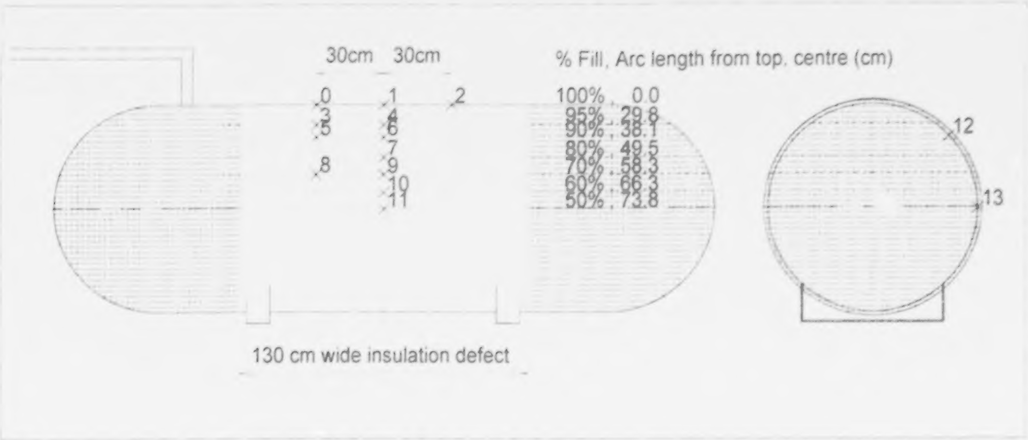
30cm
30cm
% Fill, Arc length from top, centre (cm)
0
1
2
3
4
5
6
7
8
9
10
11
100% , 0.0
95% , 29.8
90% , 38.1
80% , 49.5
70% , 58.3
60% , 66.3
50% , 73.8
12
13
130 cm wide insulation defect

Figure 4.23: Wall thermocouple layout for Test 04-W5

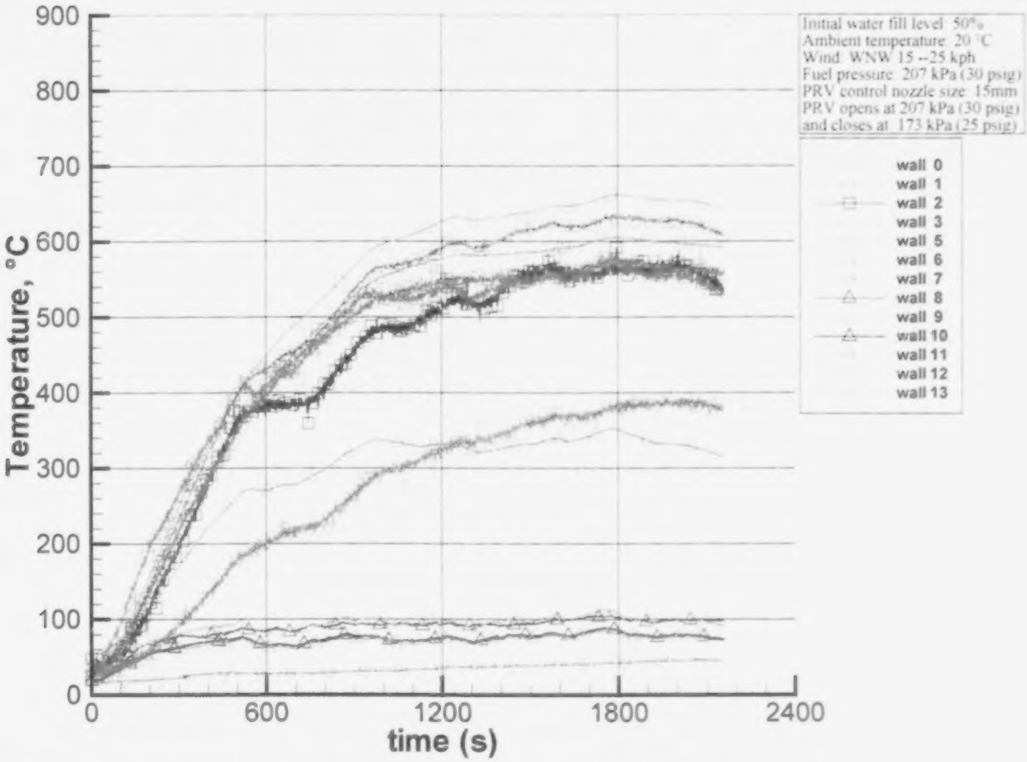

Figure 4.24: Wall temperature, Test 04-W5 (16% area insulation defect, 50% fill)

The wind was strong during this test, 16-24 km/h from the west and southwest.

Figure 4.25 shows lading temperatures for the central thermocouple bundle. Based on the liquid heating rate and the exposed area, it is estimated the flame had an effective blackbody temperature of 850-900°C, in excellent agreement with the fire standard that requires 871 ±56°C.

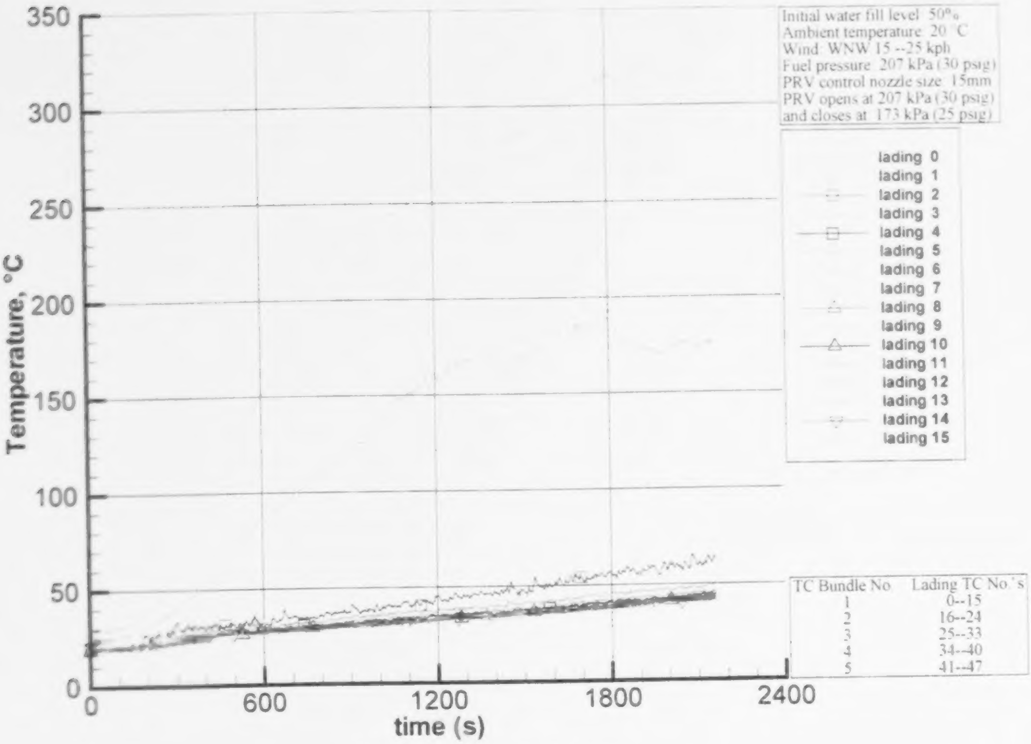

Figure 4.25: Lading temperature (TC bundle 1), Test 04-W5

4.4.3 Large Thermal Defect Test 04-3

Fire intensity for Test 04-2 was inadequate because of a restriction in the liquid propane supply to the burner system evaporator. Once the fuel supply problem was solved, it was necessary to repeat the large thermal defect test conditions.

As in Test 04-2, the tank for 04-03 was filled and purged with 1300 L of propane, about 71% fill by volume. The PRV was set to pop at 2.63 MPa (381 psig) and close at 2.39 MPa (346 psig). The simulated PRV had a 15 mm orifice.

Figures 4.26 and 4.27 show wall thermocouple layout and temperature results, respectively.

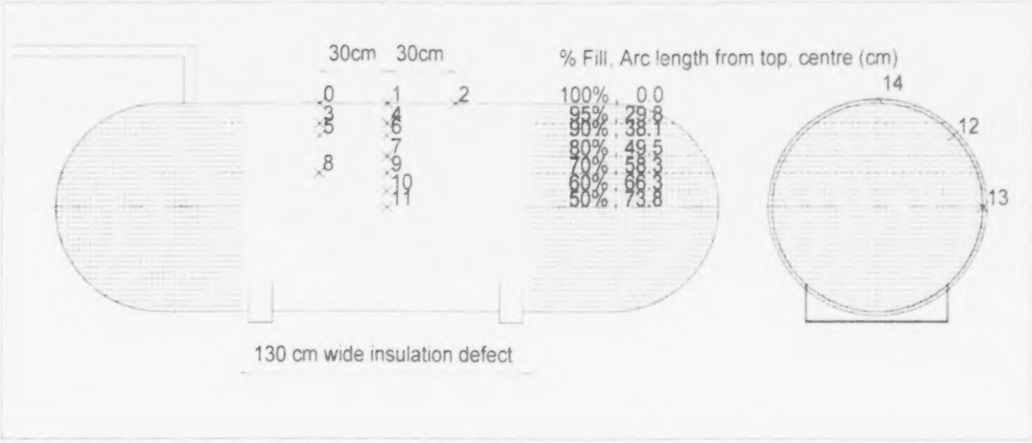
30cm
30cm
% Fill, Arc length from top, centre (cm)
0
1
2
3
4
5
6
7
8
9
10
11
100% , 0.0
95% , 29.8
90% , 38.1
80% , 49.5
70% , 58.3
60% , 66.3
50% , 73.8
14
12
13
130 cm wide insulation defect

Figure 4.26: Wall thermocouple layout for Test 04-3

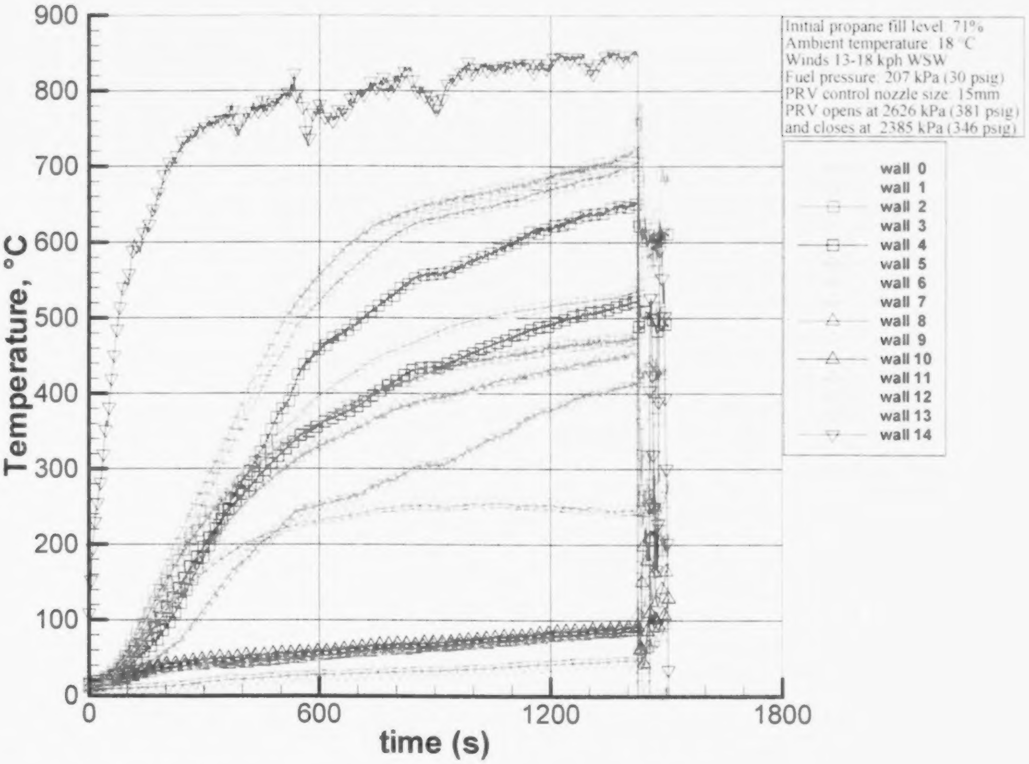

Figure 4.27: Wall temperature, Test 04-3 (16% area insulation defect)

Wind was from the southwest at about 13-18 km/h. The wind pushed the flame slightly along the tank towards the PRV pipe end of the tank, but the fire looked good visually.

The wall temperature rise rate suggests an adequate fire. The steel jacket quickly rose to about 800°C, as expected. It then continued to rise to above 840°C as the vapour space wall temperature increased. These temperatures suggest that the fire had an effective blackbody temperature in the range of 860-870°C, a credible hydrocarbon pool fire.

Tank pressure rose slowly due to the jacket and the 25% fire condition. By 700 seconds the peak wall temperature was 600°C. By the 1200 second mark, the wall temperature was 680°C. The tank failed at 1420 seconds (24 minutes). The tank pressure was about 2.55 MPa (370 psig) and the PRV never opened (Figure 4.28). It is expected the PRV would have opened at about 25 minutes.

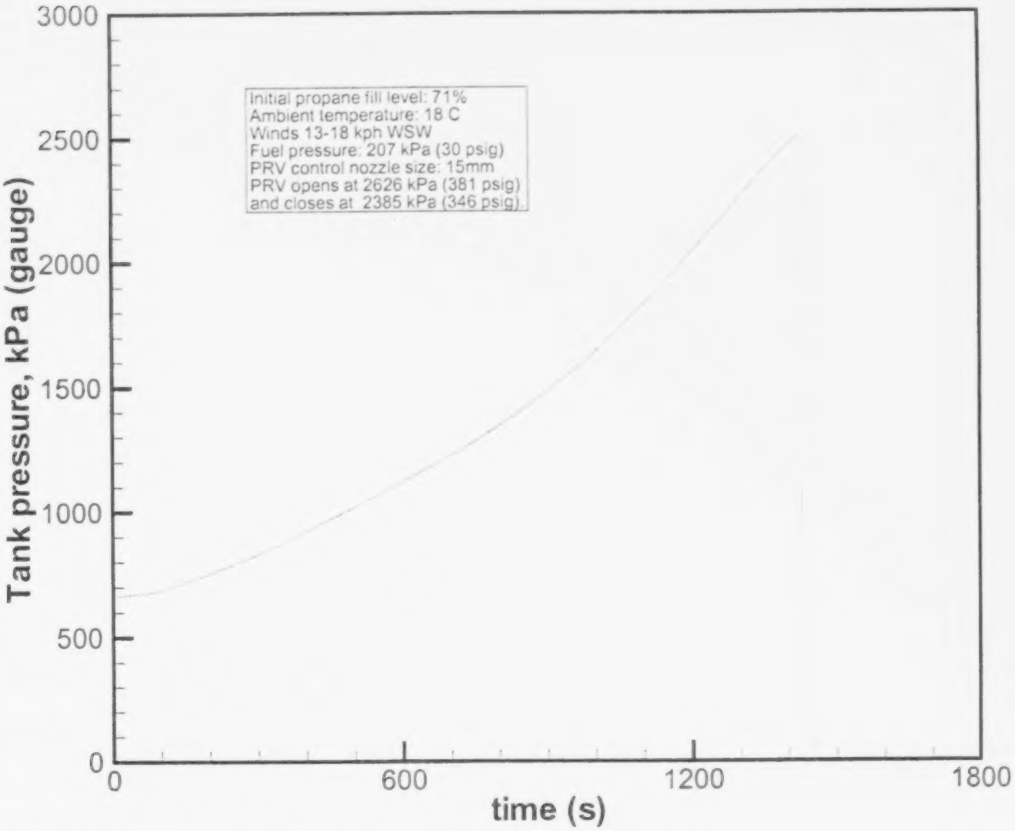

Figure 4.28: Tank pressure, Test 04-3

Note that this was a 16% insulation area defect case and it was expected that the pressurization rate would be much slower than an unprotected case. If we base the time on energy input alone we would expect PRV pop at about 2/0.16 x 2 = 25 minutes. Dividing by 0.16 accounts for the 16% defect and the factor 2 accounts for the presence of the steel jacket (50% reduction in heat flux).

The fact that the PRV never opened may explain the very high wall temperatures in the vapour space. The wall temperature exceeded 700°C and the vapour reached a temperature of about 300°C. Simulations suggest the wall should have not exceeded 640°C with PRV cycling. When the PRV opens, hot vapour is vented and replaced with cool vapour near the saturation temperature. Test 04-4 was similar to this test, but with a lower PRV pressure setting. Results and comparisons to this test are made in section 4.5.

The important thing to note about this test is that the entire vapour space got very hot when the defect was in the vapour space. Note that this tank simulated a tank with 16% defect area and yet the entire vapour space (even under the insulation) saw wall temperatures exceeding 500°C. This observation is additionally supported by pictures showing the discoloured paint in the vapour space, Figure 4.29.

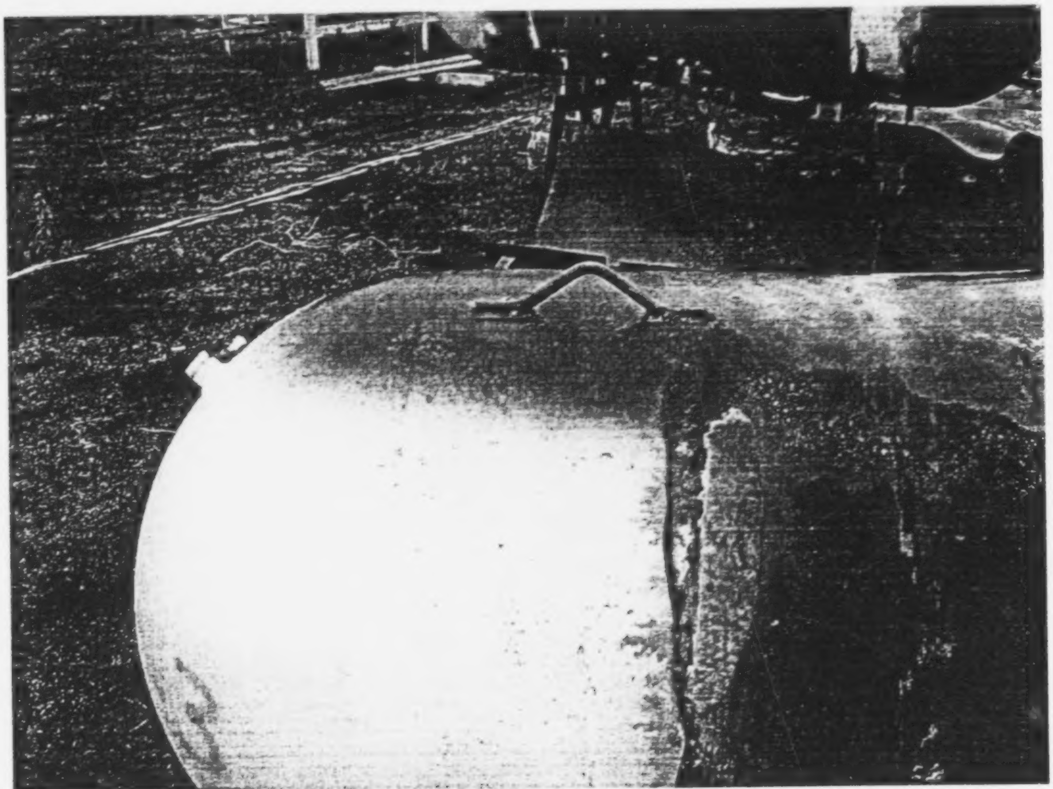

Figure 4.29: Test 04-03 burned vapour space wall under insulated area (not under fire)

The failure started as a split that ejected propane under the jacket. The jacket was deformed and split open at the tack weld line near the tank top, but remained in position, Figure 4.30. The tank did not BLEVE.

Figure 4.31 shows the lading temperature readings from the central thermocouple bundle. The liquid average temperature was only about 37°C at failure, well below the saturation temperature for the measured tank pressure at time of failure. The tank started at 71% full and 12°C. At 37°C, the fill should have been about 77% full by volume.

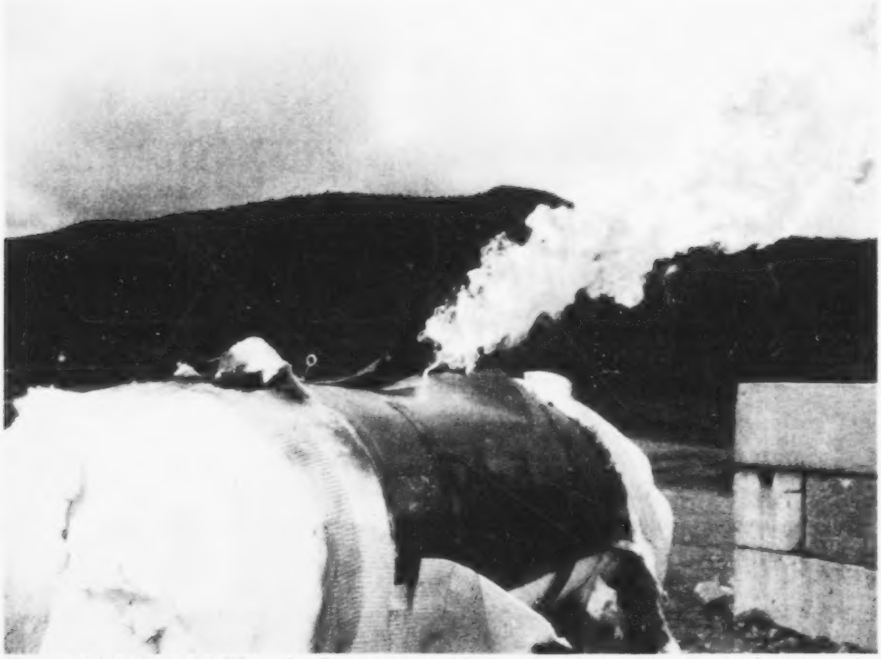

Figure 4.30: Test 04-03 tank after rupture (the steel jacket split open at the top tack weld)

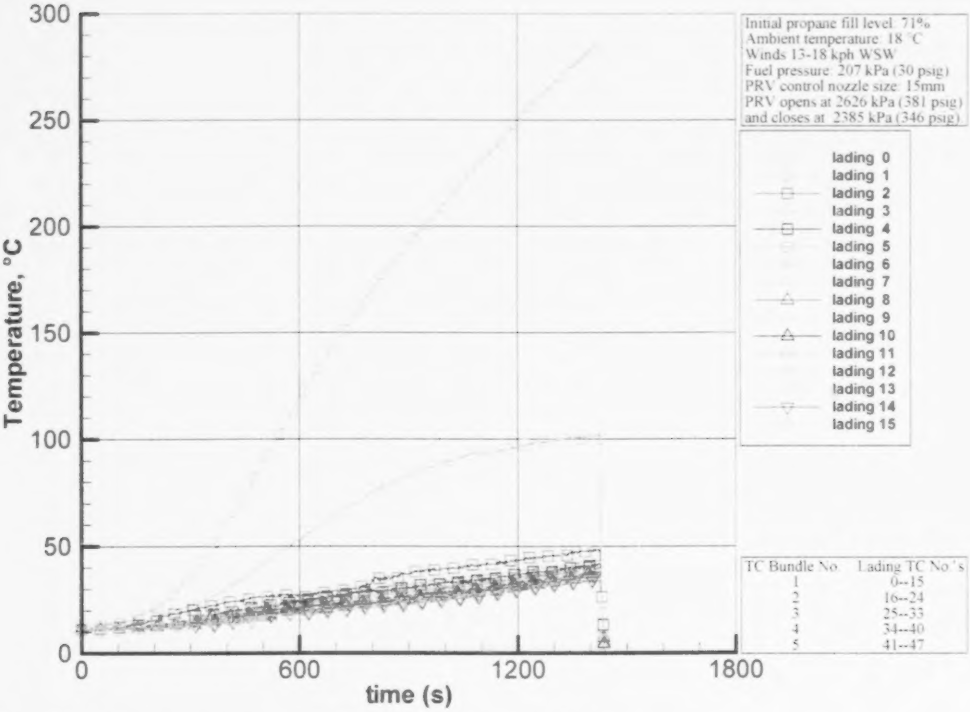

Figure 4.31: Lading temperature (TC bundle 1), Test 04-3

Just before failure, the peak wall temperature increased rapidly to about 780°C. It is likely that the tank shell had bulged to make direct contact with the hotter jacket.

The tank failed along the top nearer to the PRV end of the tank, with a 35 cm long axial fissure, Figure 4.32. The wind effect on the fire would have moved the peak wall temperature in this direction relative to the tank centre. The maximum tear width was only 3.2 cm and the vertical deformation from the top of the tank was 7.6 cm. The wall was not thinned to a knife edge but rather showed a rough failure surface (ductile fracture) about 2 mm thick (original wall thickness 7.1 mm). Severe bulging was observed and the wall clearly came into contact with the jacket late in the test.

The vapour space wall was burned and discoloured under the jacket and the vapour space wall under the insulation was also badly discoloured. This indicates the entire vapour space was very hot. The PRV did not have a chance to open resulting in a very hot vapour space. The measured vapour temperature near the tank top was about 280°C at failure.

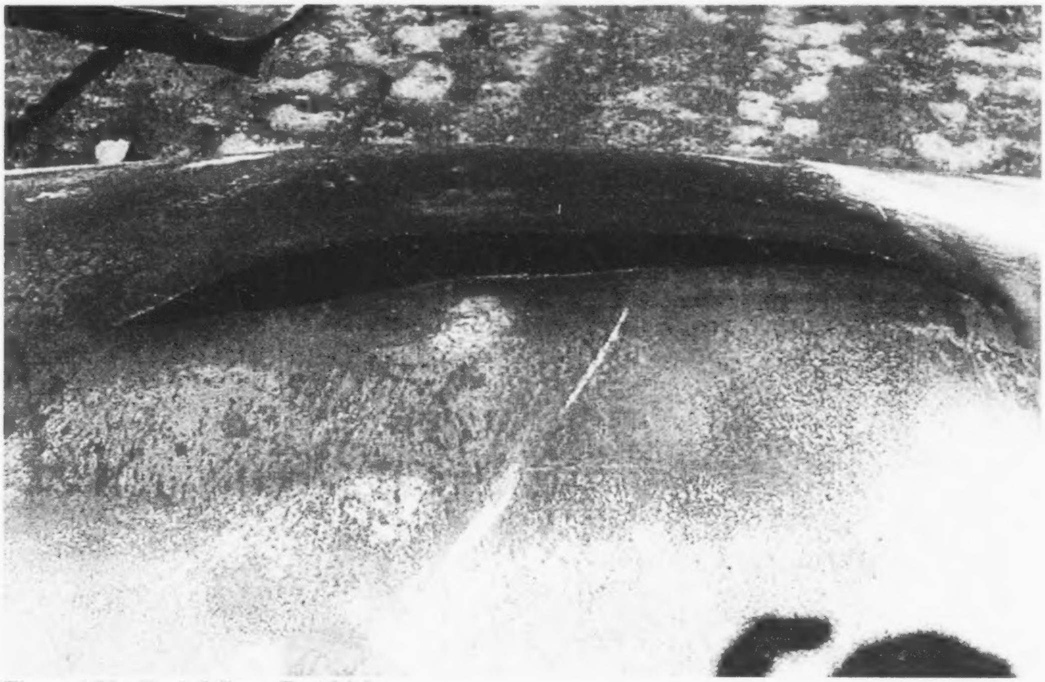

Figure 4.32: Tank failure, Test 04-3

This test involved a tank with about 16% defective insulation. It failed in 24 minutes. Applying crude scaling to a tank-car with 16% defective insulation, one would expect failure in a time period about three times longer (i.e., the ratio of the tank-car diameter to the test tank diameter), a time of 72 minutes. This is well under the 100-minute minimum time requirement.

After the jet release, the tank was left about 30% full of liquid propane at atmospheric pressure. It was allowed to burn empty. By the following morning the fire was out and the tank was empty and ice-free.

This tank did not BLEVE because:

i) The liquid temperature was low.
ii) Wall heating was not wide spread enough.
iii) The jacket may have slowed the depressurization rate upon initial failure and may have reduced the power of the phase change and pressure transient.

The release was a massive jet, producing a strong cooling effect on the tank vapour space and thinned wall region. There would also have been liquid droplet impact. This stressful condition did not result in a BLEVE.

The conclusion is that, even at high fill levels, a tank with a jacket in place and exposed to a credible fire will fail.

4.5 Large Thermal Defect, Low Hoop Stress, Test 04-4

This test was a repeat of test 04-3 (16% insulation area defect) with the following modifications:

i) PRV set pressure was reduced, popping at 2.12 MPa (308 psig) and closing at 1.93 MPa (280 psig), giving about a 20% reduction in hoop stress.
ii) Propane fill was increased to 78%.
iii) Burner fuel pressure was initially reduced from 206 to 172 kPa (30 to 25 psig).

The test was designed to see how much better the tank would survive under less severe pressure and fire conditions. The changes were predicted to delay failure to around the 35-minute mark. At 35 minutes, the lading temperature should be isothermal and a strong explosion was expected. If there was no BLEVE, then the jacket may have a beneficial effect. Note the outer steel jackets used to cover the insulation defect areas in these tests were not properly scaled in terms of structure (i.e., the jacket was the same thickness as the full-scale tank at 3 mm).

The test started at 11:39, but after 10 minutes, the fire was stopped because it was clear it was not hot enough. Figures 4.33 and 4.34 show the wall thermocouple layout and wall temperatures for this initial attempt, respectively. The jacket temperature did not exceed 700°C and it should have been around 800°C. The jacket temperature will rise rapidly to near the fire temperature. Fuel pressure was increased back to 206 kPa (30 psig) and the fire was restarted at 12:03. Figure 4.35 shows wall temperature readings that indicate the fire was then adequate.

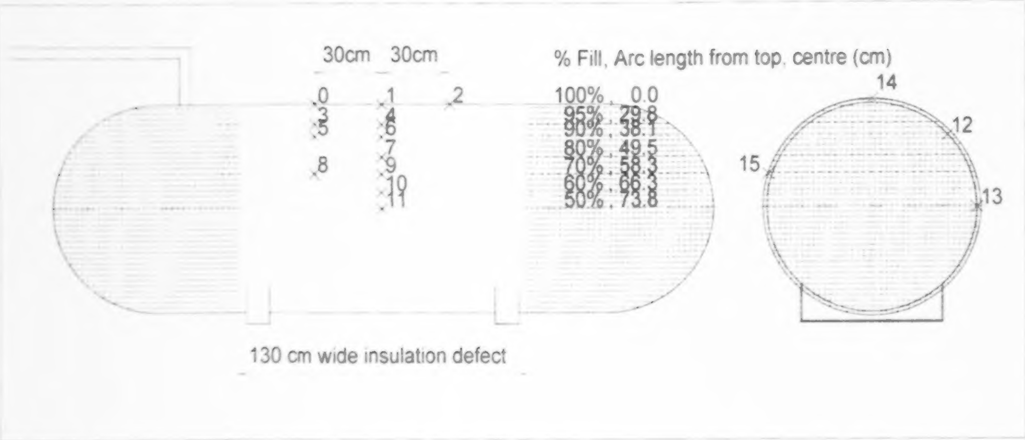
30cm
30cm
% Fill, Arc length from top, centre (cm)
0
1
2
3
4
5
6
7
8
9
10
11
100% , 0.0
95% , 29.8
90% , 38.1
80% , 49.5
70% , 58.3
60% , 66.3
50% , 73.8
14
12
15
13
130 cm wide insulation defect

Figure 4.33: Wall thermocouple layout for Test 04-4

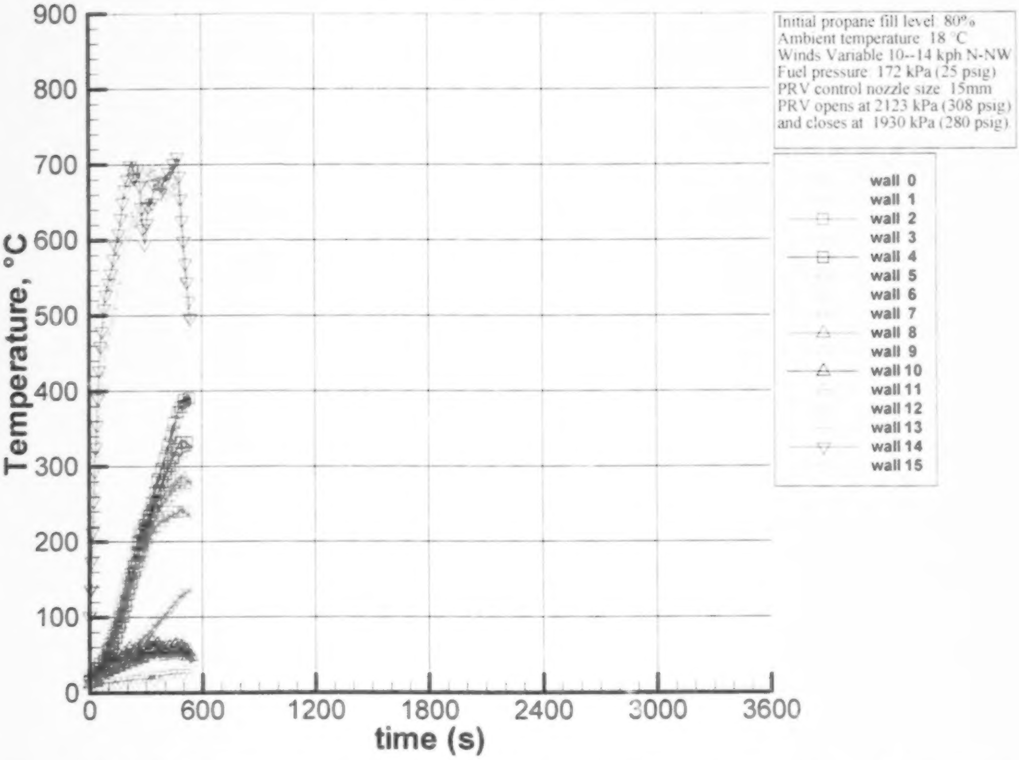

Figure 4.34: Wall temperature, Test 04-4a (16% insulation defect, low hoop stress). Run aborted to increase fuel pressure

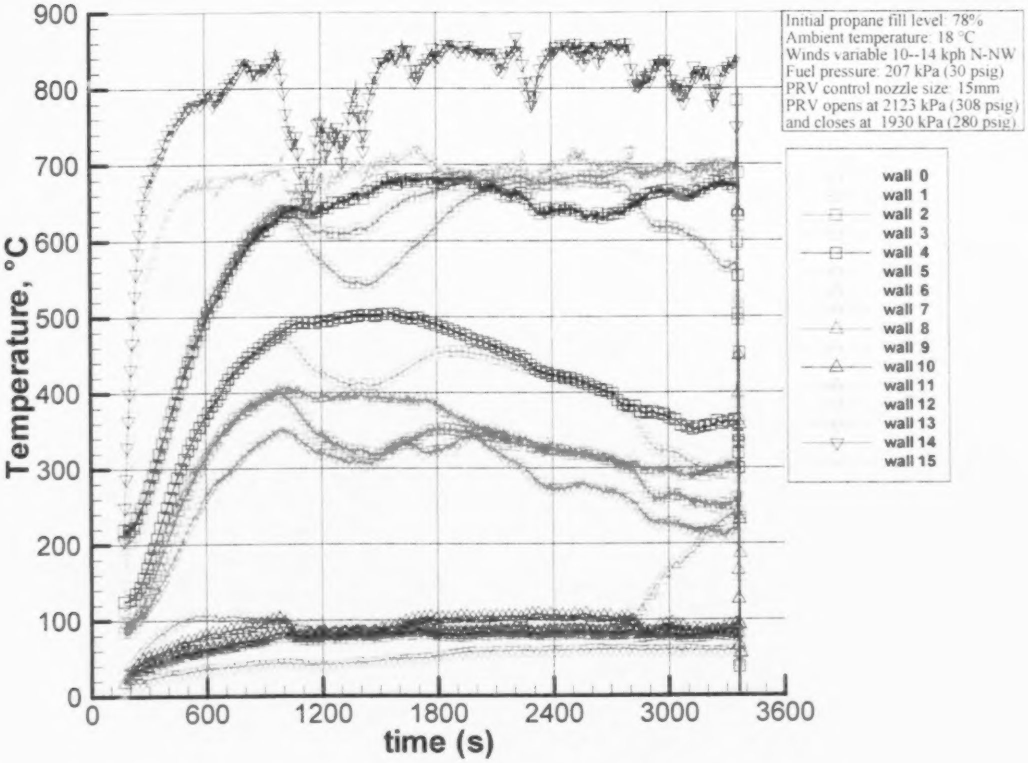

Figure 4.35: Wall temperature, Test 04-4b (16% insulation defect, low hoop stress)

The outer steel jacket temperature rose rapidly to peak at about 850°C, suggesting a fire temperature in the range of 870-900°C. The peak tank wall temperature levelled off around 680°C. For one period of about 8 minutes, the fire dropped below 700°C. The wind caused fluctuations in the fire, clearly seen in the jacket and wall temperature data.

The tank failed at 53 minutes (after start of second fire), much longer than predicted for the high wall temperatures achieved. The SA 455 steel was tougher than expected. If the time span when the fire was poor were removed from the test duration period, the adjusted failure time would be about 30-35 minutes, which is more in line with expectations.

The failure was a jet release once again. Figures 4.36 and 4.37 show the tank soon after the jet release and the failure opening respectively. The lading was isothermal (Figure 4.38) and near the superheat limit, so there was a lot of energy available in the tank at the time of failure. It could well be that the jacket slowed the depressurization and suppressed the strong pressure transient that could have restarted the crack to give a BLEVE.

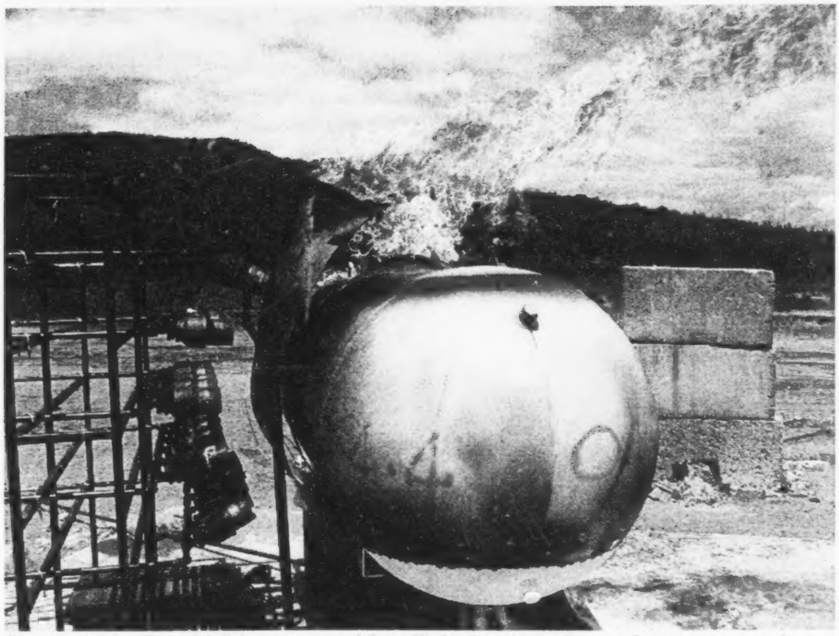

Figure 4.36: Test 04-04 rupture with split jacket (note burned vapour space)

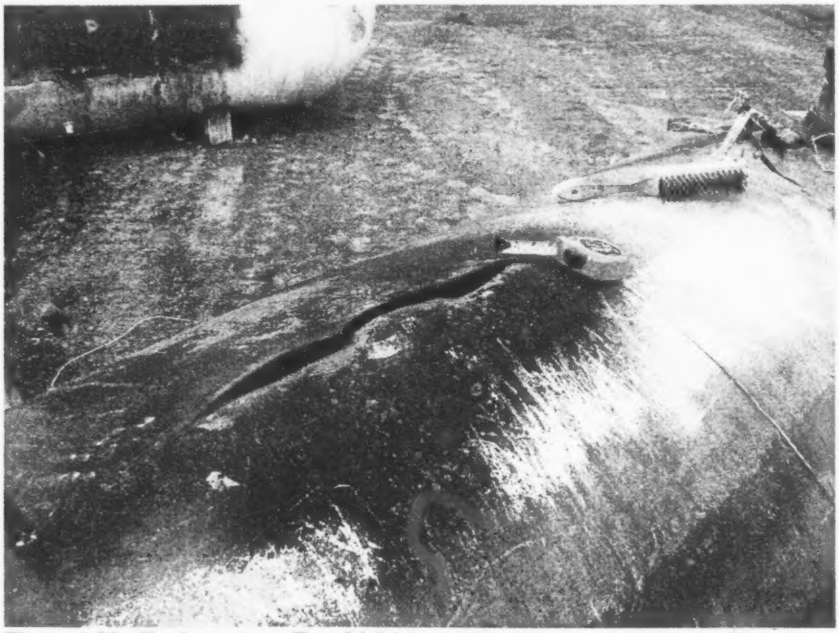

Figure 4.37: Tank rupture, Test 04-04 (note jagged tear, suggesting wall made contact with jacket and jacket provided some support)

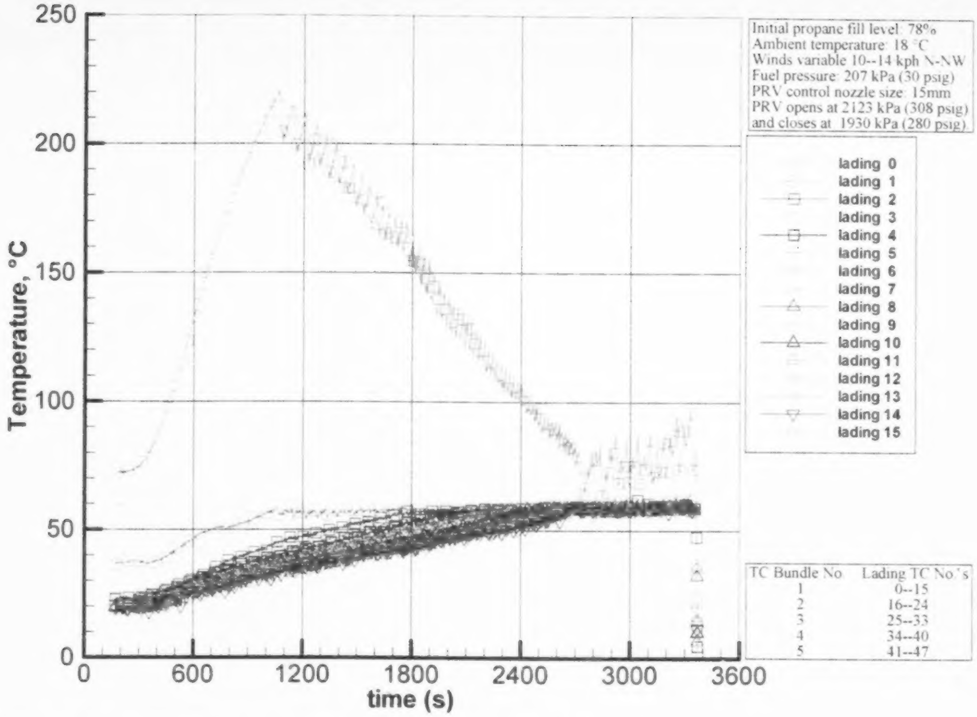

Figure 4.38: Lading temperature (TC bundle 1), Test 04-4

Jacket temperatures were very similar to the high hoop-stress version of this test, Test 04-3. Table 4.2 provides a comparison of some salient parameters between the high and low hoop-stress tests. Wall temperatures were a little different. In Test 04-3 the wall temperatures were still rising and above 700°C at failure at 1400 seconds. However, in Test 04-4 wall temperatures levelled off at 680-690°C, evening out at 3200 seconds. This was probably due to the cooler vapour space with the PRV cycling and a slightly higher propane fill level.

Table 4.2: Comparison of results for high and low hoop-stress test pair

	Fill Level	PRV Open	Failure Time	Peak Wall T	T Vapour	T Liquid
Test 04-3 High Stress	71%	2.63 MPa never opened	24 min	720°C	70°C	40°C
Test 04-4 Low Stress	78%	2.12 MPa 79 cycles	53 min	700°C	280°C	60°C

4.6 Small Thermal Defect, Test 04-5

This test involved a tank with an 8% insulation defect area. The "small" defect was 65 cm (26 in.) wide, spanning almost the entire tank circumference except for the bottom 20-30 degrees. This defect was half the width of the previous large defects tested. The remainder of the tank was insulated with 13 mm tank car ceramic fibre insulation. Again, the white surface of the tank wall was painted black in the region of the defect to ensure a high emissivity.

As in the large insulation defect case, Test 04-3, the tank was filled and purged with 1300 L of propane, about 71% fill by volume. The PRV was set to pop at 2.63 MPa (381 psig) and close at 2.39 MPa (346 psig). The simulated PRV had a 15 mm orifice.

The test began with the wind 11 km/h from the SSW. The test started off well and by the 2000 second mark the jacket temperature was 860°C and the wall temperature was 700°C. Figures 4.39 and 4.40 show the wall thermocouple layout and wall and jacket temperature results, respectively. The wind then picked up and for about 1000 seconds and the wall and jacket temperatures dropped substantially. The wind then recovered and the test continued with rising wall temperatures. The tank failed with a minor rupture at about 3550 seconds.

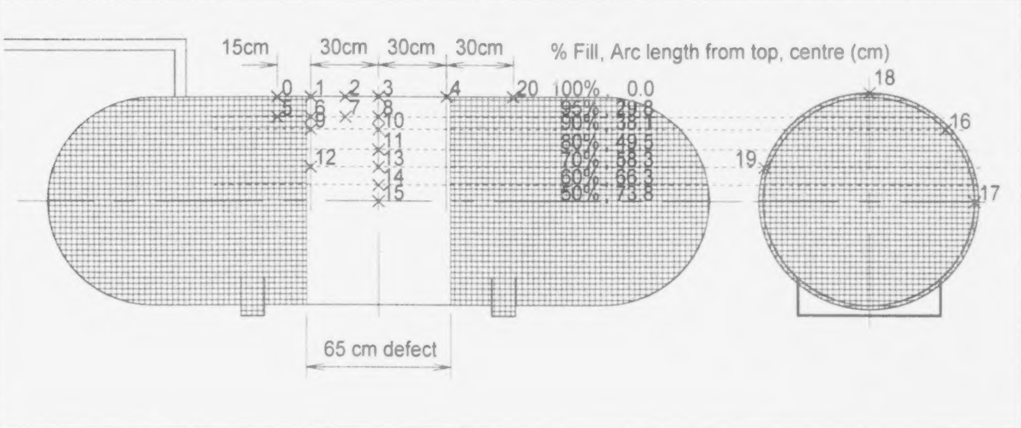
15cm
30cm
30cm
30cm
% Fill, Arc length from top, centre (cm)
0
1
2
3
4
20
5
6
7
8
9
10
11
12
13
14
15
100% , 0.0
95% , 29.8
90% , 38.1
80% , 49.5
70% , 58.3
60% , 66.3
50% , 73.8
18
16
19
17
65 cm defect

Figure 4.39: Wall thermocouple layout for Test 04-5

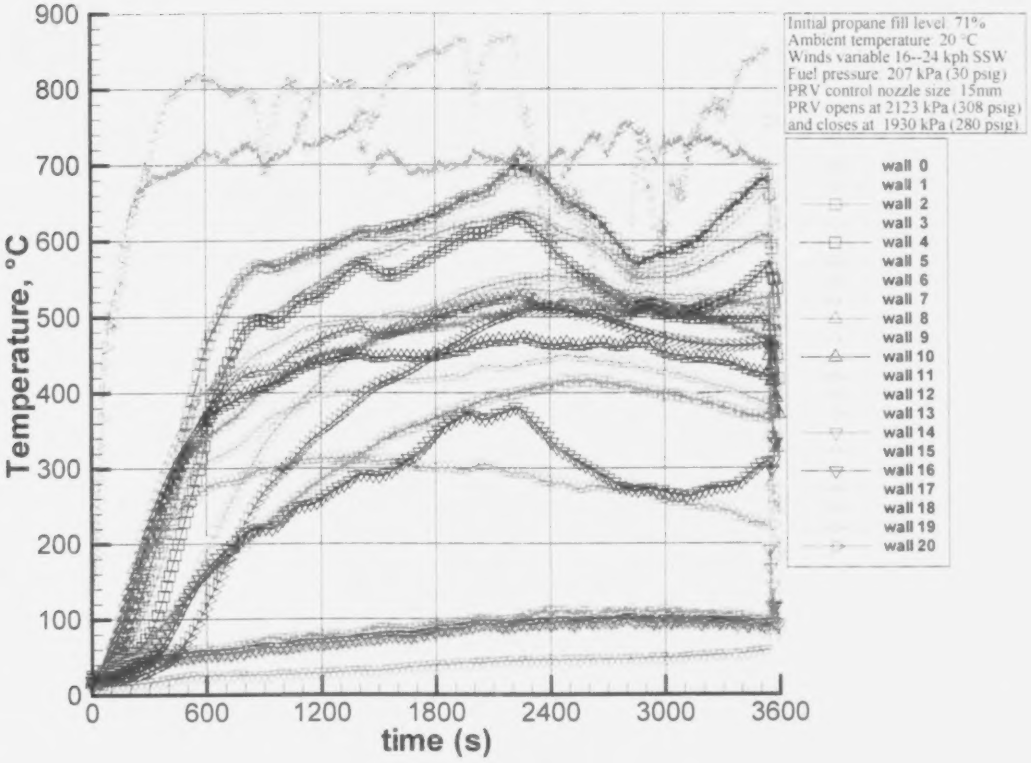

Figure 4.40: Wall temperature, Test 04-5 (8% insulation defect). Flame lifted or shifted for approximately 1200 seconds of the test duration

The PRV initially opened at 2130 seconds (35.5 minutes) and cycled 16 times (Figure 4.41) before the tank had a minor rupture. The split was so small the jet did not tear the jacket open (Figure 4.42). The tank was engulfed in a swirling fire from the leaking propane. After the tank had cooled and the outer steel jacket was removed, the tear opening in the tank wall was measured to be 64 mm long, with a maximum opening width of 2 mm. There was a vertical deformation of 51 mm from the surface of the tank. The tear was not large enough to effectively depressurize the tank, and the test was ended by dumping and burning the liquid propane.

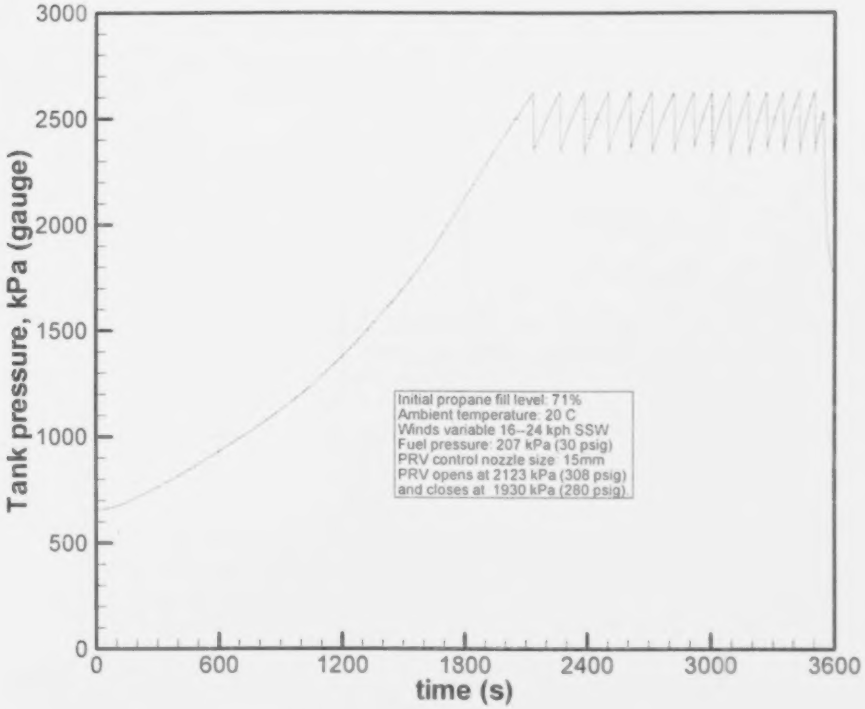

Figure 4.41: Tank pressure, Test 04-5

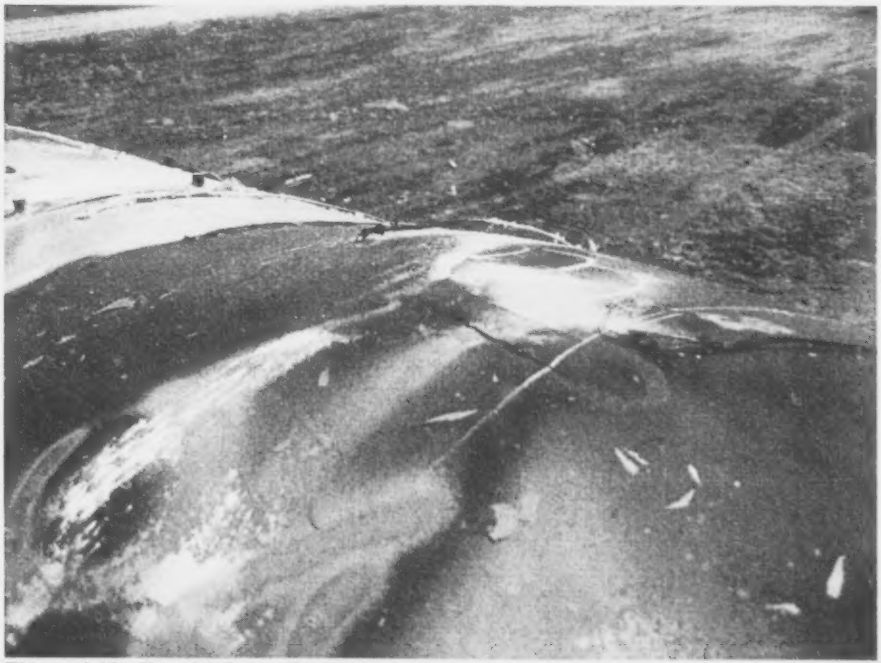

Figure 4.42: Test 04-5, small rupture with small insulation defect (again, tank wall contact with the outer steel jacket is suspected)

Of special note is that the entire vapour space wall was very hot. The tank wall temperature under the insulation near the end of the tank exceeded 500°C, far higher than predicted.

This result shows that even a relatively narrow insulation defect, 65 cm (26 in.), can result in a tank rupture if the tank is able to pressurize. If the defect size were scaled by tank wall thickness, this would represent a defect length of about 1.3 m on a tank-car.

The tank failed in about 3600 seconds but about 1200 seconds was with low fire heating (wind effecting fire). If the time at lower fire is subtracted from the time to failure seen in the test, it suggests that the tank could have failed in about 2400 seconds (40 minutes) under ideal fire conditions. Even this correction does not go far enough – if we extrapolate from the wall temperature plots, the failure could have occurred as early as 36 minutes. If we scale this by the tank diameter, the tank-car fail time would be about 109 minutes, which is outside the 100-minute limit. In other words, this defect appears to be close to the upper limit of allowable defect length.

4.7 Results Summary

In this test series, 500-gal. tanks were used as models for 33,000-gal. tank-cars. The fire was designed to represent a full-scale pool fire with an effective blackbody temperature in the range of 871 ±56°C. The plan was to have similar stress conditions in the tanks so that failure would also be similar.

Time to failure is affected by the heat-up time of the steel and is related to the wall thickness. Failure time is also related to the heating of the liquid, and this depends on the tank volume-to-surface area ratio (i.e., approximately the tank diameter). Because of these two effects, it was predicted that everything would happen about three times faster for the 500-gal. tank than the 33,000-gal. tank. For example, an unprotected tank-car would fail in a fire in about 24 minutes. The 500-gal. tank in baseline Test 04-6 failed in 8 minutes.

These tests were conducted with about 25% fire engulfment. This condition should give vapour space peak wall temperatures very similar (but slightly lower) to 100% engulfment, but the tank should pressurize and empty through the PRV about four times slower. This means the tanks should fail a little later than if they were 100% engulfed.

Test results are summarized in Table 4.3. Figure 4.43 shows top-centre tank wall-temperature data for the pertinent tests.

Table 4.3: Test summary

	Test 04-1: **Baseline, No Jacket, No Insulation**	**Test 04-2:** **3 mm Steel Jacket and 13 mm thick Ceramic Fibre Insulation with 16% Area Defect**	**Test 04-3:** **3 mm Steel Jacket and 13 mm thick Ceramic Fibre Insulation with 16% Area Defect**	**Test 04-4:** **3 mm Steel Jacket and 13 mm thick Ceramic Fibre Insulation with 16% Area Defect Lower Hoop Stress**	**Test 04-5:** **3 mm Steel Jacket and 13 mm thick Ceramic Fibre Insulation with 8% Area Defect**	**Test 04-6:** **Baseline, No Jacket, No Insulation**
PRV Settings	2.63 MPa 9% blowdown	2.63 MPa 9% blowdown	2.63 MPa 9% blowdown	2.12 MPa 9% blowdown	2.63 MPa 9% blowdown	2.63 MPa 9% blowdown
Nozzle	15 mm	15 mm	15 mm	15 mm	15 mm	15 mm
PRV Pipe Fitting	2 inch	2 inch	2 inch	2 inch	2 inch	2 inch
Initial Fill	78%	71%	71%	78%	71%	80%
Approximate Volume	1430 L	1300 L	1300 L	1430 L	1300 L	1460 L
Fuel Pressure	30 psi	30 psi	30 psi	30 psi	30 psi	30 psi
Wall Thickness	7.1 mm	7.1 mm	7.1 mm	7.1 mm	7.1 mm	7.1 mm
Initial Lading Temperature	15°C	15°C	11°C	21°C**	13°C	14°C
Wind Conditions	Light 2-4 km/h E Flame lifted or shifted: 1800 s 30.0 min	7-16 km/h Variable NW-SW Flame lifted or shifted: 4200 s 70.0 min	13-18 km/h WSW Flame lifted or shifted: 250 s 4.2 min	Variable 10-14 km/h N-NW Flame lifted or shifted: 1200 s 20.0 min	16-20 km/h SSW Variable Flame lifted or shifted: 800 s 13.3 min	10-14 km/h WNW Flame lifted or shifted: 0 s 0 min
Time to Failure	2645 s 44.1 min	NA	1425 s 23.8 min	3360 s 56.0 min	3545 s 59.1 min	480 s 8.0 min
Adjusted Time to Failure*	11 min	NA	20 min	24-36 min	30-46 min	8.0 min
PRV Pops	44	42	0	79	16	0
Fill at Failure	70%	NA	71%	64%	65%	80%
Time to First PRV Pop	786 s 13.1 min	2678 s 44.6 min	NA	1063 s 17.7 min	2133 s 35.6 min	NA
Time to Destratify	NA	4600 80 min	NA	2550 42.5 min	NA	NA
Liquid Temp	45-69°C	Uniform at 69°C at 4600 s	37°C	60°C	50°C	40°C
Peak Wall Temp at 6 Minutes	175°C	107°C	256°C	274°C	149°C	620°C
Peak Wall Temp at Failure	720°C	NA	705°C	702°C	665°C	720°C
Time to 427°C Peak Wall Temp	1460 s	2300 s	468 s	480 s	574 s	166 s
Type of Failure	Strong BLEVE	None	Jet Release	Jet Release	Jet Release	Jet Release
Initial Jet	0.1 s	NA	NA	NA	NA	NA
Number of Pieces	1	NA	1	1	1	1
Failure Description	Completely Flattened End caps separated Wall thinning evident	NA	Tear length 343 mm Max. Tear Width 32 mm Vertical deformation 76 mm Wall thinning evident	Tear length 457 mm Max. Tear Width 19 mm Vertical deformation 76 mm Some wall thinning, irregular	Tear length 64 mm Max. Tear Width 2 mm Vertical deformation 51 mm Wall thinning evident	Tear length 368 mm Max. Tear Width 45 mm Vertical deformation 89 mm Wall thinning evident
Final Location of Tank	On Pad	On Pad, On Stand	On Pad, On Stand	On Pad, On Stand	On Pad, On Stand	On Pad, On Stand
Comments	- wind direction was a problem, wind from E caused flame to lift from tank -wind changed to W and tank failed within 8 minutes -Broken Windows at approx. 170 m from blast	- fire was fuel starved - replaced 1/2" copper line with 1" pipe and filled tank for water test - wall reached 640°C under jacket in 10 min. for water test with modified fuel supply line				- tank failed so rapidly, liquid was still cool - PRV did not have chance to activate - no BLEVE

***(Adjusted Time to Failure) = (Time to Failure) - (Time Flame Lifted or Shifted)**

****Initially 15°C, 21°C after re-start**

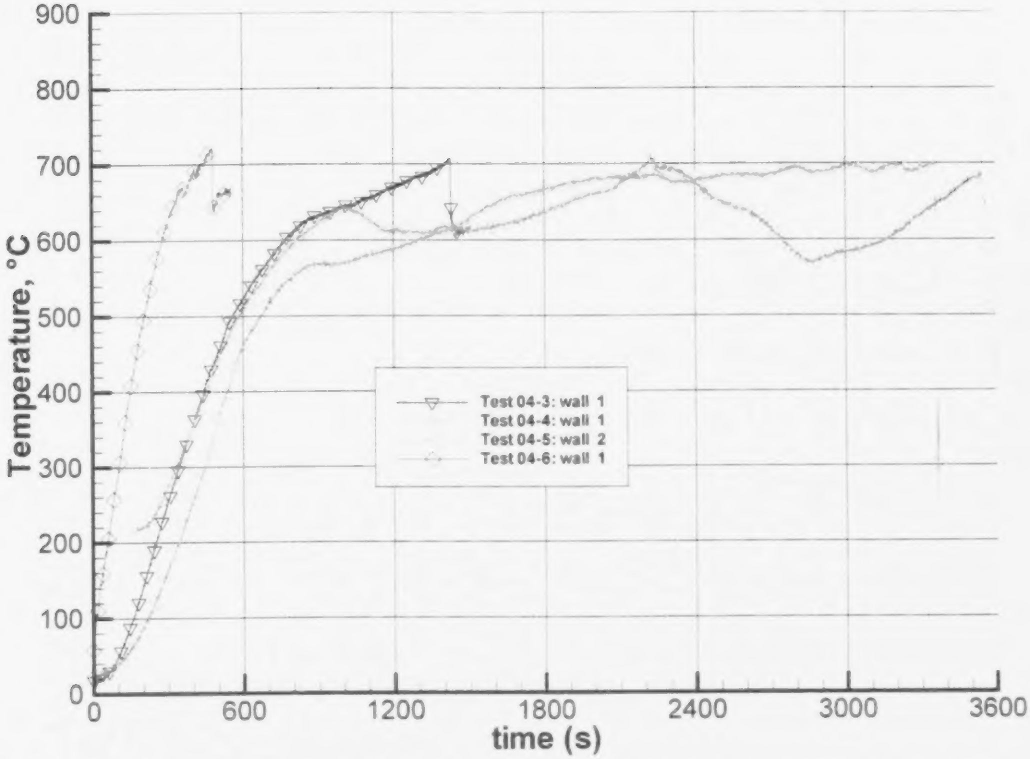

Figure 4.43: Tank wall temperature for tests 04-3, 04-4, 04-5, and 04-6 (thermocouple located at top and centre of the tank)

The peak wall temperature data in Figure 4.43 show the expected trends for the data set. The baseline (no protection), Test 04-6, has the most rapid wall heating, followed by lower heating rates for the large insulation defect cases, Tests 04-3 and 04-4. As expected, the lowest heating rate was seen with the small insulation defect, Test 04-5. The plots clearly show when fire intensities dropped due to wind effects. The two tests with 16% defect (high 04-03 and low 04-04 hoop stress cases) should have virtually the same wall temperature plots. The reason they do not is due to wind effects.

The following comments highlight the results of this test series:

i) The baseline tank, Test 04-6, failed in 8 minutes, suggesting fire conditions and tank conditions were credible. It also suggests scaling to the full-scale tank car using the tank diameter is valid.

ii) The tank with the large insulation defect, 16% area defect, with 25% fire exposure (100% of defect under fire) failed in 24 minutes. If scaled to a tank-car, this would predict failure in 72 minutes, well under the required minimum 100-minute mark.

iii) The tank with the smaller insulation defect, 8% area defect, with 25% fire exposure (100% of defect under fire) should have failed in approximately 36 minutes (corrected for poor fire exposure). Scaled to a tank-car, this would predict failure in 109 minutes, just over the required minimum 100-minute mark.

5.0 Conclusions

The main conclusions from this work are as follows:

i) The baseline test resulted in tank failure in 8 minutes. If this is scaled by the tank diameter, then an unprotected tank-car failure could be expected at about 24 minutes. This agrees well with the RAX 201 test and suggests that the scaling approach is valid.

ii) The fire temperature ranged between about 700 and 927°C. When the fire was below 816°C it was not considered credible and adjustments to some tests were necessary. In most cases, the fire was between about 820 and 870°C, which is in line with fire-test standards. Credible liquid hydrocarbon pool fires are in the range of 800-950°C [12].

iii) The entire vapour space got very hot, including areas not exposed to fire and under thermal protection. This is partly due to high vapour temperatures before the PRV is activated. With small defects the PRV can take a long time to pop and this can give very high vapour temperatures (> 300°C).

iv) The jacket temperatures were in line with expectations based on thermal modelling. With good fire contact the jacket temperatures were in the range of 780-860°C. This would be quite close to the effective fire temperature.

v) The cooling effect of the liquid surface did not appear to be as strong as previously believed. The tanks failed with high fill levels (higher than 70%). Tank pressurization was in line with expectations. The tank pressurizes much faster than predicted by single-node thermal models such as AFFTAC. The time to PRV action is inversely proportional to the defect fraction. We also know from previous testing that pressurization depends on the fill level and the location of the heating.

vi) The SA 455 steel as tested was tougher than expected based on minimum properties of SA 455 (minimum UTS = 480-515 MPa, actual test steel was approximately 610 MPa). Modelling based on minimum properties of SA 455 suggested the wall should fail when the wall temperature reached about 650°C. The wall temperatures reached 720°C at failure in the present tests.

vii) The SA 455 seems to have stress-rupture properties very similar to the TC 128 used in tank-cars.

viii) For the tank tested, with the fire conditions used, an 8% insulation defect resulted in tank failure in about 36 minutes (corrected for poor fire). This scales to about 109 minutes for a rail tank-car if scaled by the tank diameter. This suggests that an 8% insulation defect is near the upper limit of allowable defects for the conditions tested.

6.0 Recommendations

It is recommended that further medium-scale tests be conducted to firm up conclusions relating to:

i) tanks with high fill levels (initial fill > 0.95)
ii) smaller defects
iii) effect of condition of remaining thermal protection

Following these tests, it may be appropriate to conduct full-scale tests to confirm study conclusions.

References

1. Birk AM, VanderSteen JDJ, 2003, *Burner Tests on Defective Thermal Protection Systems, TP 14066E*, Transportation Development Centre, Transport Canada.
2. Birk AM, 2000, *Review of AFFTAC (Analysis of Fire Effects on Tank Cars) Thermal Model, TP 13539E*, Transportation Development Centre, Transport Canada.
3. Birk AM, Cunningham MH, 1999, *Thermographic Inspection of Tank-Car Insulation: Field Test Manual, TP 13517E*, Transportation Development Centre, Transport Canada.
4. Birk AM, Cunningham MH, 2000, *Tank-Car Insulation Defect Assessment Criteria: Thermal Analysis of Defects, TP 13518E*, Transportation Development Centre, Transport Canada.
5. Birk AM, Yoon KT, 2004, *High Temperature Stress-Rupture Tests of Sample Tank-Car Steels, TP 14356E*, Transportation Development Centre, Transport Canada.
6. Townsend W, Anderson CE, Zook J, Cowgill G, 1974, *Comparison of Thermally Coated and Uninsulated Rail Tank-Cars Filled with LPG Subjected to a Fire Environment, FRA-OR&D 75-32*, US DOT Report.
7. Moodie K, Cowley LT, Denny RB, Small LM, Williams I, 1988, Fire Engulfment Test of a 5 Tonne LPG Tank, *Journal of Hazardous Materials* 20:55-71.
8. Droste B, Schoen W, 1988, Full Scale Fire Tests with Unprotected and Thermal Insulated LPG Storage Tanks, *Journal of Hazardous Materials* 20:41-54.
9. Birk AM, Cunningham MH, Ostic P, Hiscoke B, 1997, *Fire Tests of Propane Tanks to Study BLEVEs and Other Thermal Ruptures: Detailed Analysis of Medium Scale Test Results, TP 12498E*, Transportation Development Centre, Transport Canada.
10. Anderson CE, 1982, *Rail Tank Car Safety by Fire Protection*, 6th International Fire Protection Seminar.
11. Rew PJ, Hulbert WG, Deaves DM, 1997, Modelling of Thermal Radiation from External Hydrocarbon Pool Fires, *Trans IChemE* 75(B):81-9.
12. Bainbridge BL, Keltner NR, 1988, Heat Transfer to Large Objects in Large Pool Fires, *Journal of Hazardous Materials* 20:21-40.
13. Nakos JT, Keltner NR, 1989, The Radiative -Convective Partitioning of Heat Transfer to Structures in Large Pool Fires, ASME publication HTD-Vol 106, *Heat Transfer Phenomena in Radiation, Combustion and Fire*, 381-387, National Heat Transfer Conference.
14. Hottel HC, Sarofim AF, 1967, *Radiative Transfer*, New York, McGraw-Hill Book Company.
15. Carey VP, 1992, *Liquid Vapor Phase Change Phenomena*, Washington, Hemisphere Publishing Corp.
16. Holman JP, 1976, *Heat Transfer*, New York, McGraw Hill Book Company.
17. Boyer HE, 1988, *Atlas of Creep and Stress Rupture Curves*, Metals Park, Ohio, ASM International.
18. Rohsenow WM, Hartnett JP, Ganic EN, 1985, *Handbook of Heat Transfer Fundamentals*, New York, McGraw-Hill Book Company.
19. Baum MR, Butterfield JM, 1979, Studies of the Depressurization of Gas Pressurized Pipes During Rupture, *Journal of Mechanical Engineering Science* 21(4):253-61.

20. Balke C, Heller W, Konersmann R, Ludwig J, 1999, *Study of the Failure Limits of a Tank Car Filled with Liquefied Petroleum Gas Subjected to an Open Pool Fire Test, BAM Project 3215*, Federal Institute for Materials Research and Testing (BAM).
21. Birk AM, VanderSteen JDJ, Davison C, Cunningham MH, Mirzazadeh I, 2003, *PRV Field Trials -- The Effects of Fire Conditions and PRV Blowdown on Propane Tank Survivability in a Fire, TP 14045E*, Transportation Development Centre, Transport Canada.
22. Pierorazio AJ, Birk AM, 1998, *Evaluation of Dangerous Goods Pressure Relief Valve Performance -- Phase II: Small Vessel PRV Tests, TP 13259E*, Transportation Development Centre, Transport Canada.
23. Birk AM, Cunningham MH, 1994, *A Medium Scale Experimental Study of the Boiling Liquid Expanding Vapour Explosion, TP 11995E*, Transportation Development Centre, Transport Canada.
24. Birk AM, 2005, *Thermal Model Upgrade for the Analysis of Defective Thermal Protection Systems, TP 14368E*, Transportation Development Centre, Transport Canada.
25. Birk AM, 1996, Hazards from BLEVEs: An Update and Proposal for Emergency Responders, *Journal of Loss Prevention in the Process Industries* 9(2):173-81.

Appendix A: Fire Condition Verification

The design criteria for the burner array required that the burners produce a flame front that was equivalent to an engulfing fire with an effective black body temperature of 871 ±56°C.

The effective blackbody fire temperature can be estimated by examining the heat transferred to the liquid lading using these two formulae:

$$Q_{Liq} = \rho_{Liq} V_{Liq}\, C_p\, (dT_{Liq\,Avg}/dt) \tag{A.1}$$

$$Q_{Liq} = A_{Liq}\, \varepsilon\, \sigma\, F_{12}\, (T^4_{fire} - T^4_{Wall}) \tag{A.2}$$

Equation A.1 can be used to calculate the heat transfer rate to the liquid lading, Q_{Liq} (kW) when the following values are known or can be estimated:

ρ_{Liq},	liquid lading density. Estimate based on tank pressure and average liquid temperature.
V_{Liq},	liquid lading volume.
C_p,	specific heat of the liquid lading. Estimate based on tank pressure and average liquid temperature.
$dT_{Liq\,Avg}/dt$,	heating rate of the liquid. This was estimated from lading thermocouple data using an algorithm (written for MATLAB) that sorts the liquid and vapour phase readings and then averages the readings for each phase. Further details of this algorithm are presented in Appendix B.

Radiative heat transfer to the liquid-wetted tank wall is given by Eqn. A.2. It can be used to estimate the fire temperature, T_{fire}, when the following values are known or can estimated:

Q_{Liq},	heat transfer rate to the liquid lading. Estimated from Eqn. A.1.
A_{Liq},	the liquid-wetted wall area exposed to flame. This was estimated to be liquid wetted wall covered by the visible flame for un-insulated tanks and assumed to be the un-insulated wetted wall area covered by visible flame for insulated tanks.
$\varepsilon = 0.9$,	emissivity of the tank or jacket surface. The steel surface was assumed to have an emissivity of 0.9.
σ	Stefan-Boltzmann constant.
$F_{12} = 1$,	the view factor from the tank to the fire.
T_{wall},	liquid wetted wall temperature estimate, based on wall thermocouple readings.

An equation solving software package with thermodynamic property functions (Engineering Equation Solver) was used to solve for the two unknowns Q_L and T_{Fire}. Table A.1. displays input data and the estimates for Q_L and T_{Fire} for each of the tests.

Table A.1: Fire temperature verification data and results.

	A_{liq} (m^2)	$DT_{Liq\ Avg}/dt$ (°C/s)	P_{tank} (kPa)	$T_{Liq\ Avg}$ (°C)	T_{Wall} (°C)	V_{Liq} (m^3)	Q_L (kW)	T_{fire} (°C)
Test 04-1	1.50	0.0259	1350	21.8	100	1.47	51.2	637.6
Test 04-2	1.22	0.0119	1108	22.6	650	1.34	21.4	744.1
Test 04-3	1.22	0.0208	1030	19.8	790	1.34	37.4	897.6
Test 04-4	1.33	0.0217	1425	29.7	680	1.47	43.2	826.3
Test 04-5	0.55	0.0137	1220	21.9	710	1.34	24.7	887.2
Test 04-6	1.50	0.0643	1480	28.4	78	1.47	127.7	865.8

The results show that, as suspected, Tests 04-1 and 04-2 had insufficient fire conditions. In all other tests, it appears that the burner system delivered a flame that was equivalent to an engulfing fire with an effective black body temperature in the required range of 871 ±56 °C.

Appendix B: Lading Temperatures

B.1 Lading Thermocouple Location

Figure B.1 shows the location and number scheme for the five lading-thermocouple bundles.

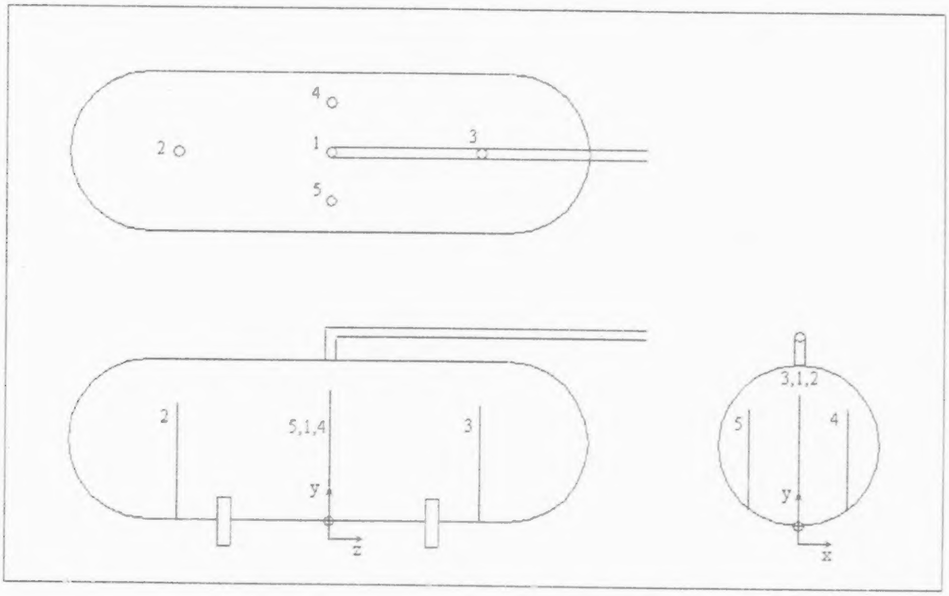

Figure B.1: Thermocouple bundle location.

Figure B.2 shows how the fill angle is defined.

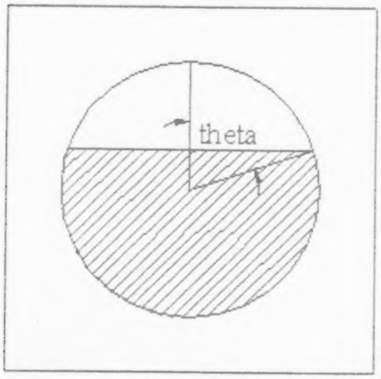

Figure B.2: Fill angle.

Table B.1 gives the bundle number and Cartesian coordinates for each lading thermocouple.

Table B.1: Tank coordinates of individual thermocouples.

t/c	Fill	B#	x(in)	y(in)	z(in)		t/c	fill	B#	x(in)	y(in)	z(in)
T0	0.9	1	0	30.9	0		T24	0.1	2	0	6.1	-35
T1	0.8	1	0	27.3	0		T25	0.8	3	0	27.3	35
T2	0.75	1	0	25.7	0		T26	0.75	3	0	25.7	35
T3	0.7	1	0	24.2	0		T27	0.7	3	0	24.2	35
T4	0.65	1	0	22.7	0		T28	0.65	3	0	22.7	35
T5	0.6	1	0	21.3	0		T29	0.6	3	0	21.3	35
T6	0.55	1	0	19.9	0		T30	0.5	3	0	18.5	35
T7	0.5	1	0	18.5	0		T31	0.4	3	0	15.7	35
T8	0.45	1	0	17.1	0		T32	0.25	3	0	11.3	35
T9	0.4	1	0	15.7	0		T33	0.1	3	0	6.1	35
T10	0.35	1	0	14.3	0		T34	0.8	4	11.5	27.3	0
T11	0.3	1	0	12.8	0		T35	0.75	4	11.5	25.7	0
T12	0.25	1	0	11.3	0		T36	0.6	4	11.5	21.3	0
T13	0.2	1	0	9.7	0		T37	0.5	4	11.5	18.5	0
T14	0.15	1	0	8	0		T38	0.4	4	11.5	15.7	0
T15	0.1	1	0	6.1	0		T39	0.25	4	11.5	11.3	0
T16	0.8	2	0	27.3	-35		T40	0.1	4	11.5	6.1	0
T17	0.75	2	0	25.7	-35		T41	0.8	5	-11.5	27.3	0
T18	0.7	2	0	24.2	-35		T42	0.75	5	-11.5	25.7	0
T19	0.65	2	0	22.7	-35		T43	0.6	5	-11.5	21.3	0
T20	0.6	2	0	21.3	-35		T44	0.5	5	-11.5	18.5	0
T21	0.5	2	0	18.5	-35		T45	0.4	5	-11.5	15.7	0
T22	0.4	2	0	15.7	-35		T46	0.25	5	-11.5	11.3	0
T23	0.25	2	0	11.3	-35		T47	0.1	5	-11.5	6.1	0

Table B.2 shows which thermocouples are present in each of the bundles.

Table B.2: Thermocouple layout for each bundle type.

fill	angle (°)	height(in)	Centre	Sides	Ends
10%	132.1	6.1	x	x	X
15%	124.6	8	x		
20%	118.4	9.7	x		
25%	113	11.3	x	x	X
30%	107.9	12.8	x		
35%	103.2	14.3	x		
40%	98.7	15.7	x	x	X
45%	94.3	17.1	x		
50%	90	18.5	x	x	X
55%	85.7	19.9	x		
60%	81.3	21.3	x	x	X
65%	76.8	22.7	x	x	
70%	72.1	24.2	x	x	
75%	67.1	25.7	x	x	X
80%	61.6	27.3	x	x	X
90%	48	30.9	x		

B.2 Average Lading Temperature Calculations

Average liquid and average vapour temperatures were required to calculate heat transferred to the lading for use in various calculations. To do this it was necessary to go through the lading thermocouple data (48 thermocouples) and determine for each time step, whether each thermocouple was in the vapour or in the liquid. This was accomplished using MATLAB code. The input to the code was the lading temperature and pressure data as well as the information about when the PRV was open or closed.

It was assumed that the pressure in the tank corresponded to the saturation pressure given the temperature at the interface. This is generally accepted in the literature [1]. The program compared each recorded temperature to the saturation temperature given the recorded tank pressure. This was done using the propane saturation curve and polynomial curve fit equations, Equations B.1 and B.2. If the temperature was greater than the calculated saturated temperature, the thermocouple was said to be in the vapour and if it was lower, it was in the liquid. Swelling, splashing, and thermal expansion complicated this matter somewhat, and upon initial calculation, some thermocouples showed evidence of moving from the liquid to the vapour and back to the liquid several times.

$$P_{sat} = 8.512 \cdot 10^{-4} \cdot T^3 + 0.154 \cdot T^2 + 14.724 \cdot T + 477.517 \qquad \text{(B.1)}$$

$$T_{sat} = 5.492 \cdot 10^{-9} \cdot P^3 - 3.212 \cdot 10^{-5} \cdot P^2 + 8.873 \cdot 10^{-2} \cdot P - 35.247 \qquad \text{(B.2)}$$

The program was adjusted using several correction routines and checks:

- A range of 1°C was used as a transition range. A thermocouple in the liquid was not considered to move into the vapour region until its temperature was 1°C greater than the saturation temperature given the tank pressure.
- The fill level was not allowed to decrease while the PRV was closed.
- Typically, when a thermocouple moves from the liquid to the vapour, the temperature sees a sudden rise in temperature. If a change was sensed, the program checked the previous two and the next two time steps to ensure the right trends were being predicted.
- If a thermocouple moved into the vapour region, all the thermocouples above that thermocouple had to be in the vapour. An error was given if this wasn't the case.
- While a thermocouple was allowed to move back and forth from the vapour to the liquid, only one thermocouple on each bundle was allowed to do this at a time. Once a lower thermocouple made a transition from liquid to vapour, the thermocouple immediately above it was considered to be in the vapour for the remainder of the test.

The program calculates the average liquid and vapour temperatures for each time step, with each thermocouple given an equal weight.

Reference

1. Venart JES et al. 1988. Experiments on the Thermo-Hydraulic Response of Pressure Liquified Gases in Externally Heated Tanks with Pressure Relief. *Plant/Operations Progress* 7:139-144.

Appendix C: Tank Fill Level

Liquid level inside the tank determines the size and shape of the vapour space. This is a critical factor that influences convection and radiation of heat in the vapour space and the size and shape of the area of maximum shell temperature.

This appendix contains additional details regarding the pressure relief system described in the main body of the report (Section 3.4.1.2), the calculation method used to determine mass flow of propane from the tank, and a section showing tank pressure and liquid level results for the tests.

C.1 Pressure Relief System

The system used to control tank pressure and determine propane mass flow from the tank is described in Section 3.4.1.2. A computer controlled pressure relief system was used to mimic the performance of an idealized real pressure relief valve.

- The PRVs normally used in the test tank is rated for 2565 scfm (standard cubic feet per minute) of air at 300 psi gauge (250 psi + 20% overpressure).
- Using the density of standard air (1.2 kg/m^3) this corresponds to 1.49 kg air/s.
- Assuming a flow coefficient through the original PRV of approximately 80% and air at 300 psi and 25°C, the effective nozzle diameter is calculated to be 21.6 mm.
- Using the same valve, propane at 275 psi and 150°C would be discharged at 1.35 kg propane/s.

Given that a smooth converging nozzle with a high flow coefficient (0.99) was used in the field testing, the nozzle throat diameter can be calculated.

- Using propane at 275 psi and 150°C and a valve with a 99% flow coefficient, a nozzle diameter of 19.4 mm was calculated.

In order to reduce the frequency of the valve cycling, a 15 mm nozzle was used.

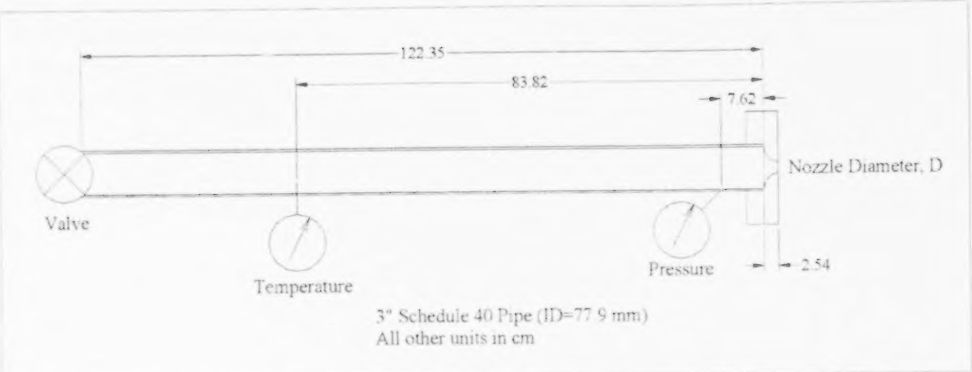

Figure C.1: PRV Nozzle (Instrumented for Mass Flow Calculations)

In a real accident scenario, a PRV will sometimes see two phase flow if the tank is very full when the PRV first opens. Any liquid that exits the tank in the experimental set up, however, is going to evaporate before the valve. The calculations presented in this thesis assume a single-phase flow.

The nozzle was manufactured according to ASME fluid meter standards. The figure shows proper dimensions.

C.2 Mass Flow Calculations

The mass flow calculations presented below assumes a single phase, choked and isentropic flow at the nozzle, and treat the superheated propane vapour as an ideal gas. An EES (Engineering Equation Solver--F-Chart Software) program used the built-in propane data to perform the calculations. The program reads in the nozzle temperature and pressure for each time step (10 readings per second) and outputs the accumulated mass flow with time. The following steps were employed:

- Assuming a specific heat ratio ($k=c_p/c_v$) of 1.1 and using Equation C.1 (an ideal gas, compressible flow relationship) for a converging nozzle, the pressure ratio between the throat pressure and the stagnation pressure was calculated to be 0.59.

$$\frac{P_{throat}}{P_{stag}} = \left[\frac{2}{k+1}\right]^{\frac{k}{k-1}} \tag{C.1}$$

- The point where the pressure and temperature measurements were made was assumed to be a stagnation point and the pressure ratio calculated above was used to determine the pressure in the nozzle (throat). This assumption is reasonable because the cross sectional area of the pipe was over 11 times bigger than the area of the nozzle.

- For a check, the real value of the specific heat ratio was calculated given the measured pressure and temperature in the nozzle. The value for k was in the range of 1.07 to 1.13 for a practical range of nozzle temperatures.
- The pressure data was used to determine when the valve was open and when it was closed. This was possible because the pressure takes a dramatic change when the valve opens and closes. The PRV position data recorded by the data acquisition system was found to be inadequate because it recorded when the signal was sent to the valve and not when the valve actually opened and closed.
- Using the tabulated propane data in EES, the enthalpy and entropy were calculated for the stagnation point using the measured temperature and pressure.

$$h_{stag}=h(T,P) \tag{C.2}$$

$$s_{stag}=s(T,P) \tag{C.3}$$

- Assuming isentropic expansion, the enthalpy was calculated at the throat, given P_{throat} and the entropy, again using the tabulated propane data in EES.

$$h_{throat}=h(P_{throat},s_{stag}) \tag{C.4}$$

- Using the enthalpy at the stagnation point and at the nozzle, the velocity at the nozzle was determined using Equation C.5.

$$h_{throat}+\frac{(v_{throat})^2}{2}=h_{stag} \tag{C.5}$$

- Using the tabulated density, the calculated velocity, measured nozzle diameter, and an assumed nozzle discharge coefficient of C_D=99%, the mass flow rate was calculated.

$$\dot{m}=C_D\cdot\rho\cdot v\cdot A \tag{C.6}$$

- The mass flow rate was integrated over time to find the total mass that had exited the tank. The amount of mass that had exited the tank at any given time was determined by Equation C.7.

$$m_{exit} = \int_0 \dot{m} \cdot dt \qquad \text{(C.7)}$$

C.3 Tank Fill Level Results

Figure C.2 shows tank pressure results for the four tests with similar fire conditions. The final rapid pressure drop for each data set indicates the point at which the tank shell fails. In the baseline and the large defect tests the pressure control system does not have a chance to cycle before the tank fails. Therefore, the tank fails with the initial fill mass of propane. The low hoop stress and small defect tests both exhibit a number of PRV cycles during the test period.

Cumulative mass flow from the low hoop stress and small defect tests are shown in Figure C.3. Fill level and propane mass inside tank versus time is shown in Figures C.4 and C.5 respectively. The fill level at any time is simply determined by subtracting the cumulative mass flow through the flow nozzle to that time from the initial fill level of the tank.

Appendix D: Water Fill Tank Tests Data Plots

Fire tests on 500-gallon tanks containing water were conducted as a final calibration check of the burner system. Burners were to deliver a flame that was equivalent to an engulfing fire with an effective black body temperature of 871 ±56 °C.

The burner fuel pressure necessary to achieve the desired fire intensity was 30 psig. This was determined from Water Tests 1 and 2 where the pressure was 20 and 40 psig respectively. Twenty-five burners were set about 9-10 inches from the tank surface, angled as depicted in Figure D.1.

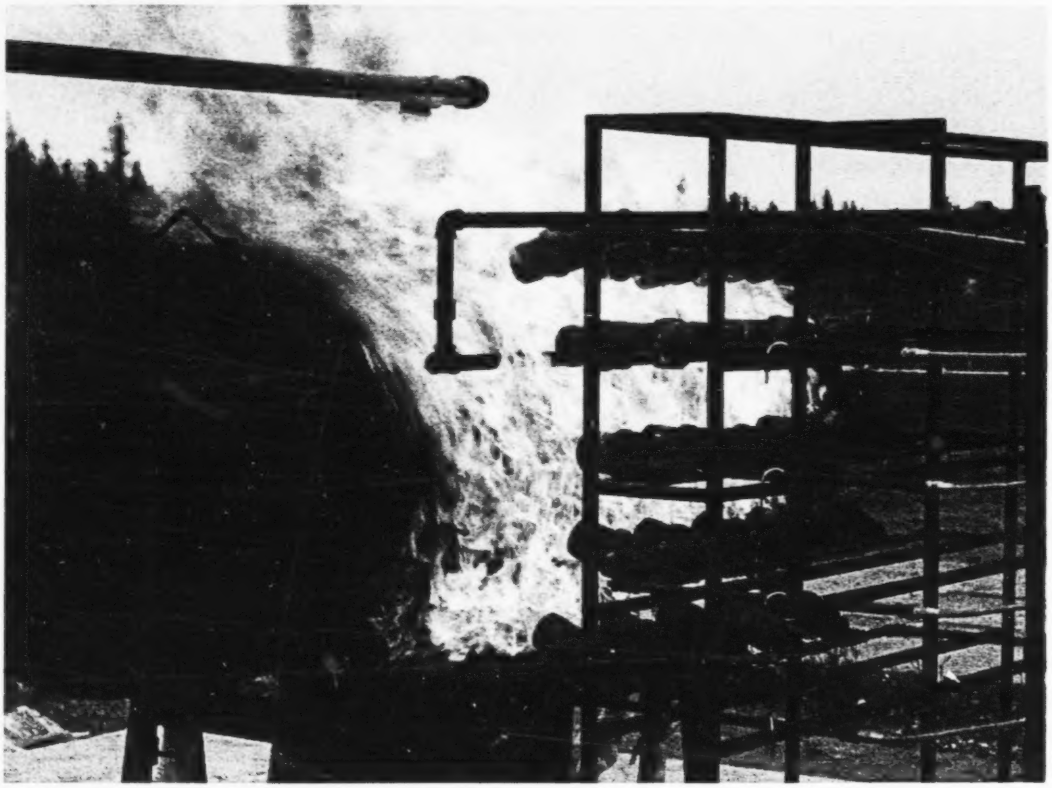

Figure D.1: Burner system in operation. Note luminous pool-fire-like flame, and flame wrapping around tank with wind from right to left (northwest wind).

Burner flames were sooty and luminous and produced a flame that looked very much like a hydrocarbon pool fire.

Flame contact was excellent (see figure above) when the wind was W or WNW. Contact was poor when wind was from the east. Prevailing winds at the test site are from the west. Therefore, it was decided to attempt to conduct tests with west winds only.

Figures D.2 and D.3 show the wall thermocouple layout used in the Water Fill Tank Tests.

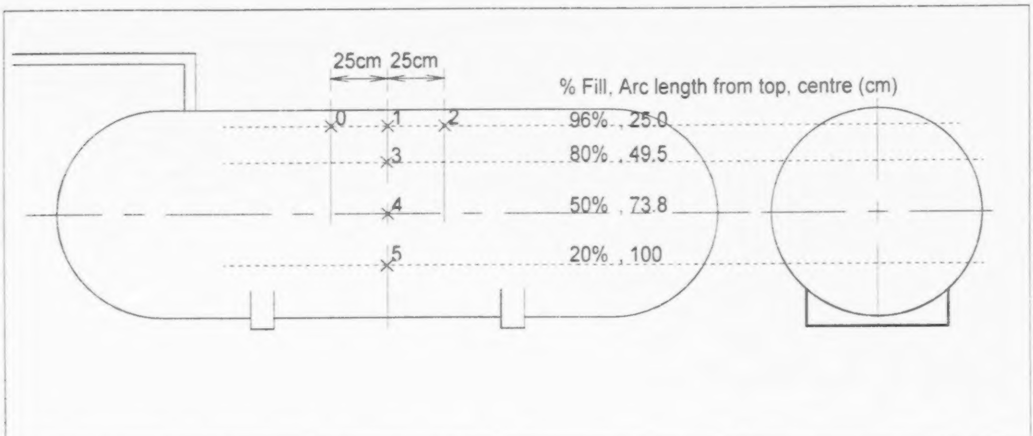
25cm
25cm
% Fill, Arc length from top, centre (cm)
0
1
2
3
4
5
96% , 25.0
80% , 49.5
50% , 73.8
20% , 100

Figure D.2: Wall thermocouple layout for Water Tank Tests 04-W1, 04-W2, 04-W3 and 04-W4.

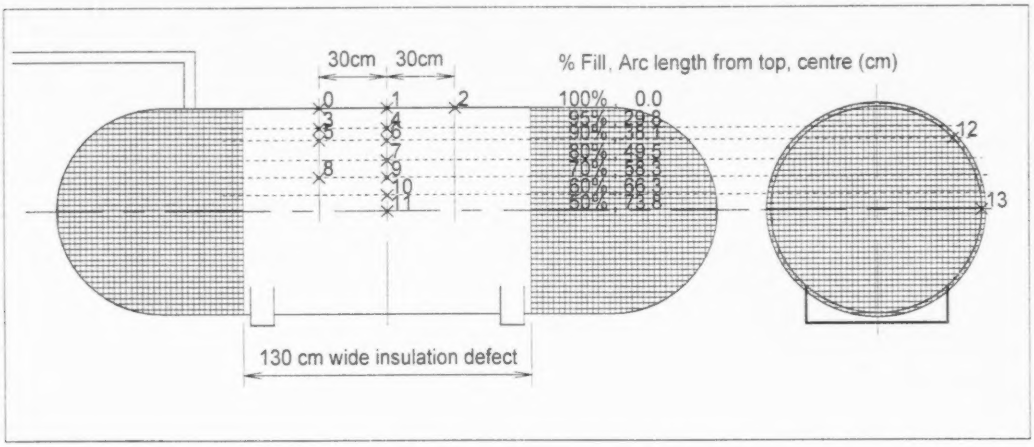
30cm
30cm
% Fill, Arc length from top, centre (cm)
0
1
2
3
4
5
6
7
8
9
10
11
12
13
100% , 0.0
95% , 29.8
90% , 38.1
80% , 49.5
70% , 58.3
60% , 66.3
50% , 73.8
130 cm wide insulation defect

Figure D.3: Wall thermocouple layout for Water Fill Tank Test 04-W5.

The following figures are presented below for each of the water fill tests:

- Wall Temperature
- Lading Temperature Data (Bundle 1)

Appendix F: Error Analysis

There were two sources of error observed in the tests:

- errors associated with the accuracy of the instruments
- errors associated with the instrument installation

Table F.1 summarizes the errors associated with the instruments, while subsections below discuss installation errors. The errors associated with the instruments were in acceptable ranges, but in some cases, installation methods resulted in significant errors.

Table F.1: Accuracy of Instruments

Measurement	Device	Accuracy
Lading Temperature	Type K Thermocouple	+/- 1°C
Tank Wall Temperature	Type K Thermocouple	+/- 1°C
Tank Pressure	Pressure Transducer	+/- 12 kPa
PRV Nozzle Pressure	Pressure Transducer	+/- 12 kPa
PRV Nozzle Temperature	Type K Thermocouple	+/- 1°C

The errors can also be categorized according to relative size:

- Large, significant errors include wall temperature measurements and initial fill estimation.
- Small, less significant errors include lading pressure, lading temperature, nozzle pressure, and nozzle temperature measurements.

F.1 Wall Temperature Errors

A new method of wall thermocouple installation was used in this series of tests. Wall thermocouples were welded with a spot welder to the surface of the tank. The fabrication method is presented in Appendix I. This method appears to have resulted in a significant improvement in accuracy and reliability over the previously used mechanical attachment method. Some preliminary testing of the wall thermocouples was done in conjunction with burner development tests, where an instrumented piece of pressure vessel steel was exposed to a torch fire. A difference of 5 to 10°C was seen between the steady measured thermocouple temperature and the temperature measured with a hand-held IR thermometer at temperatures near 500°C. The major source of error is due to conduction of heat to or from the measurement point through the thermocouple leads.

F.2 Lading Pressure and Temperature Errors

Temperatures and pressure within the tank were measured more accurately than the wall temperatures. Conduction errors were much smaller for lading thermocouples while pressure transducers were calibrated before the tests. The average vapour and liquid temperature calculations do contain errors, however. The largest amount of uncertainty results from the difficulty in determining exactly when a thermocouple moves from the liquid to the vapour and the errors in the installed thermocouple height.

To validate the process, a manual check was done. The thermocouple data file was opened into a spreadsheet and by manually inspecting the trends on a plot and comparing the temperature to the saturation temperature, it was decided when a thermocouple moved from the liquid to the vapour. The manual results were compared to the output of the program and it was seen that the two methods were comparable. The maximum difference of approximately 12°C between the two methods was seen in the average vapour temperatures. Moodie et al (1988) reported that liquid frothing and swelling made it very difficult to determine the exact location of the liquid/vapour interface in their testing.

F.3 Mass Flow Errors

The mass flow calculations depended on the measured nozzle temperature and pressure. Errors in either the measurements or calculations can result in an erroneous total mass flow and final fill at failure.

A pressure ratio between the throat pressure and the stagnation pressure of 0.59 was assumed for the calculations. This assumption was based a specific heat ratio of k=1.1. In reality, the specific heat ratio, and thus the pressure ratio depends on the nozzle temperature. The data was studied to understand the sensitivity of this parameter. For this test, given tabulated propane data and the measured nozzle temperature, the specific heat ratio ranged from 1.134 to 1.069. Table F.2 shows that varying the pressure ratio in this range has a very little effect on the total mass flow calculation.

Table F.2: Effects of Varying Nozzle Pressure Ratio on Mass Flow

P_{throat}/P_{stag}	K	total mass flow	% Different
0.57	1.172	606.3 kg	-0.20%
0.58	1.122	607.0 kg	-0.07%
0.59	1.075	607.4 kg	0.00%
0.6	1.029	607.6 kg	0.02%
0.61	0.985	607.4 kg	-0.01%

Although the errors associated with the nozzle thermocouple and pressure transducer are well within acceptable ranges, the errors can propagate through the calculations. The effect of changing the temperature, pressure, or both at the same time can be studied. Table F.3 shows how adjusting the measured values according to the instrument's tolerance affects the final answer. The biggest error occurs when both the pressure and the temperature are off by the maximum allowable amount.

Table F.3: Propagation of Errors in Mass Flow Calculations

Change	total mass flow	% Different
No Change	607.5 kg	0.00%
T-->T+1°C	606.1 kg	-0.20%
T-->T-1°C	609.0 kg	0.30%
P-->P+12 kPa	612.8 kg	0.90%
P-->P-12 kPa	602.3 kg	-0.80%
P-->P+12 kPa; T-->T-1°C	614.2 kg	1.10%
P-->P-12 kPa; T-->T+1°C	600.8 kg	-1.10%

Finally, a significant source of error comes from the uncertainty in the initial volume and mass of propane. It is estimated that the initial volume of the liquid propane in the tank after purging is +/- 10 litres. This corresponds to a mass of +/- 5.0 kg assuming the liquid propane was at 20°C.

Appendix G: Field Test Checklists

The following pages contain field test checklists:

- System 200 Data Acquisition and Control Procedure Checklist
- Data Acquisition Channel Settings
- PRV Test Checklist
- 35mm Camera Checklist
- High Speed Camera Checklist

G.1 System 200 Data Acquisition and Control Procedure Checklist

Pre-Test

1. Reinitialize all to default (operate menu).
2. Set all channel settings as required.
3. Start VI running.

All controls now active.

3. If saving to file is required press **save to file?**
4. Test controls
   - a) PRV.
   - b) burner valve.
   - c) burner ignition.
   - d) PRV shut-off.
   - e) Video cameras
   - f) SLR cameras
5. Press **Measurement** to begin measuring all channels
6. Verify measured data is correct.

Test Procedure

1. Turn on **PRV shut-off** (verify valve opens **3** times).
2. Turn on **igniters**.
3. Turn on **fuel valve**.
4. When ready to begin saving press **Start Recording.**
5. Turn off **igniters**.
6. When ready to begin recording on Racal press **Record**
7. Enable **PRV control**

ALL SWITCHES SHOULD BE GREEN.

G.2 Data Acquisition Channel Settings

Test			
Date		Time	
Directory			
File base			
Lading start channel		Pressure start channel	
Lading end channel		Pressure end channel	
Lading range		Pressure range	
Lading Scan Rate		Pressure Scan Rate	
Wall start channel		P1 s/n	
Wall end channel		P1 Location	
Wall range		P1 equation	
Wall Scan Rate		P2 s/n	
Fire start channel		P2 Location	
Fire end channel		P2 equation	
Fire range		Nozzle TC channel	
Fire Scan Rate		Nozzle TC range	
Air pressure ch		Nozzle Pressure ch	
		Nozzle Pressure range	
Air pressure range		Nozzle P s/n	
		Nozzle P eqn.	

Top View

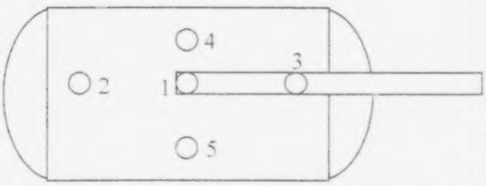

TC feedthrough numbering
1 ________
2 ________
3 ________
4 ________
5 ________

Side View

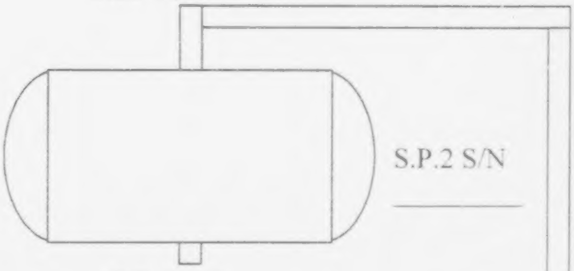

S.P.2 S/N ________

S.P.1 S/N ________
T.P. S/N ________

Notes:

____

____

____

G.3 PRV Test Checklist

Test:____________

Date:____________

Relay Box					
Both cords of relay box plugged in					
PRV shut-off pluged in					
Igniters plugged in					
Burner valve plugged in (2)					
PRV auto plugged in light on					
PRV manual plugged in					
Air line					
Compressor plugged in					
Compressor on auto					
Ball valve at compressor open					
Ball valve at receiver open					
Pressure in Air line					
Auto PRV operates					
Manual PRV operates					
PRV shut-off operates					
Igniters					
Igniters operate					
Propane Fuel					
Tank Valves open					
Manual ball valve open					
Solenoid valve operates					
Final					
PRV ball valve open					

G.4 35mm Camera Checklist

Date:____________

Test:____________

Video Cameras

B1	B2	B3	Inst. Bunk.	
☐	☐	☐	☐	Check tape is in camera and rewound
☐	☐	☐	☐	Set to camera mode
☐	☐	☐	☐	Set zoom and aim
☐	☐	☐	☐	Set manual focus
☐	☐	☐	☐	Set to record date & time
☐	☐	☐	☐	Put camera in record mode

Still Cameras

B1	B2	B3	
☐	☐	☐	**Turn cameras on**
☐	☐	☐	Check film is in camera
☐	☐	☐	Set zoom and aim
☐	☐	☐	Set to fast picture taking mode
☐	☐	☐	Set manual exposure
☐	☐	☐	**Set manual focus**

G.5 High Speed Camera Checklist

Date:___________

Test:___________

High Speed Camera

- ☐ Turn system on
- ☐ Check connections
- ☐ Check aim and focus
- ☐ Check settings (FPS, trigger point)
- ☐ Press *Ext Trig* button on front panel (Check display to ensure it engages)
- ☐ Press *Rec* button

Settings

Frames per Second: ________________________

Shutter Speed: ________________________

Trigger Point (%): ________________________

____

Record Time: ________________________

Pre-trigger record time: ________________________

Appendix H: Data Acquisition Software User's Guide

Table of Contents

H.1 Introduction H-2
H.2 System Requirements H-2
H.3 General Layout of PRV_DAQ H-3
H.4 Using PRV_DAQII H-5
    H.4.1 Start-up H-5
    H.4.2 Set-up H-5
    H.4.3 Fixed Settings H-7
    H.4.4 Running PRV_DAQII H-7
H.5 Program Structure H-9
    H.5.1 LV200.dll H-9
    H.5.2 Sub VI's H-10
    H.5.3 Graphical Programming Layout H-10
    H.5.4 Timing H-10
    H.5.5 Thermocouples H-11
    H.5.6 File output format H-11
H.6 Utility Programs H-12
H.7 Test Programs H-12
H.8 Interface Sub-VI Listing H-12

H.1 Introduction

PRV_DAQII is a data acquisition and control program that was written for the Queen's University Propane Fire Tests of Tests of August-September 2000. The program is used to remotely carry out the fire testing of propane tanks and collect temperature and pressure data during the tests.

PRV_DAQII, written using LabView 5.0, was developed specifically for the Sciemetrics System 200 data acquisition system.

H.2 System Requirements

The following hardware requirements are recommended for PRV_DAQII

1. *PIII 550* – the system can be used on a lower systems, but data acquisition rates may have to be decreased
2. *Windows 95 or 98* – the System 200 is accessed by directly reading the system memory at the interface card's base address. Windows NT does not allow the system memory to be directly addressed.
3. *1024 X 768 resolution* – the display screen was designed to be used at this resolution

H.3 General Layout of PRV_DAQ

PRV_DAQII contains both a control and data acquisition component. The control component consists of a series of toggle switches that allow various functions on the test site to be controlled remotely through the solid state relays in the System 200. The control system also includes the dead band control of a pneumatic Pressure Relief Valve. Pressure transducers on the tank supply the input for the control routine which controls the output state of the valve through a solid state relay.

The data acquisition is divided into the following 5 separate tasks:

- i) Lading temperature
- ii) Wall temperature
- iii) Fire temperature
- iv) Tank pressure
- v) Nozzle temperature and pressure
- vi) Pneumatic line pressure

The scan rate of each task can be different and therefore based on the type of instrument included in the task. These tasks can be executed in a measurement only mode as well as a measure and save to disk mode. The data is saved to disk after each sample and is not buffered in memory.

Screen Layout

The PRV_DAQII screen consists of three main areas, which are described below :

1. Switch control
   - b) Location – right hand side of upper portion of the screen
   - c) Used to :
     - i) Turn the measurement of channels on/off
     - ii) Enable/disable the automatic control of the PRV
     - iii) Turn saving on/off
     - iv) Control relays for
       - (1) Fuel line valve
       - (2) Ignitors
       - (3) Prv shut-off valve
     - v) Run PRV test – pulses PRV valve three times
     - vi) Control record/stop of the tape recorder

2. DAQ display
   - a) Location - the left hand side of the upper portion of the screen
   - b) Contains
     - i) three plots displaying :
       - (1) Tank pressure
       - (2) Lading temperature
       - (3) Wall temperature
     - ii) Switch showing current position of PRV
     - iii) Boxes for setting PRV open and close pressure.

        iv) Boolean switches to indicate which pressures are to be used for PRV control
        v) Table displaying fire temperatures
        vi) Boxes displaying
            (1) Tank pressures
            (2) Nozzle temperature
            (3) Nozzle pressure
            (4) Pressure of pneumatic line
            (5) Reference temperature for thermocouple junctions

3. Settings
    a) Location - lower portion of the screen
    b) Contains settings for the following data acquisition tasks:
        i) Lading temperature
        ii) Wall temperature
        iii) Fire temperature
        iv) Tank pressure
        v) Nozzle temperature and pressure
        vi) Pneumatic line pressure
    c) Settings for file directory and file name prefix.

H.4 Using PRV_DAQII

The following are instructions for operating PRV_DAQII :

H.4.1 Start-up

1. Double click on the PRV_DAQII icon or start LabView and open PRV_DAQII.
2. In some cases it may be required to manually find some files. A dialogue box will prompt for their locations

H.4.2 Set-up

Once the program is started, the settings for the data acquisition and control must be set if different from the current default values. Unless indicated, the settings cannot be changed while the PRV_DAQII VI is running. If settings are to be changed, stop the VI, change the settings and re-start the VI.

The following describes each setting which can be adjusted

1. File Set-up
    a) File directory – the directory name to which the files are to be saved. The directory must already exist or LabView will give an error
    b) Run name - the name of the current run that will be used as the root for all file names. The file names have the format *run-name task-name.dat*.
2. Lading Temperature
    a) Lading temperature scan rate – rate at which the lading temperature channels will be scanned and saved in samples per second.
    b) 1st TCP channel – number of the first channel to be scanned in the lading thermocouple task.
    c) Last TCP channel – number of the last channel to be scanned in the lading thermocouple task.
    d) Lading TCP range – the voltage range to be used for measuring the lading thermocouple channels

Note : all lading temperature channels must be in consecutive order on the D/A board

3. Wall Temperature
    a) Wall temperature scan rate – rate at which the wall temperature channels will be scanned and saved in samples per second.
    b) 1st TCP channel – number of the first channel to be scanned in the wall thermocouple task.
    c) Last TCP channel – number of the last channel to be scanned in the wall thermocouple task.
    d) Lading TCP range – the voltage range to be used for measuring the wall thermocouple channels

Note : all wall temperature channels must be in consecutive order on the D/A board

4. Fire Temperature
    a) Fire temperature scan rate – rate at which the fire temperature channels will be scanned and saved in samples per second.
    b) 1st TCP channel – number of the first channel to be scanned in the fire thermocouple task.

   c) Last TCP channel – number of the last channel to be scanned in the fire thermocouple task.
   d) Lading TCP range – the voltage range to be used for measuring the fire thermocouple channels

Note : all fire temperature channels must be in consecutive order on the D/A board

5. Pressure and PRV
   a) PRV relay channel – channel on the 222 board from which the solenoid for the PRV is controlled
   b) Tank Static Pressure Scan Rate – rate at which the tank pressure channels will be scanned and saved in samples per second. The PRV control loop also executes at this rate
   c) 1st pressure channel – number of the first channel to be scanned in the pressure and PRV task.
   d) Last pressure channel – number of the last channel to be scanned in pressure and PRV task.
   e) Pressure range – the voltage range to be used for measuring the pressure and PRV channels
   f) Calib Coefficients – the linear calibration coefficients for each pressure transducer in the form of $Pressure = a \cdot volts + b$
6. Mass Flow Nozzle
   a) Nozzle Scan Rate - rate at which the nozzle channels will be scanned and saved in samples per second.
   b) Nozzle TCP range – the voltage range to be used for measuring the nozzle thermocouple.
   c) Nozzle TCP channel – channel number to which the nozzle thermocouple is connected
   d) Nozzle P range – the voltage range to be used for measuring the nozzle pressure
   e) Nozzle P channel – channel number to which the nozzle pressure transducer is connected
   f) Nozzle Calib Coefficients - the linear calibration coefficients for the nozzle pressure transducer in the form of $Pressure = a \cdot volts + b$
7. Pneumatic Pressure Set-Up
   a) Air P range – the voltage range to be used for measuring the pneumatic pressure
   b) Air P channel – channel number to which the pneumatic pressure transducer is connected
   c) Air Calib Coefficients - the linear calibration coefficients for the pneumatic pressure transducer in the form of $Pressure = a \cdot volts + b$
8. PRV control (top right of screen)
   a) PRV Open Pressure – pressure in calibrated units which the PRV valve will open in dead band control. The value of the open pressure can be changed while the test is running.
   b) PRV Close Pressure – pressure in calibrated units at which the PRV valve will close in dead band control. The value of the close pressure can be changed while the test is running.
   c) Use P – indicates which pressure transducer(s) will be used as an input into the dead band control loop. The pressure transducer with the lowest channel number

is at the top. A black square indicates that the pressure transducer will be used in the dead band control. If more than one transducer is indicated, the arithmetic mean of the pressure readings is used for the PRV control. The transducers used in the average can be changed during while the test is running.

9. Channels to plot
   a) In the arrays at the right of the lading and wall temperature enter the number of the lading or wall temperatures that are to be plotted. These numbers are of the thermocouples in the tasks starting at 0 and going upwards, and not the channel number.

H.4.3 Fixed Settings

Some settings have been set within the program and cannot be set in the front panel. The channels that are fixed are outlined in the table below:

Function	Board	Channel
PRV shut-off valve	222	2
Ignitors	222	3
Fuel line valve	222	4
Racal Stop indicator	210	0 digin
Racal Record indicator	210	1 digin
Racal Stop button	210	0 digout
Racal Record button	210	1 digout

H.4.4 Running PRV_DAQII

Once the settings have been set, the following steps must be executed in sequence.

Pre-test Sequence

1. Ensure that all switches on the left hand side are off. All buttons should be red except "ignitors" which should be green.
2. Start PRV_DAQII running by pressing the run arrow on the left side of the LabView toolbar. All the control switches are now active.
3. If data is to be saved in the current session change the *Save to File* button to *Yes*.
4. To start measuring all of the channel values change the *Measurement* button to *Yes*. The test time clock is set to zero and the data in the plots cleared.

Test Sequence

5. Close PRV shut-off valve by clicking the *PRV shut-off* toggle switch. The toggle switch is green when the valve is closed.
6. Open fuel line valve by clicking on *Fuel Line Valve* toggle switch. The toggle switch is green when the valve is on.
7. Start recording to file by clicking on *Start Recording* and changing it to *Yes*. The test time clock is set to zero and the data in the plots cleared.

8. Ignite the burners by clicking on the ignitors toggle switch. The toggle switch is red when the ignitors are operating. Turn off the ignitors as soon as all of the burners are lit.
9. Once the ignitors are off, change the PRV control to enable. Do not change to enable until the ignitors are off since the ignitors may cause spikes in the pressure transducer readings resulting in premature opening of the PRV.
10. At the pre-determined delay, start the Racal recorder recording by pressing the square *REC* button. The LED above the *REC* button should turn green. The recorder can be stopped and restarted at any time by pressing the *STOP* or *REC* buttons.

Note : During a test all the buttons should be green if controls are in the correct postion.

11. To stop recording data click on the *Start Recording* button to turn it *off*.
12. To stop measuring data values, click on the *Measurement* button to turn it *off*.

H.5 Program Structure

In PRV_DAQII, all access to the System 200 boards is done through the 802 interface cards using basic library routines contained in lv200.dll. The program calls sub VI's that contain the *Call Library* function of LabView to call the functions in the DLL. All higher level programming is done within Labview.

Sub VI's have been used for repetitive tasks or to simplify the layout of the program.

H.5.1 LV200.dll

LV200.dll contains all of the command routines required for communicating with the 236, 210, and 222 boards in the System 200 chasis. The DLL was written in C++ and is based on the Level 1 C drivers supplied by Sciemetrics. The DLL was compiled as a DLL project using Visual C++ 6.0. The variable types in the original C drivers were changed to allow the DLL to be used on a 32 bit computer rather than a 16 bit architecture for which they were originally written.

LV200.dll contains the following function calls:

```
int reset222(unsigned badd);
int read222 (unsigned badd, int chan, int *state);
int write222 (unsigned badd, int chan, int state);
int init236 (unsigned badd);
int voltshlg236 (unsigned badd, int chan, int range, int
HorL,
                         int AZflag,int az236[4], float
                         *volts);
int volts236 (unsigned badd, int chan, int range, int
AZflag,
                         int az236[4],float *volts);
int tablevolts236 (unsigned badd, int size, int chans[],
int range,
                         int AZflag, int az236[4],float
                    volts[]);
int autozero236 (unsigned badd, int zeros[]);
int interthmst236 (unsigned badd, float *ohms);
int readdin210 (unsigned badd, int chan, int *state);
int readdout210 (unsigned badd, int chan, int *state);
int writedout210 (unsigned badd, int chan, int state);
int out210counts (unsigned badd, int chan, int dtoacount);
int checkbaddid(unsigned badd, int modelnumber);
int checkid(unsigned badd);
```

The purpose of the above function calls is described in the Level 1 software documentation.

H.5.2 Sub VI's

Labview programming makes use of sub-VI's which are similar to subroutines or functions in Fortran. Two types of subroutines have been used in PRV_DAQII :

1. interface sub-VI's- These sub-VI's provided an interface to the functions contained in lv200.dll using the Call Library function.
2. Programming sub-VI's - Several sub-VI's have been created for various tasks including creating TecPlot file headers, and dead band control for the PRV etc. These sub-VI's simplify repetitive tasks and make the overall code more readable.

A full listing of the sub-VI's and their function is included in Appendix 1.

H.5.3 Graphical Programming Layout

The graphical programming in the LabView diagram window of PRV_DAQII is laid out in three main units which use a combination of while loops and sequences to carry out the data acquisition and control.

1. file set-up – if the data is to be saved to file the files are opened and initialized with TecPlot headers.
2. Data acquisition – The data acquisition is set-up with five main tasks
   a) lading temperature
   b) wall temperature
   c) fire temperature
   d) tank pressure and PRV control
   e) nozzle temperature and pressure

   Each task is contained in a while loop that executes at the rate set by sample frequency for the task. For high-speed data acquisition, if any task contains more than one channel with the same settings, the tablevolts function is used. The method currently used to scan the channels with tablevolts requires that the channels be in consecutive order. This is a result of the LabView programming. The LV200.dll function can take channels in any order.
3. Switch control – several relays and digital inputs/outputs are used to control the Racal tape recorder, burner fuel valve, ignitors, and PRV shut-off valve. These controls are contained in a while loop that executes two times a second. The slightly long delay makes the system a little sluggish but prevents the system from becoming bogged down. At each execution of the loop the position of the control switches are checked and action is taken as appropriate.

H.5.4 Timing

The System 200 does not have the capability to sample at accurate intervals. In PRV_DAQ the timing of the sampling for each task is controlled by the wait Sub-VI included in each while loop. Each loop will wait the required delay and then attempt to carry out the data acquisition or control task. Since there are several tasks running simultaneously, LabView semaphores are used to ensure that only one task is accessing the boards in the System 200 at any one time. By using semaphores, when a task wants to access a board, a request for access is issued. If no other tasks are accessing the board, the task is allowed immediate access. If one or more requests for access are in line ahead, the task waits until the board is free.

Due to this requirement, the execution frequency will not necessarily be constant. Therefore, the time of acquisition is included in the data file.

H.5.5 Thermocouples

The voltages read by the System 200 are converted to temperature using the NIST thermocouple polynomials in a conversion VI adapted from a LabView supplied VI. The reference temperature at the thermocouple junction at the DA board is measured by an internal thermistor mounted on the 236 board. To increase the DA capacity, this temperature is only read at a specified interval and not when every time a thermocouple voltage is read. Currently the internal reference temperature is updated once per minute. This was found to be adequate for the rate at which the temperature in the System 200 changed. The update frequency of the reference temperature can be changed by changing the rate at which the while loop that reads the reference temperature executes.

H.5.6 File output format

One data file is saved for each DA task using the run name as a prefix. The files are named as follows :

Lading temperature file - *run-name*lading.dat
Wall temperature file - *run-name*wall.dat

Fire temperature file - *run-name*firet.dat
Tank pressure file - *run-name*tankp.dat
Nozzle data file - *run-name*massflow.dat

All data files are saved with a TecPlot header that allows them to be plotted immediately. The header contains the title of the plot and variable names. The time of acquisition of each sample is listed in the leftmost column in each file. A sample of a file is shown below:

```
Title ="tankp"
Variables ="time (s)" "tankp 0" "tankp 1" "valve position"
Zone F=Point
0.080      113.722   114.839   0.000
0.179      113.722   115.220   0.000
0.281      113.722   115.220   0.000
```

H.6 Utility Programs

Channel array.vi – creates an array of channel numbers given the first and last channel number in a string of consecutives channels
Fileopen.vi – opens a file with a TecPlot header
NIST TCP buffer.vi – uses NIST polynomials to convert a table of voltages to temperature
NIST Thermocouple.vi - uses NIST polynomials to convert a voltage to temperature
P average.vi – averages pressures for use in the PRV control
PRVcontrol.vi – controls the state of the PRV using deadband control
PRVcontrolsynch.vi – same as PRVcontrol.vi using semaphores
PRVtest.vi – cycles the PRV three times
Racal.vi – controls the stop and record functions of the tape recorder
Single P convert.vi – converts a single voltage to pressure using a linear fit
Static P convert.vi – converts a table of voltages to pressure using linear fits
Tcpconvert.vi – converts a thermocouple voltage to temperature
TecPlot header.vi – writes a TecPlot header to file
Tforchart.vi – creates a sub-array for plotting
Variable name.vi – generates the variables names for an array of channels

H.7 Test Programs

Several test programs have been written to allow measurement and control to be done separately from PRV_DAQII. These are useful for diagnostics and testing individual components of the system.

Digoutcontrol.vi – switches the digital outputs on the 210 board
PRVcycletest.vit – cycles the PRV at a specified rate
Racalrun.vi – runs the control of the Racal recorder
Relaytest.vi – allows control of all the relays on the 222 board
Tabletcptest.vi – allows an array of thermocouples to be read at a specified frequency
Thermocoupletes.vi – allows a thermocouple to be read at a specified frequency
Volttest.vi – allows a voltage to be read at a specified frequency

H.8 Interface Sub-VI Listing

Autozero.vi – measures the autozero values of the 236 board
Badd 210.vi – contains the global variable of the base address for the 210 board
Badd 212.vi – contains the global variable of the base address for the 212 board
Badd 236.vi – contains the global variable of the base address for the 236 board
Checkbaddid.vi – checks that the board at badd XXX has the expected number
Checkid.vi – checks the number of a board at the given base address
Init236.vi – carries out initialization of the 236 board
Interthermst236.vi – reads the temperature of the internal thermistor on the 236 board

Interthermst236synch.vi – same as Interthermst236.vi using semaphores
Out210counts.vi – outputs a analogue to digital count to the 210 board
Read222.vi – reads the state of a relay on the 222 board
Read222synch.vi – same as Read222.vi using semaphores
Readdin210.vi – reads the state of a digital input on the 210 board
Readdout210.vi – reads the state of a digital output on the 210 board
Reset222.vi – resets all of the relays on the 222 board to off
Tabletcp.vi – reads an array of thermocouples on the 236 board
Tabletcpsynch.vi – same as Tabletcp.vi using semaphores
TableVolts236.vi – reads an array of voltages on the 236 board
TableVolts236synch.vi – same as TableVolts236.vi using semaphores
Thermocouple.vi – reads a single temperature from the 236 board
Volts236.vi – reads a single differential voltage from the 236 board
Volts236synch.vi – same as Volts236.vi using semaphores
voltshlg236.vi – reads a single voltage between high and ground or low and ground on the 236 board
write222.vi – write the state to a relay on the 222 board
write222synch.vi – same as write222.vi using semaphores
writedout210.vi – writes the state to a digital output on the 210 board

Appendix I: Wall Thermocouple Fabrication

I.1 Overview

A new method of wall thermocouple installation was used in this series of tests. Wall thermocouples were welded with a spot welder to the surface of the tank. This method appears to have resulted in a significant improvement in accuracy and reliability over the previously used mechanical attachment method. Some preliminary testing of the wall thermocouples was done in conjunction with burner development tests, where an instrumented piece of pressure vessel steel was exposed to a torch fire. A difference of 5 to 10°C was seen between the steady measured thermocouple temperature and the temperature measured with a hand-held IR thermometer at temperatures near 500°C. The major source of error is due to conduction of heat to or from the measurement point through the thermocouple leads.

I.2 Fabrication Procedure

Wall Thermocouple Fabrication and Installation

Thermocouple Material
K-Type
24 gauge wire
Fibreglass insulation around each lead and around both pair
Omega Part No. HH-K-24

Welder
Hot Spot II TC Welder
DCC Corporation
Stored Weld Energy: adjustable, 5 to 250 Joules

The welder should only be used by competent personnel after reading the application manual and fully understanding safety issues.

Fabrication and attachment of Wall TC's is a two-step process. First, a thermocouple junction is welded. Then, the TC junction is welded to the tank wall. This helps to ensure sturdy attachment of both TC leads.

TC Fabrication
(i) Strip 1.0 -- 1.5 cm of insulation off end of TC leads
(ii) Attach base electrode to carbon block
(iii) Set weld energy dial to 30 -- 35 Joules
(iv) Grip both bare TC leads securely, approx. 6 --7 mm from end, with electrode pliers
(v) The tips of both TC leads should meet each other or else be in very close proximity
(vi) Hold tip of TC leads to carbon block/electrode with pliers
(vii) Make sure the only electric circuit between the electrodes is though TC.
(viii) Press weld button to release charge

Wall attachment
(i) Grind areas on tank wall for TC attachment and base electrode attachment with hand grinder
(ii) Attach base electrode with magnetic block to tank wall
(iii) Set weld energy dial to 40 -- 45 Joules
(iv) Grip TC leads securely, approx. 6 --7 mm from TC junction, with electrode pliers
(v) Hold TC junction to tank wall with electrode pliers
(vi) Make sure the only electric circuit between the electrodes is though TC and Tank.
(vii) Press weld button to release charge

Appendix J: Burner Development

Fire testing of this type is often carried out using liquid hydrocarbon fuelled pool fires. This type of fire is very difficult to control, since even slight winds can greatly effect the fire's behaviour. A pool fire also poses additional complications to the data acquisition process. For these reasons, an array of burners was developed to simulate a partially engulfing pool fire.

The performance objectives of the burner system design was to:

- simulate an engulfing pool fire with an estimated black body temperature in the range of 871 ± 56 °C (Canadian General Standards Board standard CAN/CGSB 43.147-2002)
- deliver the heat in a uniform, repeatable way from test to test

In addition to the above criteria, the following design guidelines were adapted during the burner development process:

- modular for easy on site assembly
- comprised of inexpensive, readily available parts
- stable flame (no blow-off tendency)
- directional stability
- uniform flame front that covers at least 1.5m x 1.5m area

J.1 Burner Design Evolution

Since a large number of burners may be required (many or all can be destroyed during tank failure), it was decided to use cheap and readily available standard pipe fittings for as much of the burner assembly as possible. The development process began with a very primitive design and progressed through more elaborate schemes, until the burner performance criteria were met. Figure J.1 shows the progression of burner designs A through D followed during the burner development process.

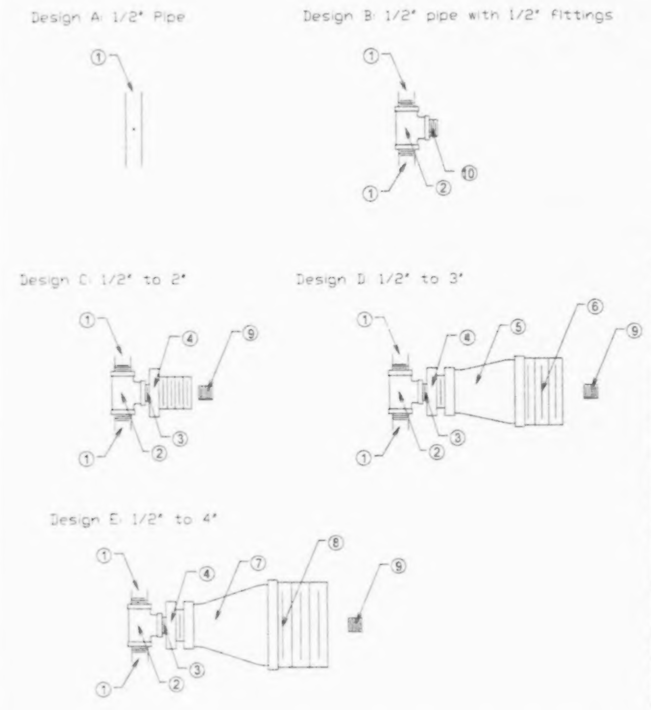

Notes:

Design A: consists of only 1/2" sch 40 pipe with various sized holes and shroud attachments

Design B: consists of 1/2" pipe supply to 1/2" pipe fittings with exchangable pipe plug nozzles

Design C: is similar to B with the addition of a modified nipple that allows the attachment of a pipe bushing to reduce the fuel velocity at the burner exit and to better control air mixing

Design D: is similar to C with the addition of a pipe reducer coupling to exagerate the effects of the modifications made in Design C

Design E: is similar to D with larger exit dia

Item No.	Part Name	Matl	Dwg. No.	Req
12				
11				
10	Plug, 1/2" NPT	Steel	10	
9	Plug, 3/8" NPT	Steel	9	
8	Nipple, 4" sch 40	Steel		
7	Reducer, 4" to 2" NPT	Steel		
6	Nipple, 3" sch 40	Steel		
5	Reducer, 3" to 2" NPT	Steel		
4	Bush, 2" to 1/2" NPT	Steel	4	
3	Nipple, 1/2" sch 40	Steel	3	
2	Tee, 1/2" NPT	Steel		
1	Pipe, 1/2" sch 40	Steel		

Thermal Hazards Laboratory
Queen's University at Kingston
Kingston, Ontario, CANADA

Title: Burner Designs

Dwg. No.:

Drawn by: D.J. Poirier	Tolerances
Scale:	Frac. ± 1/32 .X ±.05 .XX ±.005
Date: 040226	Angles ±.5

Figure J.1: Burner design evolution.

Design A, a simple pipe with holes drilled in it, lacked both flame stability and luminousity. This was not a surprise as there was no means of anchoring the flame (bluff body or diffuser) or control of air entrainment into the fuel jet.

Design B, a pipe tee with a modified pipe plug, performed no better than Design A, for basically the same reasons.

Design C added a modified concentric pipe bushing burner body, Figure J.2, and a modified pipe cap fuel nozzle, Figure J.3, to Design B and was a marked improvement in both stability and luminousity, Figure J.4. However, directional stability could be improved.

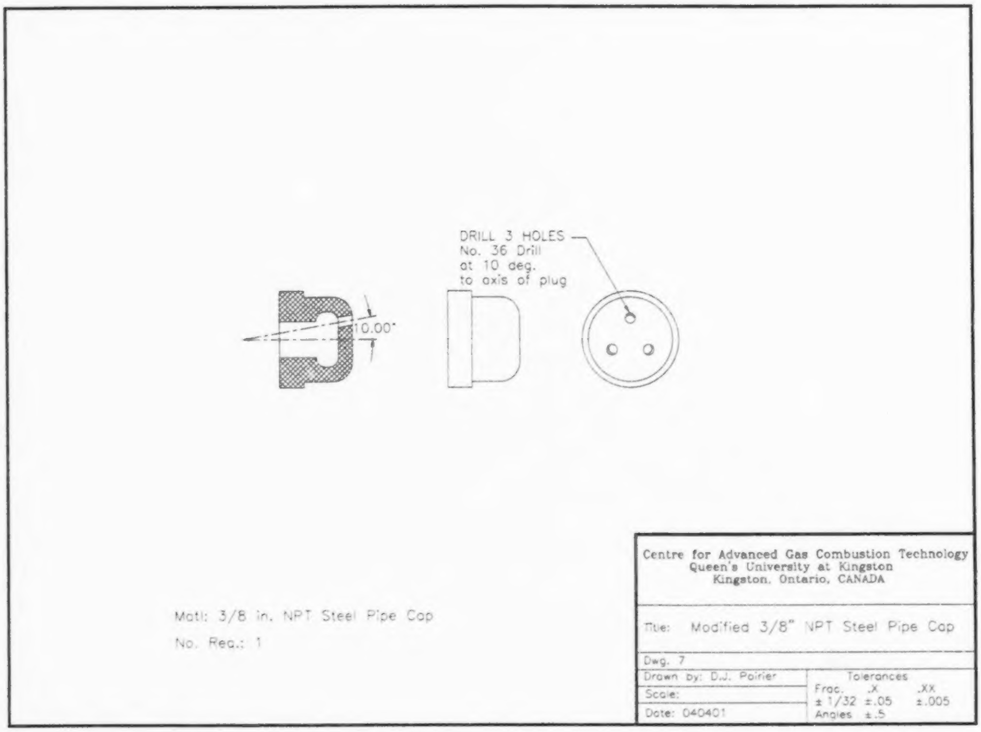
DRILL 3 HOLES
No. 36 Drill
at 10 deg.
to axis of plug
10.00°
Matl: 3/8 in. NPT Steel Pipe Cap
No. Req.: 1
Centre for Advanced Gas Combustion Technology
Queen's University at Kingston
Kingston, Ontario, CANADA
Title: Modified 3/8" NPT Steel Pipe Cap
Dwg. 7
Drawn by: D.J. Poirier
Scale:
Date: 040401
Tolerances
Frac. .X .XX
± 1/32 ±.05 ±.005
Angles ±.5

Figure J.2: Modified pipe cap fuel nozzle.

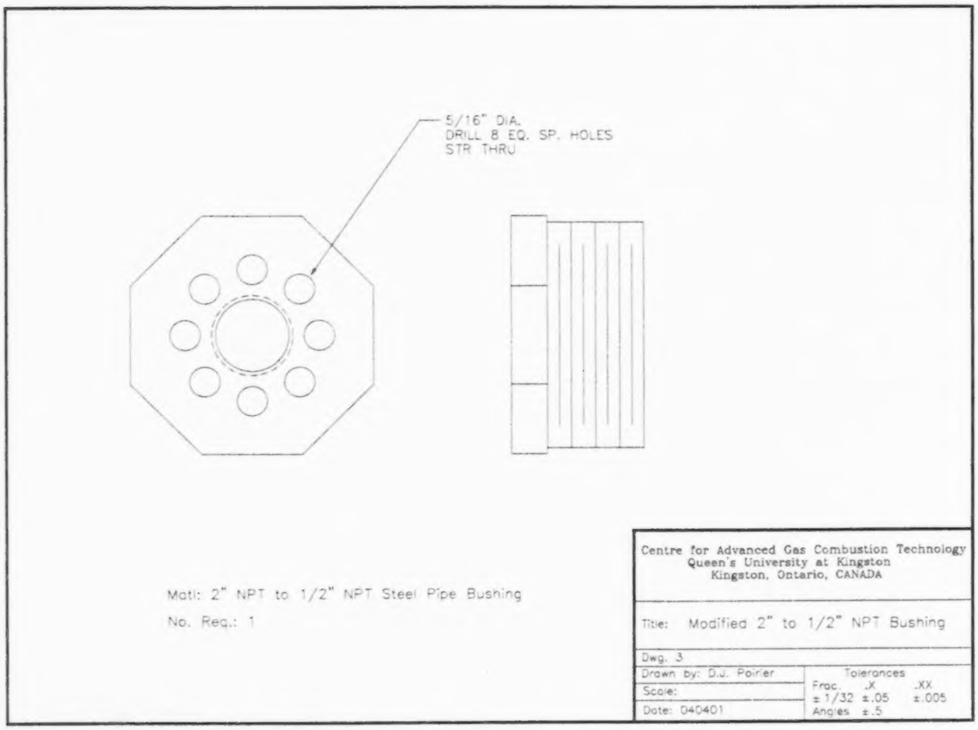
5/16" DIA.
DRILL 8 EQ. SP. HOLES
STR THRU
Matl: 2" NPT to 1/2" NPT Steel Pipe Bushing
No. Req.: 1
Centre for Advanced Gas Combustion Technology
Queen's University at Kingston
Kingston, Ontario, CANADA
Title: Modified 2" to 1/2" NPT Bushing
Dwg. 3
Drawn by: D.J. Poirier
Scale:
Date: 040401
Tolerances
Frac. .X .XX
± 1/32 ±.05 ±.005
Angles ±.5

Figure J.3: Modified pipe bushing burner body.

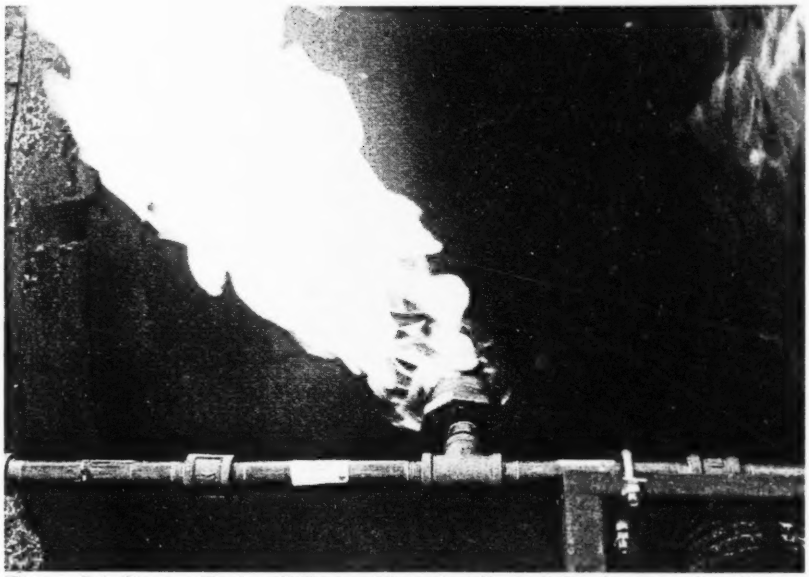

Figure J.4: Burner Design C flame. Note that flame is luminous and well attached to burner, but directional stability is not good.

Design D added a reducing coupling and large pipe nipple to Design C and produced a flame that had promising stability and luminosity characteristics, Figure J.5.

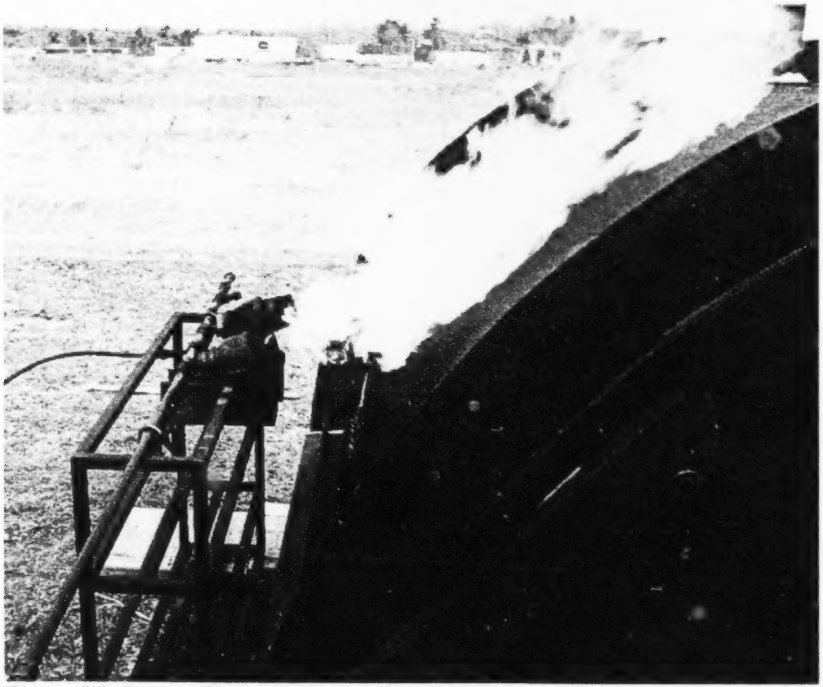

Figure J.5: Burner Design D flame. Note that flame is luminous, attached to burner and directional stability is better than Design C.

The next step was to produce and assemble arrays of Burner D to do temperature distribution tests. Figure J.6 shows a drawing for a single 5-burner array. A drawing of the evaporator assembly used to convert the liquid propane to vapour for burner firing is shown in Figure J.7. Figures J.8 and J.9 show the burner array and test shell set-up before temperature distribution testing.

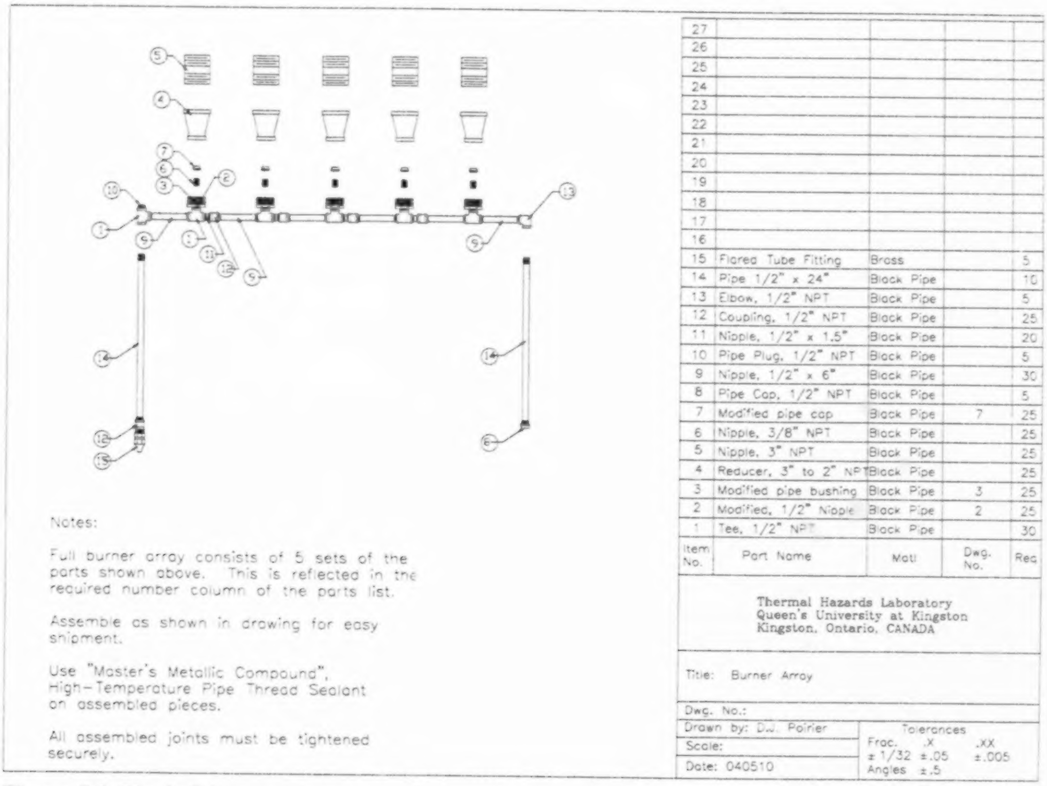

Notes:

Full burner array consists of 5 sets of the parts shown above. This is reflected in the required number column of the parts list.

Assemble as shown in drawing for easy shipment.

Use "Master's Metallic Compound", High-Temperature Pipe Thread Sealant on assembled pieces.

All assembled joints must be tightened securely.

Item No.	Part Name	Matl	Dwg. No.	Req
27				
26				
25				
24				
23				
22				
21				
20				
19				
18				
17				
16				
15	Flared Tube Fitting	Brass		5
14	Pipe 1/2" x 24"	Black Pipe		10
13	Elbow, 1/2" NPT	Black Pipe		5
12	Coupling, 1/2" NPT	Black Pipe		25
11	Nipple, 1/2" x 1.5"	Black Pipe		20
10	Pipe Plug, 1/2" NPT	Black Pipe		5
9	Nipple, 1/2" x 6"	Black Pipe		30
8	Pipe Cap, 1/2" NPT	Black Pipe		5
7	Modified pipe cap	Black Pipe	7	25
6	Nipple, 3/8" NPT	Black Pipe		25
5	Nipple, 3" NPT	Black Pipe		25
4	Reducer, 3" to 2" NPT	Black Pipe		25
3	Modified pipe bushing	Black Pipe	3	25
2	Modified, 1/2" Nipple	Black Pipe	2	25
1	Tee, 1/2" NPT	Black Pipe		30

Thermal Hazards Laboratory
Queen's University at Kingston
Kingston, Ontario, CANADA

Title: Burner Array

Dwg. No.:

Drawn by: D.J. Poirier
Scale:
Date: 040510

Tolerances
Frac. .X .XX
± 1/32 ±.05 ±.005
Angles ±.5

Figure J.6: Single 5-burner array.

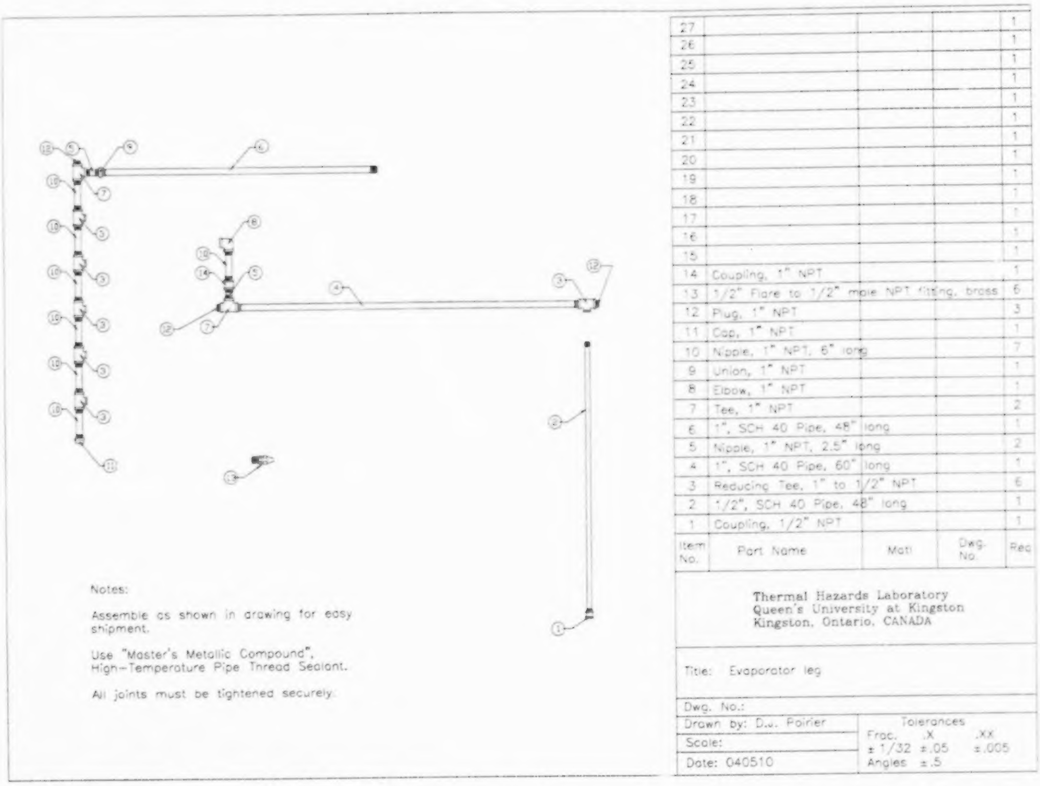

Notes:

Assemble as shown in drawing for easy shipment.

Use "Master's Metallic Compound", High-Temperature Pipe Thread Sealant.

All joints must be tightened securely.

Item No.	Part Name	Mat'l	Dwg. No.	Req
27				1
26				1
25				1
24				1
23				1
22				1
21				1
20				1
19				1
18				1
17				1
16				1
15				1
14	Coupling, 1" NPT			1
13	1/2" Flare to 1/2" male NPT fitting, brass			6
12	Plug, 1" NPT			3
11	Cap, 1" NPT			1
10	Nipple, 1" NPT, 6" long			7
9	Union, 1" NPT			1
8	Elbow, 1" NPT			1
7	Tee, 1" NPT			2
6	1", SCH 40 Pipe, 48" long			1
5	Nipple, 1" NPT, 2.5" long			2
4	1", SCH 40 Pipe, 60" long			1
3	Reducing Tee, 1" to 1/2" NPT			6
2	1/2", SCH 40 Pipe, 48" long			1
1	Coupling, 1/2" NPT			1

Thermal Hazards Laboratory
Queen's University at Kingston
Kingston, Ontario, CANADA

Title: Evaporator leg

Dwg. No.:
Drawn by: D.J. Poirier
Scale:
Date: 040510

Tolerances
Frac. .X .XX
± 1/32 ±.05 ±.005
Angles ±.5

Figure J.7: Evaporator design.

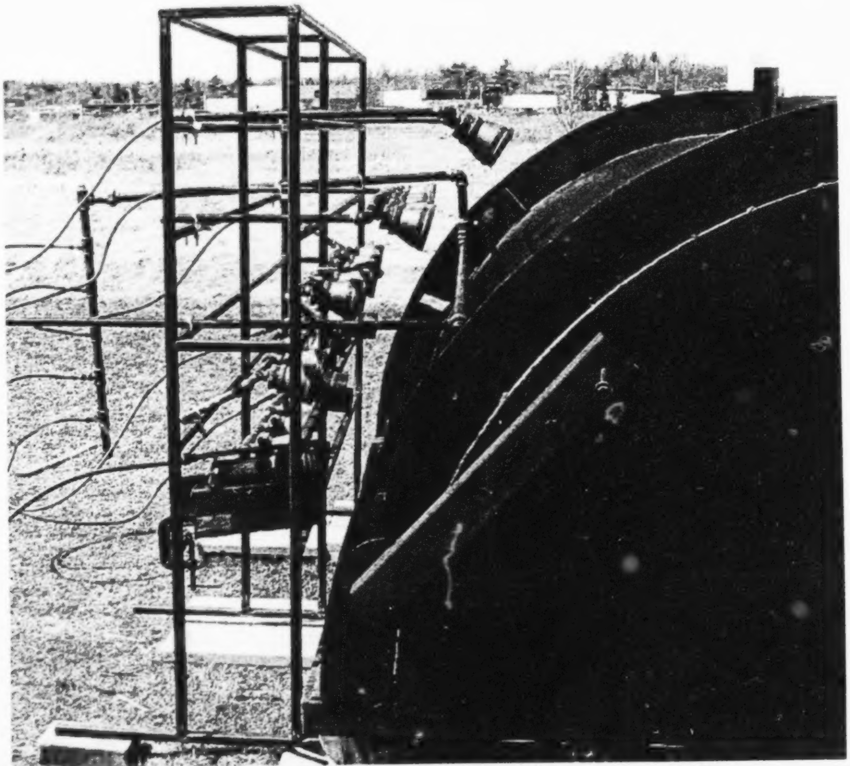

Figure J.8: Side-view of five 5-burner arrays on 1/4 section test shell.

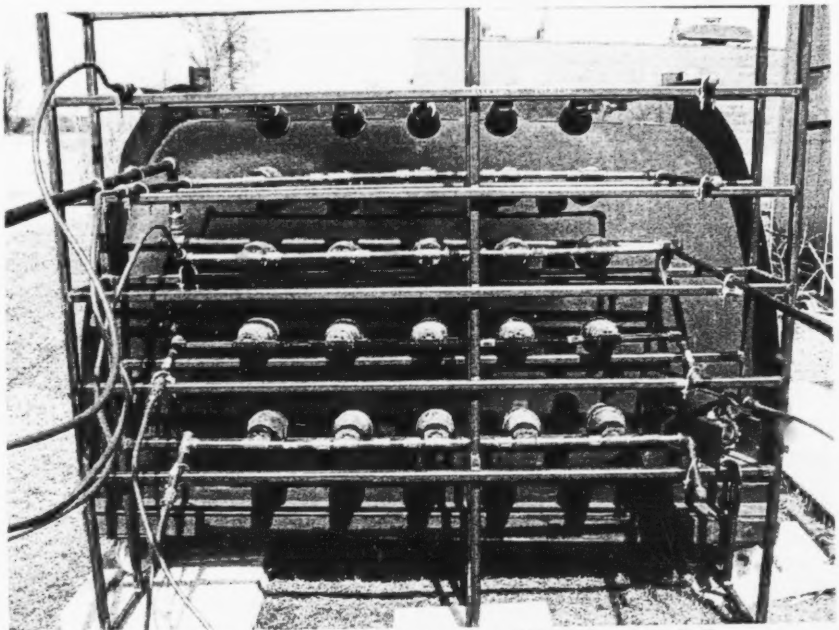

Figure J.9: Back view of five 5-burner arrays on 1/4 section test shell.

Liquid propane was supplied to the evaporator at approximately 205 kPa (30 psi). Figure J.10 shows a side-view of the flame sheet produced by the 5x5 array of burners. Note the luminous flame, as is characteristic of pool fires.

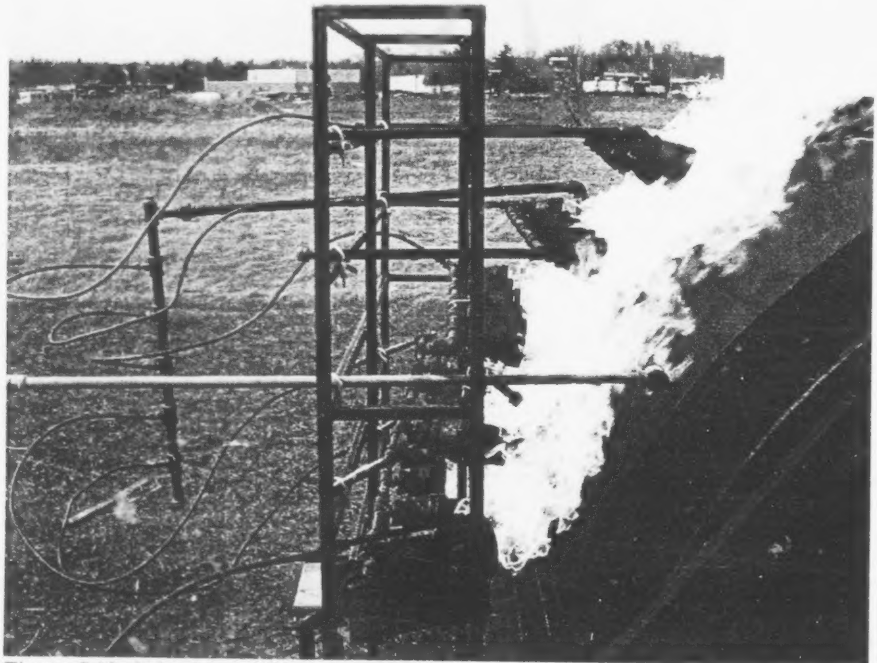

Figure J.10: Side view of flame from five 5-burner arrays on 1/4 section test shell. Note frost on evaporator inlet.